PUB-5428

ERNEST ORLANDO LAWRENCE BERKELEY NATIONAL LABORATORY

Laboratory Directed Research and Development Program
FY 1996

February 1997

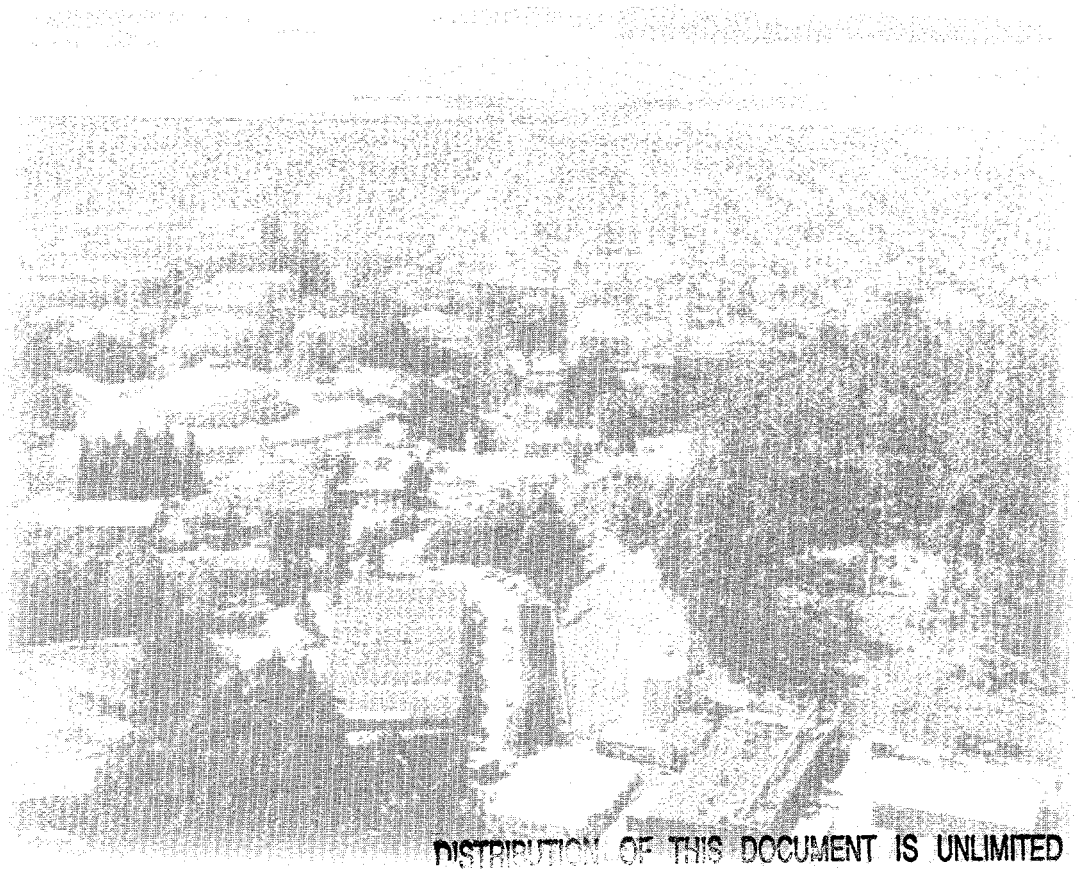

PUB-5428

Report on
Ernest Orlando Lawrence
Berkeley National Laboratory

Laboratory Directed Research and Development Program

FY 1996

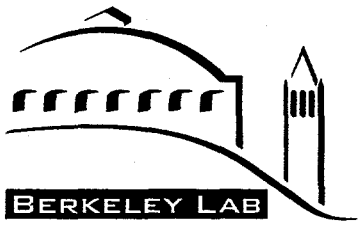

ERNEST ORLANDO LAWRENCE
BERKELEY NATIONAL LABORATORY
UNIVERSITY OF CALIFORNIA
BERKELEY, CALIFORNIA 94720

Prepared for the U.S. Department of Energy under Contract No. DE-AC03-76SF00098

Table of Contents

Introduction

The *Ernest Orlando Lawrence Berkeley National Laboratory (Berkeley Lab) Laboratory Directed Research and Development Program FY 1996* report is compiled from annual reports submitted by principal investigators following the close of the fiscal year. This report describes the projects supported and summarizes their accomplishments. It constitutes a part of the Laboratory Directed Research and Development (LDRD) program planning and documentation process that includes an annual planning cycle, projection selection, implementation, and review.

The Berkeley Lab LDRD program is a critical tool for directing the Laboratory's forefront scientific research capabilities toward vital, excellent, and emerging scientific challenges. The program provides the resources for Berkeley Lab scientists to make rapid and significant contributions to critical national science and technology problems. The LDRD program also advances the Laboratory's core competencies, foundations, and scientific capability, and permits exploration of exciting new opportunities. Areas eligible for support include:

- Work in forefront areas of science and technology that enrich Laboratory research and development capability;
- Advanced study of new hypotheses, new experiments, and innovative approaches to develop new concepts or knowledge;
- Experiments directed toward proof of principle for initial hypothesis testing or verification; and
- Conception and preliminary technical analysis to explore possible instrumentation, experimental facilities, or new devices.

The LDRD program supports Berkeley Lab's mission in many ways. First, because LDRD funds can be allocated within a relatively short time frame, Berkeley Lab researchers can support the mission of the Department of Energy (DOE) and serve the needs of the nation by quickly responding to forefront scientific problems. Second, LDRD enables the Laboratory to attract and retain highly qualified scientists, and supports their efforts to carry out world-leading research. Finally, the LDRD program also supports new projects that involve graduate students and postdoctoral fellows, thus contributing to the education mission of the Laboratory.

Berkeley Lab has a formal process for allocating funds for the LDRD program. The process relies on individual scientific investigators and the scientific leadership of the Laboratory to identify opportunities that will contribute to scientific and institutional goals. The process is also designed to maintain compliance with DOE Orders, in particular DOE Order 5000.4A and DOE draft Directive 413, dated October 28, 1996. From year to year, the distribution of funds among the scientific program areas will change. This flexibility optimizes the Laboratory's ability to respond to opportunities.

Berkeley Lab LDRD policy and program decisions are the responsibility of the Laboratory Director. The Director has assigned general programmatic oversight responsibility to the Deputy Director for Research. Administration and reporting on the LDRD program is supported by the Directorate's Office for Planning and Communications. LDRD accounting procedures and financial management are consistent with the Laboratory's accounting principles and stipulations under the contract between the University of California and the Department of Energy, with accounting maintained through the Laboratory's Chief Financial Officer.

In FY 1996, Berkeley Lab was authorized by the Department of Energy to establish a funding ceiling for the LDRD program based on 3% of the Laboratory's FY 1996 operating and capital equipment budgets. This funding level was provided to develop new scientific ideas and opportunities and allow the Laboratory Director an opportunity to initiate new directions. However, budget constraints limited available resources, so only $6.2 M was expended for operating and $0.6 M for capital equipment.

In FY 1996, scientists submitted 145 proposals requesting over $22 M. A total of 60 projects were funded, with awards ranging from $6 K to $457 K. These projects are summarized in Table 1.

Table 1: FY 1996 Laboratory Directed Research and Development Program.

Investigator	Project Title	($)
Accelerator and Fusion Research Division		
Christine Celata Richard Donahue Ehud Greenspan Ka-Ngo Leung Paul Luke Peter Zawislanski	A Neutron Logging Instrument for Earth Sciences Applications	179,900
Alan Jackson Clyde Taylor	"Superbend"—A 5 T Bending Magnet Design for the ALS	245,600
Howard Padmore Jacques Millaud Thomas Earnest David Nygren	Advance Towards the Next Generation of Pixellated Detectors for Protein Crystallography	166,400
Howard Padmore	Using Microdiffraction to Measure Local Strain in Microelectronic Devices	155,900
Neville Smith	Spin Polarized Photoemission Studies of Magnetic Surfaces, Interfaces, and Films	200,200
William Turner	Technology for an International Proton Collider at High Energy and Luminosity	150,800
Chemical Sciences Division		
John Arnold	Network Silicates With Porphyrin Backbones: Novel Solids and Catalysts	79,600
David Chandler Martin Head-Gordon William Miller	Molecular Theory Center	69,000
Charles Harris	Magnetic Properties and Electron Localization at Interfaces	98,300

Table 1. Continued.

Investigator	Project Title	($)
Computer Sciences Departments		
John Bell Nancy Brown Phillip Colella Michael Frenklach	High Fidelity Simulation of Diesel Combustion	99,900
Earth Sciences Division		
Mark Conrad Terrence Leighton Bob Buchanan	Characterization and Monitoring of Subsurface Biologic Activity Using Stable Isotope Soil Gas Analyses	49,600
Jennie Hunter-Cevera Hoi-Ying Holman Tamas Torok	Bioavailability and Degradation of Aromatic Hydrocarbons from Soil	170,300
Karsten Pruess George Brimhall	Reactive Chemical Transport in Geologic Media	16,300
Erika Schlueter Dale Perry	Developing High Resolution Synchrotron X-ray Techniques to Study Natural Porous Media	120,300
Garrison Sposito	Molecular Geochemistry of Clay Mineral Surfaces	25,900
Don Vasco Lane Johnson	Advanced Computing for Geophysical Inverse Problems	34,300
Jiamin Wan	Microbial Transport and Microbial and Nutrient Delivery in Subsurface Environments	78,200
Energy and Environment Division		
Susan Anderson	Sediment Toxicity and Site Restoration at the Mare Island Naval Shipyard	60,200
Ronald Cohen	Instruments for the in situ Detection of NO and NO_2 and Their Precursors	129,800
Michael Frenklach	Mechanism and Modeling of Soot Formation in Hydrocarbon Flames	75,000
Arlon Hunt	Manganese Oxide Aerogels for Lithium Batteries	75,100
Jay Keasling	Kinetics and Modeling of Anaerobic TCE Degradation for in situ and ex situ Applications	60,500

Table 1. Continued.

Investigator	Project Title	($)
Rolf Mehlhorn	Decontamination Technology for Marine Sediments	5,900
Tihomir Novakov	Composition and Sources of Marine Cloud Condensation Nuclei	74,900
Richard Russo Richard Fish	Metal-Specific Chemical Sensors Using Polymer Films for Non-Proliferation and Environmental Applications	81,100
Stephen Selkowitz Mary Ann Piette Frank Olken Max Sherman	Building Performance Assurance with Building Life-Cycle Information Systems	278,800
Engineering Division		
Eugene Binnall Joseph Katz Charles Fadley Helmuth Spieler Jorge Zaninovich	Development of Next-Generation Detectors for Use at the Advanced Light Source	119,800
Deborah Hopkins Bill Edwards Carol Corradi Kurt Nihei Larry Myer Seiji Nakagawa	Non-Destructive Evaluation and Testing of Vehicle Bodies and Components	50,100
Information and Computing Sciences Division		
William Johnston William Greiman Brian Tierney	High-Speed Distributed Data Handling	216,800
William Johnston Horst Simon	Scientific Computing on Networks of Workstations	129,200
Life Sciences Division		
Aloke Chatterjee William Holley Saira Mian Björn Rydberg	Computational Investigation of Chromatin Structure	80,000
Joe Gray	Techniques for Discovery of Disease-Related Genes	457,100

Table 1. Continued.

Investigator	Project Title	($)
Teresa Head-Gordon George Oster	Computational Biology	60,900
Paul Kaufman	Mechanism of Chromatin Assembly During DNA Replication	33,300
Jon Nagy	Screening a Combinatorial Peptide Library for Ability to Promote Reversion of Tumor Cells into Nonmalignant Cells	22,900
Daniel Rokhsar	Theoretical Model for DNA Structure and Function	50,000
David Schild	Role of Recombinational Repair in Mammals: Analysis in Yeast of the Human DNA Repair Gene XRCC3	50,000
Peter Walian	Crystallization and Structure Determination of Integrin $\alpha_{IIb}\beta_3$, a Platelet Membrane Protein Receptor	89,900
Paul Yaswen	Isolation of Genetic Supressor Elements in Human Mammary Epithelial Cells	40,000
Materials Sciences Division		
John Arnold Eugene Haller Edith Bourret	New Chemistry for Epitaxial Growth of *p*-Type Gallium Nitride and Its Alloys	132,900
Deborah Charych Lutgard De Jonghe Amir Berman Marca Doeff Pieter Stroeve	Synthesis of Oriented Nanoparticulate and Dense Crystalline Ceramic Films Using Biomimetic Membranes	70,900
Dung-Hai Lee	Universal Properties at the Critical Point of Quantum Hall Plateau Transitions	50,200
Steven Louie Marvin Cohen John Morris, Jr. Daryl Chrzan	Determining Macroscopic Materials Properties from Microscopic Calculations	44,500
Werner Meyer-Ilse John Brown David Attwood	Biological X-ray Microscopy	100,900

Table 1. Continued.

Investigator	Project Title	($)
Zi Qui	Investigation of Nanometer Magnetism by Using Surface Magnetooptic Kerr Effect (SMOKE)	50,100
Antoni Tomsia Rowland Cannon	Functionally Graded Ceramic-Metal Architectures for High Temperature Applications	70,800
Michael Van Hove	MSD Theory and NERSC Computation for ALS Experiments	86,000
National Energy Research Scientific Computing Center		
C. William McCurdy Thomas Rescigno	Electron and Photon Collisions with Molecules, Clusters, and Surfaces	88,100
Nuclear Science Division		
Claude Lyneis	A Third-Generation ECR Ion Source	157,600
Physics Division		
Murdock Gilchriese	Pixel Detectors for Charge Particle Detection	119,600
Hans Wenzel Richard Kadel	Photosensor for Use in a High Magnetic Field	120,800
David Nygren Douglas Lowder Martin Moorhead Gilbert Shapiro George Smoot Robert Stokstad	System Design and Initial Electronic Engineering for a km-Scale Neutrino Astrophysical Observatory	138,000
Saul Perlmutter Gerson Goldhaber Donald Groom Alex Kim	Exploring Scientific-Computational Collaboration: NERSC and the Supernova Cosmology Project	44,400
Ravi Malladi James Sethian	Level Set Methods for Medical Image Analysis	48,900
Structural Biology Division		
Stephen Holbrook Rosalind Kim	Synthesis, Crystallization and Characterization of 5S Ribosomal RNA	130,800

Table 1. Continued.

Investigator	Project Title	($)
Stephen Holbrook	Determination of Macromolecular Structure by *ab initio* Phasing of Crystallographic Diffraction Data	57,200
Cross-Divisional		
Robert Bergman Mark Alper Jonathan Ellman Peter Schultz Alexis Bell Enrique Iglesia Heinz Frei Jay Keisling	New Chemistry for Pollution Prevention: Selective Catalyst	378,800
Eleanor Blakely Thomas Budinger William Chu Theodore Phillips	Biology of Boron Neutron Capture Therapy (BCNT)	128,900
Thomas McKone Sally Benson Nancy Brown Joan Daisey Lois Gold Jane Macfarlane	SELECT: An Integrated Framework for Assessing Transport, Exposure, Health Risk, and Clean-up Cost for Subsurface Contamination	322,700
Stanley Goldman Tamas Torok	Use of rRNA Gene Sequencing and Signature Lipid Biomarker Analysis to Assess and Monitor Microorganisms in Damaged Environments	251,000
TOTAL		6,774,900

Accelerator and Fusion Research Division

A Neutron Logging Instrument for Earth Sciences Applications

Principal Investigators: Christine Celata, Richard Donahue, Ehud Greenspan, Ka-Ngo Leung, Paul Luke, and Peter Zawislanski

Project No.: 96001

Funding: $179,900 (FY96)

Project Description

The purpose of this project is to use Berkeley Lab technological advances in ion sources and gamma-ray detectors to make a significant enhancement in the capability of neutron logging tools. Neutron logging instruments consist of a neutron generator and gamma-ray detector packaged so as to fit into a small (2-inch-diameter) borehole. Analyzing the gamma ray spectrum due to neutron capture and inelastic scattering in the subsurface allows elements in the medium to be identified. Applications include oil and mineral exploration; detection of contraband; explosives, including land mines; and basic geological studies.

For Year 1 of the project we proposed to miniaturize the Berkeley Lab rf-driven ion source for use in neutron logging. It was expected that this ion source could increase the neutron flux over that of existing tubes by at least an order of magnitude. We also proposed to fabricate a large CdZnTe gamma-ray detector (≈ 2 cm^3) for use in the instrument. CdZnTe offers the advantages of higher efficiency per unit volume, better energy resolution, and better survivability than the NaI scintillator plus photomultiplier tube system used in most present neutron logging tools. Moreover, unlike germanium detectors, it operates at room-temperature.

Accomplishments

The goals set for the first year of this project have been met, and in some cases exceeded. The rf-driven ion source and its impedance-matching network were successfully miniaturized. Output current can be as high as 35 mA per pulse, in contrast to 1 mA for commercial sources. Characterization of the beam shows that it is 80 to 95% monatomic, as opposed to approximately 15% for commercial sources. This is important, since the nuclei which compose di- and triatomic particles will not be at optimum energy when they reach the neutron production target, thus compromising neutron production efficiency. With this high monatomic percentage and the high output current, the prototype is projected to produce a factor of two to three orders of magnitude more neutrons than commercial sources. This will decrease counting times and increase sensitivity and range of the instrument. It also provides the flux necessary for three-dimensional localization of detected substances, if this proves feasible.

Commercial neutron tubes have used the impact of deuterium on tritium (D-T) for neutron production. The deuterium-on-deuterium (D-D) reaction, with a cross section for production a hundred times lower, has not been able to provide the necessary neutron flux. The new source makes high flux D-D neutron sources feasible. This will greatly increase the lifetime of the neutron tubes, which is unsatisfactory at present. For field applications, it greatly reduces transport and operation safety concerns. For applications such as mine detection, where thermal neutrons are presently used, the use of the lower energy D-D neutrons (2.45, rather than 14, MeV) also would decrease the size of the neutron moderator.

A 1.5 cm $\times$ 1.5 cm $\times$ 1 cm CdZnTe detector with front end electronics was fabricated—the largest CdZnTe detector ever made using the coplanar grid collection technique developed at Berkeley Lab. This technique is the only known way to reach an energy resolution and efficiency level reasonable for our applications. A compact, sealed detector module containing the front end electronics and detector biasing network has been fabricated and tested. The output of the detector module interfaces directly with a portable amplifier/multichannel analyzer. Energy resolution of 3.1% full width at half maximum (FWHM) has been achieved at 1.33 MeV. This is slightly better than NaI. The limits on the energy resolution have been traced to non-uniform charge transport properties of the material. We believe that with better materials and further optimization of the coplanar grid electrodes, resolution of approximately 1% FWHM can be achieved. A

second CdZnTe crystal has been procured, and preliminary evaluation has shown that it also possesses some degree of non-uniformity. Further tests using the coplanar grid structure are needed to fully determine the detector performance.

Three-dimensional Monte Carlo calculations have enabled us to explore the advantages and deficiencies of the CdZnTe detector for this application, and the applicability of the neutron logging tool to problems other than its traditional applications. We have calculated the efficiency of the detector, and found it to be, per unit volume, three times higher than germanium or NaI at 2 MeV. Calculations also show that background from neutron capture by the cadmium of the detector can be reduced to insignificant levels by the use of a 0.5-cm-thick shield of B_4C around the detector. Using three-dimensional simulations that include the borehole and fractured or porous media of known composition, we have shown that neutron logging would be a very useful tool for locating non-aqueous phase liquids (NAPLs), which are widespread contaminants of DOE and non-DOE sites. The modeling also indicates that the tool will be able to trace the flow of water through ~1-mm-wide fractures if chlorine is added to the water.

We have enjoyed a highly successful collaboration among participants from three divisions at Berkeley Lab and the Nuclear Engineering Department at the University of California at Berkeley. We have drawn expertise from diverse fields (built up for other DOE activities) for future potential use in environmental assessment, mine detection, geological experiments involving flow through fractured media, and, possibly, oil exploration.

Publications

L.T. Perkins, C. Celata, Y. Lee, K.N. Leung, D.S. Picard, R. Vilaithong, M.C. Williams, and D. Wutte, "Development of a Compact, RD-Driven, Pulsed Ion Source for Neutron Generation," to be published in *Proceedings of 14th International Conf. on Applications of Accelerators in Research and Industry*, Denton, Texas, Nov. 6–9, 1996, AIP Press (1996).

C.M. Celata, R. Donahue, K. Leung, P.N. Luke, L.T. Perkins, P.T. Zawislanski, Ernest Orlando Lawrence Berkeley National Laboratory, and E. Greenspan and D. Hua, U.C. Berkeley, "A New Intense Neutron Generator and High-Resolution Detector for Well-Logging Applications," presented at the 1996 IEEE Science Symposium, Anaheim, California, Nov. 2–8, 1996, and submitted for publication (refereed) in the conference proceedings.

C.M. Celata, R. Donahue, K. Leung, P.N. Luke, L.T. Perkins, P.T. Zawislanski, Ernest Orlando Lawrence Berkeley National Laboratory, and E. Greenspan and D. Hua, U.C. Berkeley, "A New Intense Neutron Generator and High-Resolution Detector for Well Logging Applications," presented at the 3rd Annual Topical Conference on Industrial Radiation and Radioisotopes Measurement Applications, Rayleigh, North Carolina, Oct. 7–9, 1996.

A patent application on the miniaturized ion source will be submitted.

"Superbend"—A 5 T Bending Magnet Design for the ALS

Principal Investigators: Alan Jackson and Clyde Taylor

Project No.: 95002

Funding: $245,600 (FY96)
$292,500 (FY95)

Project Description

The Advanced Light Source (ALS) can be upgraded by replacing some of the gradient bend magnets with superconducting (SC) dipoles and adding extra quadrupoles to match the lattice functions. For operation at 1.9 GeV, the short dipoles (~4 T, operating at 1.5 GeV) can be ramped to ~5.1 T. These dipoles would provide bend-magnet synchrotron radiation with a critical energy of 6 keV, which is much better-suited to protein crystallography and other small sample x-ray diffraction and adsorption studies than what is currently available at the ALS. Figure 1(a) and (b) indicate the improved flux and brightness in the spectral range of interest (comparing the superbends with the normal ALS and Advanced Photon Source bends). We will design, build, and test a prototype magnet at the Advanced Photon Source to verify the concept. It is anticipated that, supported by ARIM funding, the changeover (ALS-II) could occur in FY97 if the concept is successful. The proposed design is unique; yet it would seem that similar magnets could be developed for other light sources and accelerators.

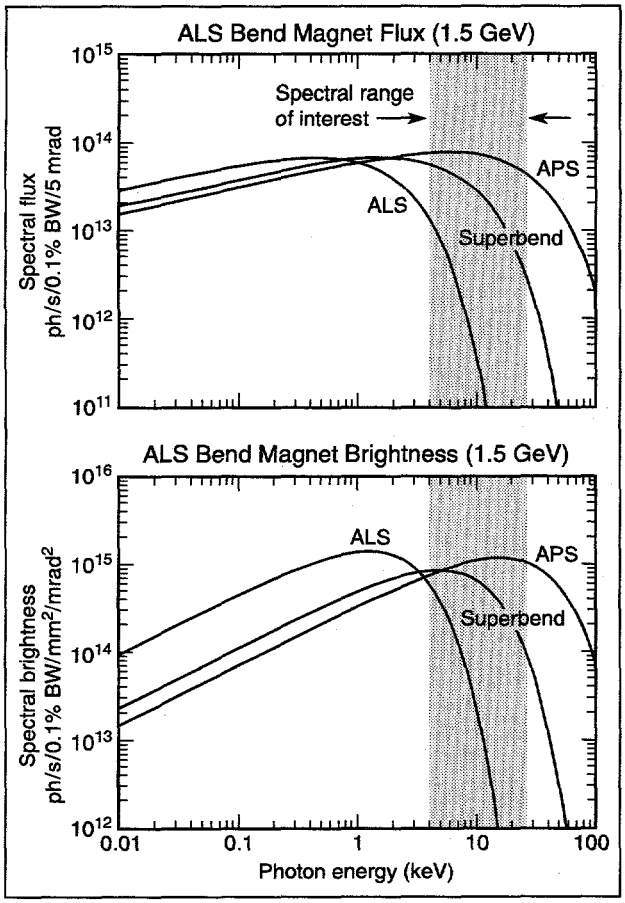

Figure 1. Flux and brightness of synchrotron light from the Superbend compared with normal bend magnet radiation at the ALS and Advanced Photon Source.

The C-shaped "cold iron" design has an "internal" pole-piece iron driven to about 5.5 T and a magnetic length of only ≈24 cm along the beam direction. The magnet (in its cryostat) must be installed around the existing ALS beam line. Since the magnet is very short, end effects are determined by the gap. To bring the pole faces as close together as possible, some material will be removed from the aluminum beam line walls at the bend locations. The magnet design will be reviewed by ALS staff and a prototype magnet will be constructed and tested. These results will be the basis for building three magnets for installation in ALS-II.

Accomplishments

In FY96, after having studied several designs the previous year, we had three coil sets built by Wang NMR, Inc., using surplus SSC superconductor wire and three different construction methods. All achieved the operating current required for 1.9 GeV operation. However, the critical current of these coils is much higher than was achieved after numerous quenches, and an additional operating current "margin" must be demonstrated before the coils can be considered qualified for operation in the ALS. Also, it appears that the coil does not recover from local instantaneous temperature "spikes" (probably caused by epoxy cracking). One potential solution, currently under investigation, is a magnet with a higher ratio of copper to superconductor and with rectangular wire for higher packing density. Figure 2 shows one of the coils of the SB 3 set. The coils are wound around a laminated iron pole and a 1-mm-thick layer of copper surrounds each coil for cooling purposes. The aluminum alloy ring provides radial structural support.

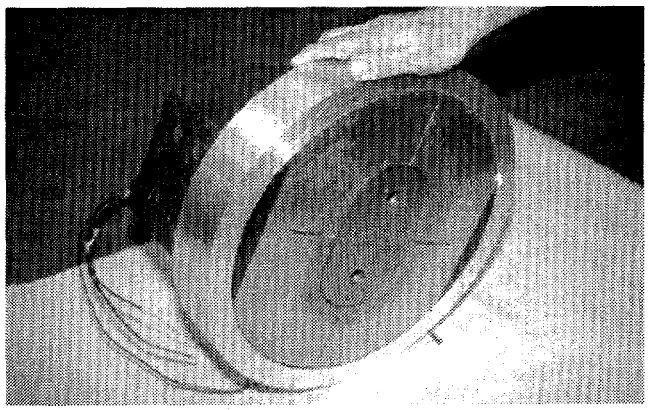

Figure 2. Photograph of one of a set of test coils (SB 3) with a 12 cm ×18 cm "racetrack" shaped laminated iron pole. The 20 cm I.D. ×3-cm-thick aluminum ring provides radial structural containment. The copper cooling plate is slotted to limit eddy currents.

Advance Towards the Next Generation of Pixellated Detectors for Protein Crystallography

Principal Investigators: Howard Padmore, Jacques Millaud, Thomas Earnest, and David Nygren

Project No.: 95010

Funding: $166,400 (FY96)
$293,700 (FY95)

Project Description

To develop fast x-ray area detectors for time-resolved and static crystallography, we pursue the massively parallel instrumentation of pixel detector arrays. This will lead to a large area detector technology with outstanding rate and dynamic range capability. The system will be capable of handling rates as high as 5×10^8 x-rays/s/cm^2. It will revolutionize time-resolved diffraction studies and significantly improve static crystallography studies currently based on CCD detectors.

The approach is to fabricate separate arrays of PIN diodes (pixels) and the instrumenting Application Specific Integrated Circuit (ASIC). The interconnections between the detector and the ASIC will use Flip Chip Technology. The resulting modules will be assembled in larger arrays.

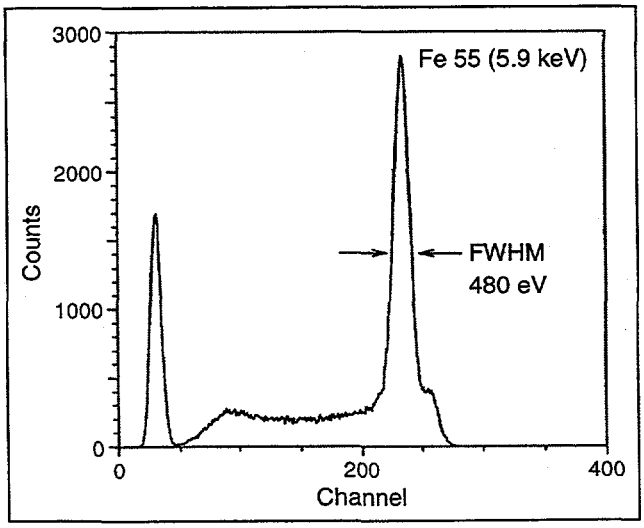

Figure 3. Output of a single pixel when irradiated with x-rays from a Fe55 source under the following conditions: bias voltage +80 V, temperature 25°C, detector 300-μm-thick Si, peaking time = 100 ns, and shaping time 1 μs.

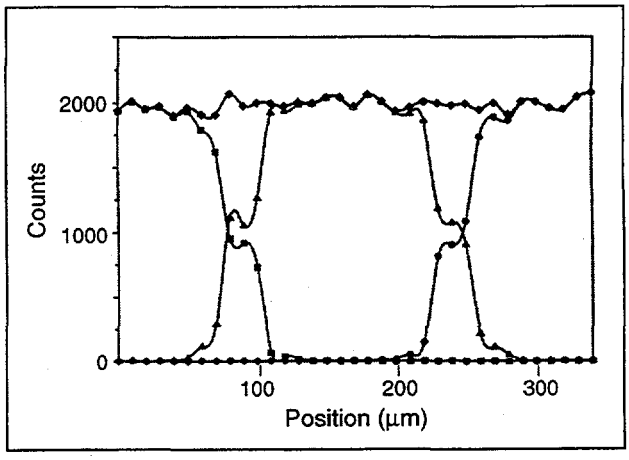

Figure 4. Response of adjacent pixels (Pixel 1, circles; Pixel 2, triangles; Pixel 3, squares; total, diamonds). Beam size for the test was 35 μm; pixel pitch, 150 μm. There is very little cross-talk between adjacent pixels.

Accomplishments

An 8×8 pixel array detector has been hybridized to a matching ASIC and an ASIC capable of instrumenting a 16×16 pixel array has been fabricated. The latter device shows full functional performance although the noise performance needs some adjustments. Parametric testing has identified the source of the excess noise. Solutions to the problem have been implemented and an enhanced design will soon be submitted to fabrication. Enhancements to eliminate or drastically reduce instantaneous current surges have been implemented in the column architecture. Advances in ASIC technology as well as in circuit design point to the feasibility of smaller pixels (~125 μm).

Systematic characterization of 8×8 array detector systems has provided results that confirm the superiority of the approach compared to imaging plates or phosphor screen/CCD detectors. In particular, the counting noise level of individual pixels is of the order of 0.01 counts/s above an energy level of 2 keV. Taking in account the maximum counting rate of 1 MHz, this indicates a maximum dynamic range of 10^8. Although it is likely that system noise will somewhat reduce this figure, it is clear that the dynamic range will remain far in excess of the 50,000 currently achievable with CCDs. Spatial resolution measurements using a rotating anode source, a 35 μm collimator and a micrometric stage show that the 8×8 array system could twice as good as a CCD detector.

Publications

E. Beuville, J-F. Beche, C. Cork, V. Douence, T. Earnest, J. Millaud, D. Nygren, H. Padmore, B. Turko, G. Zizka (Lawrence Berkeley National Laboratory); P. Datte and N-H. Xuong (University of California, San Diego), "A 16×16 Pixel Array Detector for Protein Crystallography," presented at the Conference on Pixellated Detectors, Bari, Italy, March 1996.

E. Beuville, J-F. Beche, C. Cork, V. Douence, T. Earnest, J. Millaud, D. Nygren, H. Padmore, B. Turko, G. Zizka (Lawrence Berkeley National Laboratory); P. Datte and N-H. Xuong (University of California, San Diego),"Photon Counting 2-D Smart Pixel Array Imager for Protein Crystallography," presented at the SPIE meeting, Denver, Colorado, August 1996.

N-H. Xuong, P. Datte (University of California, San Diego); E. Beuville, T. Earnest, J. Millaud, D. Nygren, H. Padmore (Lawrence Berkeley National Laboratory), "An Extremely Fast Direct Photon Counting Detector for Protein Crystallography," presented at the XVII Congress of the Int. Union of Crystallography, Seattle, Washington, August 1996.

Using Microdiffraction to Measure Local Strain in Microelectronic Devices

Principal Investigator: Howard Padmore

Project No.: 96028

Funding: $155,900 (FY96)

Project Description

This proposal was intended to enable the development of x-ray diffraction techniques on a microscopic scale. The primary use of such instrumentation will be to extend traditional measurements of stress in blanket thin films from large areas to ones less than a single grain in size.

Of particular importance is the application of microdiffraction to measurements of strain in microelectronic and micromagnetic devices. For example, in microelectronic devices, there are three main causes of strain:

1. Operational differential thermal expansion caused by dielectric and resistive heating.
2. Static differential thermal expansion caused by the encapsulation of Al-Cu interconnects in SiO_2 at elevated temperatures during fabrication.
3. Current induced "electromigration" stress.

In each case, it is important to be able to evaluate the thin film stress in smaller than grain sized areas. Our project centers around developing instrumentation to enable the measurement of strain in Al-Cu interconnect lines, and in W plugs used to connect individual interconnects at 1 micron spatial scale. It will also be applied to a wide variety of other thin film systems.

Accomplishments

The experimental geometry consists of a four-crystal (two-channel cut, double-bounce crystals) monochromator, followed by a Kirkpatrick-Baez (K-B) mirror pair. The monochromator is retractable from the beam, and allows switching from monochromatic to the white light Laue mode without moving the focused beam. The K-B mirror pair is designed to produce a 1 μm focus at the sample. The sample stage consists of a scanning system, a double rotation stage, and a system for moving the CCD camera. Most of the work so far has concentrated on two key elements of the system: K-B mirrors and beam diagnostics. These are discussed in detail below.

K-B Mirrors

To avoid aberrations, K-B mirrors have to be elliptical and fabricated to microradian tolerances. They also use a single layer Au coating for white light focusing, and so have to be relatively long to pick up a significant aperture at grazing incidence. We have pioneered the methods of strain-free mounting and application of controlled end couples with leaf springs that are required for accurate bending of flat substrates into an elliptical shape. We chose this route of controlled bending of flats, rather than the production of the required shape by grinding, because the required tolerances for the latter are well beyond the present state of the art. We can now achieve the required elliptical shape for a 160-mm-long mirror to microradian slope error tolerance. Focusing tests with x-rays are underway.

Beam Diagnostics

The mirrors are adjusted to high accuracy in our optical metrology laboratory. However, once installed on the beamline, they must be adjusted to the best point focus using a monitor of the x-ray spot size. Due to the number of adjustments, the measurement must be done in real time by an automated imaging system. The best way to do this is to convert the x-rays to visible light using a phosphor, and then image the spot using a large f-number microscope. Unfortunately, due to the great penetration depth of high energy x-rays into the phosphor material, the phosphor must be grown as a thin layer, only a few microns thick, to avoid image blurring. The imaging system is complete and under test, and we are testing thin epitaxially grown films as well as laser-ablated thin films.

Finally, the complete system components are designed and in fabrication, and we hope to start testing with model samples soon.

Publications

H.A. Padmore, M.R. Howells, S. Irick, T. Renner, R. Sandler, Y-M Koo, "Some New Schemes for Producing High Accuracy Elliptical X-ray Mirrors by Elastic Bending," *SPIE* **2856**, 145 (1996).

Spin Polarized Photoemission Studies of Magnetic Surfaces, Interfaces, and Films

Principal Investigator: Neville Smith

Project No.: 94027

Funding: $200,200 (FY96)
$409,900 (FY95)
$124,300 (FY94)

Project Description

The principal objective of this project, namely, to introduce techniques of spin-polarized photoemission and magnetic circular dichroism at the ALS, has been accomplished. An electron spin analyzer has been installed on the photoemission system of Beamline 9.3.2 and the experimental program is about to begin. Circularly polarized x-rays are being generated on Beamline 7.0 using a quarter-wave retarder of the transmission multilayer type. Preliminary experiments in magnetic circular dichroism in photoemission from Gd have already been performed.

Accomplishments

Spin-Polarized Photoemission

A decision was made quite early on to go with the "MicroMott" design philosophy. A collaboration was established with UC-Davis and Florida State University, and Professor David Lind of FSU manufactured the spin analyzer under contract to Berkeley Lab. The analyzer was attached to the detection end of the Scienta photoemission analyzer operated on Beamline 9.3.2 by Professor Charles Fadley of UC-Davis. The first spin-polarized photoemission spectra should be obtained soon.

Figure 5 shows a schematic of the MicroMott detector. The basic principle is to accelerate the electrons emerging from the Scienta energy analyzer and bombard them into a gold foil. From the asymmetry in

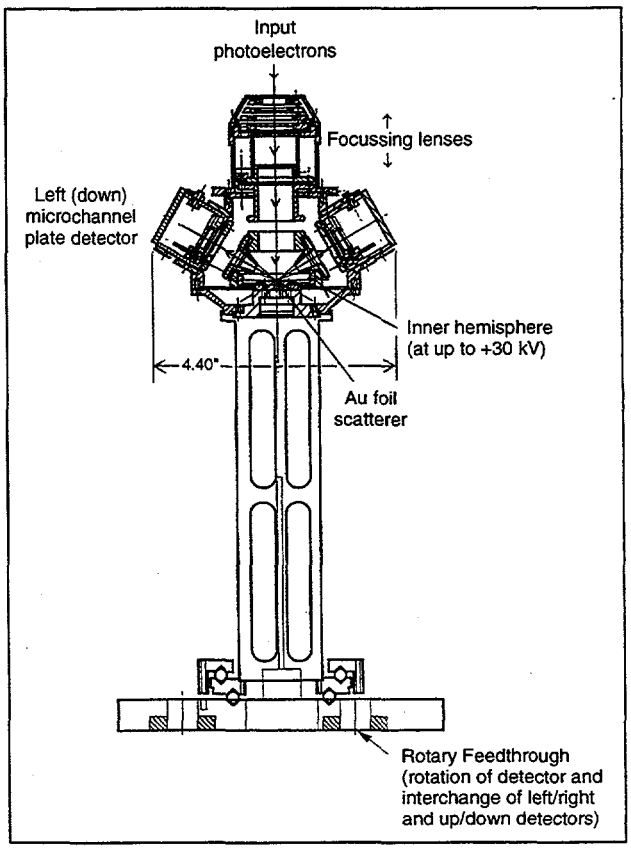

Figure 5. Schematic of the MicroMott spin analyzer installed on Beamline 9.3.2 at the Advanced Light Source.

backscattering, monitored using microchannel plates, spin polarization of the incoming beam can be deduced. The detector is mounted on a differentially pumped rotary feedthrough that permits interchange of left/right and up/down detectors. Another mechanism permits interchange of the spin detector with a multidetector for high performance in the spin-integrated mode.

Circularly Polarized X-rays

A quarter-wave phase shifter of the transmission multilayer type has been designed, built, and installed on Beamline 7.0. This work was done in collaboration with Dr. Jeff Kortright of LBNL/MSD.

The principle of the phase shifter is shown in Fig. 6. A multilayer film composed of suitable materials (Mo/Si) with a suitable periodicity will induce a phase change between s- and p-polarized radiation that can be arranged to be 90 degrees. A mechanism incorporating all the desired angular degrees of freedom has been constructed and installed in an appropriate 1-meter section of Beamline 7.0. Tests of the phase shifter, also shown in Fig. 6, are seen to be excellent.

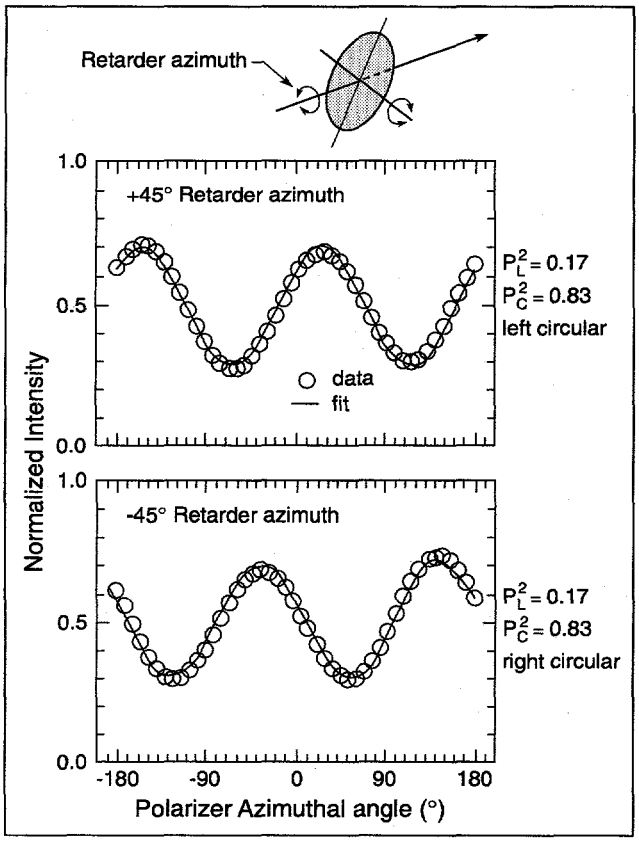

Figure 6. Geometry and performance of the transmission multilayer phase retarder installed on Beamline 7.0.1 at the Advanced Light Source.

Some preliminary experiments have already been done with this instrument. Circular dichroism has been observed in photoemission from a Gd film. It is anticipated that there will be a demand for this capability from the users of the ultraESCA chamber on Beamline 7.0. These include James Tobin (LLNL), Roy Willis (Penn State), Z.-Q. Qiu (UC-Berkeley), among others.

Magnetic circular dichroism offers a contrast mechanism in x-ray microscopy. The M edges of the elemental ferromagnets (Fe, Co and Ni) fall within the operating photon energy range of the transmission multilayer phase retarder. We therefore plan to perform magnetic spectroscopy experiments using the STXM and SPEM microscopes on Beamline 7.0.

Technology for an International Proton Collider at High Energy and Luminosity

Principal Investigator: William Turner

Project No.: 95001

Funding: $150,800 (FY96)
$206,000 (FY95)

Project Description

The purpose of this project was to develop design approaches and fabrication techniques for applying Berkeley Lab (LBNL) accelerator technology expertise to possible U.S. participation in the construction of the Large Hadron Collider (LHC) at CERN. An international co-operation agreement between CERN and DOE is now in place and an interim implementing arrangement detailing the contributions of the DOE laboratories is nearing completion. In addition to LBNL, the other participating laboratories are BNL and FNAL. According to the implementing arrangement, the U.S. laboratory contributions will focus on the Interaction Regions (IRs) and radio frequency (rf) straight section. LBNL's specific responsibilities will include design and analysis of high gradient superconducting quadrupoles; fabrication of superconducting cable; design and fabrication of cryostats and collimators for the IR quadrapoles; and design and fabrication of neutral particle absorbers for the

IRs. The LHC is scheduled to be completed in the year 2005. In FY95-96, we developed and clarified our technical role in support of the U.S. LHC accelerator collaboration.

Accomplishments

During FY96, conceptual designs and analysis of the beam tube vacuum system were worked out for the approximately 4 km of ambient temperature straight insertions of the LHC. It was not possible to include all of this within the scope of the final implementing arrangement. However, the neutral dumps and quad collimators in the two high luminosity IRs were included in this work and remain as part of the project.

During FY96, the main technical task in the Superconducting Magnet Program was the design of a high gradient quadrupole for the LHC interaction regions. This was a collaborative effort: the original magnetic design and the superconducting cable design work was done by Berkeley Lab, while the mechanical and thermal design was done by FNAL. The U.S. team is proposing a two-layer quadrupole made from existing SSC strand, with 15-mm-wide cable, in contrast to a four-layer, narrow cable design that is being proposed by KEK in Japan (Fig. 7). At this time, CERN is encouraging both teams to carry their design through the prototype stage and then, if the designs meet the CERN operating requirements, to build quadrupoles for two interaction regions each. The main technical challenges of the two-layer design are first, fabricating high aspect ratio cable, and then, winding coils with this cable. Both inner and outer layer cables were successfully made at LBNL. This cable was then sent to FNAL for coil winding tests, also successful. In October 1996, we made enough inner layer and outer layer cable for the first prototype quadrupoles, which will be built and tested at FNAL during FY97.

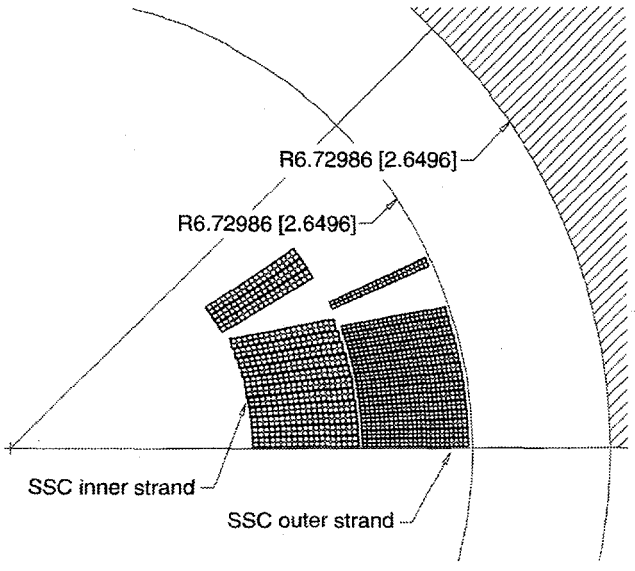

Figure 7. A two-layer IR quad using SSC wire.

Seven publications reporting results were completed. A collaboration between LBNL, FNAL, and BNL reported progress on the design of a high gradient IR quad, which achieved a maximum gradient exceeding the required 250 T/m with a two-layer coil. A second publication reported on the design, fabrication and testing of the wide (15.4 mm), high-aspect-ratio (~13.4) superconducting cable required for this design. Coil fabrication methods being worked out indicate that the inner and outer coils can be fabricated from the same high-aspect-ratio cable with minimal degradation of critical current. Additional related work was done to test the performance of existing FNAL quadrupoles at the superfluid He temperature where the LHC IR quads will operate. Two publications dealt with beam tube vacuum in large hadron colliders. One of them extended the theory of ion desorption stability to the cold, cryosorbing beam tube temperatures of the LHC. The cold beam tube of LHC was found to have a rather large safety margin for ion desorption stability. The second vacuum paper dealt with conditions in the next generation of hadron colliders beyond LHC.

Publications

J.D. Adam, D. Leroy, L.R. Oberli, D. Richter, M. Wilson, R. Wolf, H. Higley, A. McInturff, R. Scanlan, A. Nijhuis, H. ten Kate, and S. Wessel, "Rutherford Cables with Anisotropic Transverse Resistance," presented at the 1996 Applied Superconductivity Conference, Pittsburg, Pennsylvania, August 25–30, 1996.

R. Scanlan, A. McInturff, C. Taylor, S. Caspi, D. Dell'Orco, H. Higley, S. Gourlay, R. Bossert, J. Brandt, and A. Zlobin, "Design and Fabrication of a High Aspect Ratio Cable for a High Gradient Quadrupole Magnet," LBL-38307 (1996).

A. Lietzke, A. McInturff, R. Scanlan, R. Bossert, S. Feher, S. Gourlay, M. Lamm, P. Limon, F. Nobrega, J. Ozelis, and A. Zlobin, "Superfluid Performance of Tevatron IR Quad Heaters," LBL-38310 (1996).

R. Bossert, S. Feher, S. Gourlay, T. Heger, J. Kerby, M. Lamm, P. Limon, P. Mazur, T. Nicol, F. Nobrega, D. Orris, J. Ozelis, T. Peterson, P. Schlaback, J. Strait, J. Tompkins, A. Zlobin, A. Lietzke, A. McInturff, and R. Scanlan, "Tests of Fermilab Low Beta Quadrupoles," presented at the 1996 Applied Superconductivity Conference, Pittsburg, Pennsylvania, August 25–30, 1996.

R. Bossert, S. Gourlay, T. Heger, Y. Huang, J. Kerby, M. Lamm, P. Limon, P. Mazur, F. Nobrega, J. Ozelis, G. Sabbi, J. Strait, A. Zlobin, S. Caspi, D. Dell'Orco, A. McInturff, R. Scanlan, J. Van Oort, and R. Gupta, "Development of a High Gradient Quadrupole for the LHC Interaction Regions," presented at the 1996 EPAC Conference, Barcelona, Spain, May 1996.

W.C. Turner, "Ion Desorption Stability in Superconducting High Energy Physics Proton Colliders," *J. Vac. Sci. Technol.* **A14**, 2026 (1996).

W.C. Turner, "Beam Tube Vacuum in Low Field and High Field Very Large Hadron Colliders," *Proceedings of 1996 DPF/DPB Summer Study on New Directions for High Energy Physics*, Snowmass, Colorado, June 24 – July 12, 1996.

Chemical Sciences Division

Network Silicates With Porphyrin Backbones: Novel Solids and Catalysts

Principal Investigator: John Arnold

Project No.: 96003

Funding: $79,600 (FY96)

Project Description

The ability of chemists to control chemical and physical properties on the molecular scale has been the major driving force in synthetic chemistry over the last hundred years. It is only quite recently, however, that attention has been focused on more complex *supramolecular* systems, where small molecules are employed as templates for the synthesis of complex two- and three-dimensional framework structures. We intend to lead this research into a new area of study by fabricating robust arrays incorporating porphyrin backbones, held together by strong siloxane linkages built using sol-gel chemistry. If this approach is successful it will lead to a new class of materials, engineered by molecular chemistry to control structural relationships and pore sizes.

In concert with the idea of building new supramolecular compounds, a second aspect of this work will apply this chemistry to the preparation of new heterogeneous porphyrin-based catalysts for alkane oxidation and olefin epoxidation. Over the years, numerous models have been prepared in attempts to mimic enzyme active sites, such as those in cytochrome P-450. To prevent degradation of the catalytically active site, nature employs protein sheaths to control the local environment. We propose to exert similar control by building frameworks using the chemistry described herein. Since they are based on molecular chemistry, these systems combine the attractive features of both homogeneous catalysts (mainly "tunability" and control of the catalyst center) with those of solid-phase heterogeneous catalysts, such as aluminosilicates. This synergism between homogeneous and heterogeneous catalysis may result in the development of a new range of highly selective, environmentally benign catalysts.

In addition to the catalytic potential of these compounds, we envisage a number of other interesting applications, including potential uses as sensors, large-pore molecular sieves, and magnetic and conducting solids.

Accomplishments

We have made excellent progress toward the synthesis of porphyrin monomers and will be in a position to test the first of the proposed polymerization reactions shortly. Several different strategies are being investigated, as illustrated in Schemes 1 through 3 below. The first of these is to develop

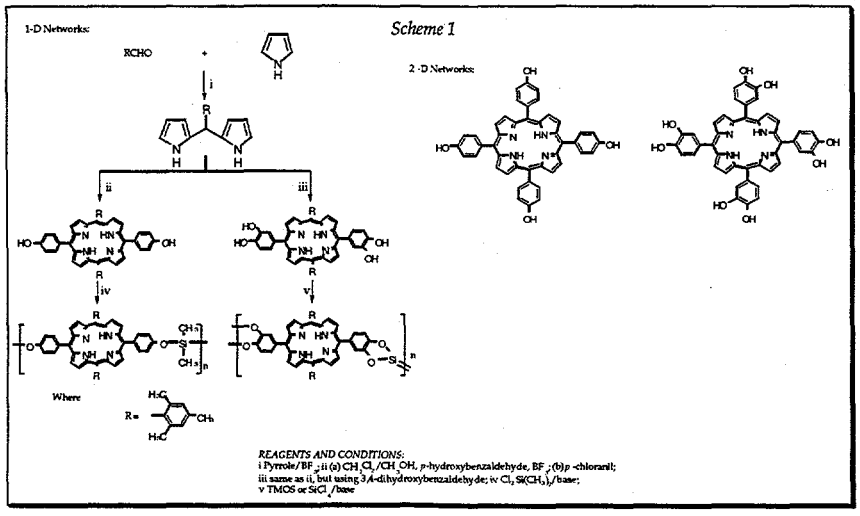

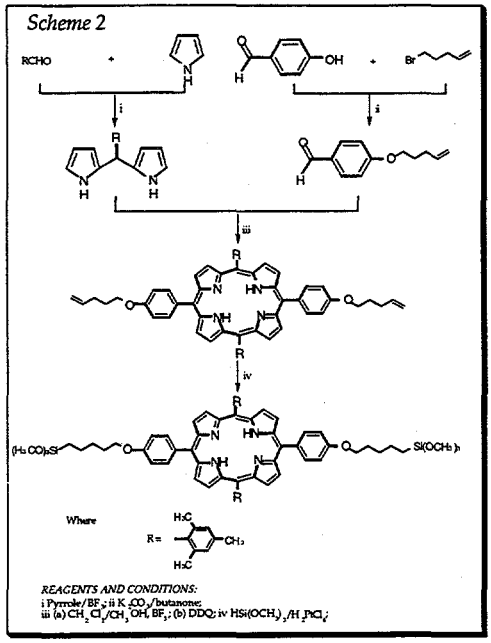

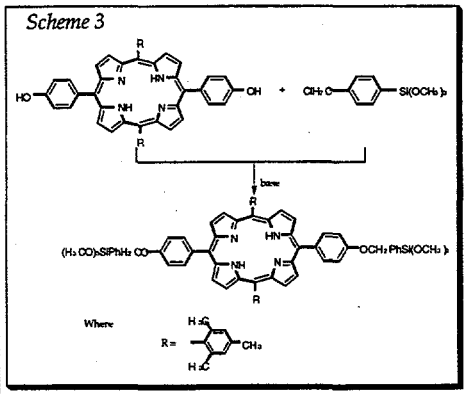

a one-dimensional model system to identify the most efficient polymerization route, which will then be applied to more complex two- and three-dimensional structures. In the process, we are discovering a wealth of new porphyrin chemistry and have prepared a number of interesting and novel molecules.

The above results are encouraging as they demonstrate that a high degree of functionality is possible in network structure building blocks. The ability to control such functionality will become increasingly important as we begin to assemble solid structures, where they will influence factors such as solubility, rates of polymerization, and pore size. We will continue to look for new ways to assemble functionalized porphyrins and for new methods to oligomerize and polymerize these monomers during the course of the project.

Publications

Qing Min Wang and John Arnold, "Design and Synthesis of One-Dimensional Metalloporphyrins," (tentative title) in preparation.

Molecular Theory Center

Principal Investigators: David Chandler, Martin Head-Gordon, and William Miller

Project No.: 96030

Funding: $ 69,000 (FY96)

Project Description

The simulation of chemical reactions of isolated reactants has become, to a great degree, commonplace in chemical theory. Typically, such simulations consist of the computation of a potential energy surface for the reaction and a classical trajectory or variational transition state approximation calculation of the reaction rate. However, much of the most important, and at the same time least-well-understood, chemical reactions occur in solution, or in the presence of heterogeneous environments, where the environments also undergo chemical change. We propose developing

and demonstrating the capability to simulate long time scale reactions in liquids based on a combination of new methods of computational statistical mechanics and ab initio density functional theory for electronic structure. We also propose developing and implementing an effective and practical semiclassical treatment of reaction dynamics coupled to many nonreactive degrees of freedom in a complex system. These developments will be applied collectively to simulate the prototypical problem of dissociation of a weak acid in water. This problem, and the many classes of reactions that will subsequently become accessible to simulation, becomes solvable only with access to the most powerful computers. Hence the program will evolve with the ever-changing technology made available for the project by NERSC.

Accomplishments

Directed Paths

The dynamics of complex systems in the molecular domain poses a challenge because the number of possible transition states grows exponentially with the dimensionality of the system. Our work addresses this problem by developing algorithms for the efficient computation of dynamical pathways connecting reactants and products in high-dimensional systems. We have derived a weight for directed paths and implemented corresponding Monte Carlo methods based on polymer sampling. During the last six months, we have refined the directed path algorithms by applying the directed path method to the problem of hydrogen-bond breaking in liquid water; we obtain the profiles of structure and energy averages along the trajectory. Our preliminary results show that along with the expected librational motion, hydrogen bonds break with an increase in the separation between the bonding waters. We are also working on the dynamics of ion dissociation in water. For the future, we will work on the pathways of water deprotonation. The self-deprotonation of water is a fundamental process in chemistry and molecular biology. The reaction leads to a change in electronic structure, which makes it necessary to couple the path sampling algorithm with the ab initio methods of quantum chemistry.

Direct Density Matrix Solvers in Electronic Structure Theory

Within electronic structure theory, we have made significant progress on two problems over the last six months. First, we have developed and implemented new methods for direct solution of the density matrix within density functional theory calculations, entirely based on spatially localized quantities. This carries two promising advantages: first, that sparsity can be exploited directly to make calculations on very large molecules much more feasible, and second, that by avoiding diagonalization we have a method which can be much more efficiently parallelized. The second area of progress is in performing Ewald summations within electronic structure calculations using local basis functions. We are in the process of implementing linear scaling solutions to the Ewald sum problem that are fully compatible with our existing linear scaling methods for treating the Coulomb interactions of electrons in isolated molecules. In addition to its intrinsic value, this work will form the basis for direct use of electronic structure methods in conjunction with the statistical mechanical techniques discussed above.

Semiclassical Methods

The third general area has been the development of semiclassical theory for the accurate computation of quantum dynamics, with the long-term goal of treating large molecular systems. Recently, we have calculated photodetachment intensities within the Franck-Condon approximation for a model two-dimensional problem (collinear H3) using a semiclassical approximation to the Green's function where the phase space average is calculated efficiently by running the trajectories in parallel on a T3D computer. Good agreement with exact quantum results is observed. Ongoing work involves calculating state-to-state reaction probabilities using similar semiclassical methods. Progress has also been made in the calculation of the thermal rate constants for chemical reactions and recombination events. These rates can be obtained directly, i.e., without reference to state-selected quantities, yet correctly (without inherent approximation) by means of the flux-flux autocorrelation function.

The bottleneck in these computations is a sparse-matrix multiplication scheme for which implementation on a massively parallel machine such as the T3D or T3E provides large savings in computational time. The method will therefore be applied to challenging systems such as $H + O_2$ which involves both reaction (to give OH + O) and recombination (to give stable HO_2).

Publications

M. Head-Gordon, C.A. White, P. Maslen, and M.S. Lee, "The Tensor Properties of Energy Gradients Within a Nanorthogonal Basis Set," in preparation.

F. Csajka, J. Marti, and D. Chandler, "Pathways Between Stable States in Complex Systems. Application to Hydrogen Bond Dynamics in Water," in preparation.

J. Marti, F. Csajka, and D. Chandler, "Pathways of Ionic Pair Dissociation in Water," in preparation.

Magnetic Properties and Electron Localization at Interfaces

Principal Investigator: Charles Harris

Project No.: 95003

Funding: $ 98,300 (FY96)
$116,200 (FY95)

Project Description

We endeavor to study magnetic properties and the spatial extent of electrons at scientifically and technologically interesting interfaces. Recent advances in Ti:sapphire laser technology and nonlinear optics have enabled us to study magnetic interfaces. High-resolution, time- and angle-resolved two-photon photoemission (TPPE) is being used to determine the spatial extent, band structure, tunneling and carrier dynamics, and magnetic splittings of electrons localized at atomically thin interfaces. Important nanometer scale structures under investigation include magnetic thin layers, metal-semiconductor junctions, and metal-polymer interfaces. The unifying theme of this work is the study of the unoccupied electronic states at interfaces where these excited states control the electronic and magnetic dynamics and/or serve as sensitive probes of important interface physics.

Thin film magnetism and layered magnetic materials are important areas of research for magnetic storage devices, nanotechnology, and the two-dimensional physics of highly correlated systems. Interface and low-dimensionality effects may dominate the physics in these systems and yield new phenomena. Magnetic coupling across ultrathin layers can induce magnetism in the substrate and adsorbate or induce magnetically dead layers in the overlayer. Potentially useful giant magnetoresistance effects have been observed in multilayer metal-on-metal systems.

The first area of study is metal-polymer interfaces. These interfaces have become technologically relevant junctions due to successful initial work on polymer LEDs (light emitting diodes) and batteries. Since metal-polymer contact is an integral feature of this class of devices, interface conduction bands form a crucial part of the electrical pathway through the device. An understanding of the band structure at the metal-polymer interface and the coupling between interface and metal states is crucial to modeling current-voltage characteristics. We will attack these problems by studying model metal-polymer junctions where the overlayers are various single- and double-bonded hydrocarbons. By studying the conduction band structure of the interface as a function of overlayer chain length, branching, and electronic structure, we will derive general principles for understanding the electronic states at metal-polymer interfaces. Important aspects to be addressed include electron localization and tunneling lifetimes.

Second, metal-semiconductor junctions comprise an important class of interfaces in microelectronics. Almost all work in the literature on such junctions concerns metal layers on semiconductor substrates. Very little research has been done for semiconductor layers on metal substrates. The TPPE techniques developed in our laboratory are uniquely suited to study the excited electronic states, including dependence on magnetic spin, and dynamics of atomically thin semiconductor layers on metal substrates. Localization effects may also be observed at these interfaces.

Third, we are investigating coherence and quantum beats in TPPE spectroscopy of interfaces. Coherence effects, which are related to the quantum-mechanical description of the interaction of light and matter, are present in time-resolved TPPE. Coherence is important in itself because it is intimately tied to the fundamental interaction of light and matter. It also complicates studies of the very short time behavior witnessed in TPPE. Quantum beats are due to

quantum-mechanical interference between closely-spaced energy levels. From studies of beat frequencies, detailed information on energy spacing and dynamics can be obtained.

Accomplishments

In FY96, we continued the development of femtosecond time-resolution in TPPE spectroscopy of metal substrates and at interfaces, with particularly important advances in the theoretical description of femtosecond electron dynamics. We have analyzed new interfacial systems and developed new approaches to TPPE spectroscopy and data analysis. The application of novel experiment and theory has proven important in furthering our understanding of the nature of coherence, momentum relaxation, quantum beats, quantum size effects, and localization by means of two-dimensional polarons. The increased wavelength range and ultrafast time-resolution of the current apparatus, in conjunction with good angle and energy resolution, have given us the capability to explore these issues.

A significant advance in the work on metal-polymer interfaces has resulted from the study and theoretical interpretation of two-dimensional localization of electrons at metal-alkane interfaces through electron localization time and momentum dependence measurements. The decay of delocalized electrons into the localized state as a function of energy is shown in Fig. 1. We have deduced key portions of the mechanism of localization: the initially delocalized electron decays within a few hundred femtoseconds to the two-dimensional small polaron localized state by means of a self-trapping mechanism that can be modeled as an activated barrier crossing. The localized electron then decays back to the metal on a time scale associated with tunneling through the potential barrier presented by the alkane layer to the metal. The quantitative model we have developed identifies the phonon mode of the overlayer responsible for self-trapping, the reorganization energy of the overlayer molecular lattice, and the energy levels involved. These data results point toward the development of a general theory connecting electron mobility (transport property) and effective mass (band structure) in low-dimensional molecular solids.

In the second area, of metal-semiconductor junctions, we studied the femtosecond dynamics of interfacial quantum well states in rare gas films on metal substrates, which serve as experimentally accessible model system semiconductor quantum wells. These experiments allowed us to follow the dynamics of excited charge carriers at a quantum well interface as a function of the quantized momentum parallel and perpendicular to the interfacial plane. By analyzing the carrier dynamics (Fig. 2) at a series of coverages and angles for the Xe/Ag(111) system, we have determined the dynamics of carriers over a sizable portion of the three-dimensional conduction band structure of Xe. We have developed a simple quantum-mechanical theory that qualitatively

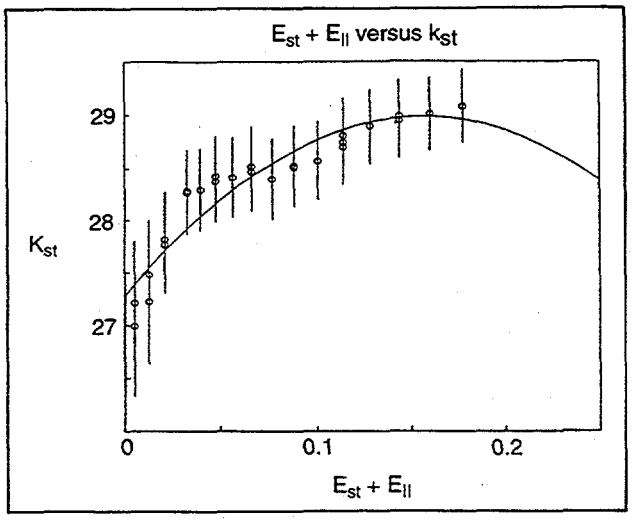

Figure 1. The trapping rate into the localized state for a bilayer of n-heptane on Ag(111) as a function of energy. This plot is a measure of the barrier to localization.

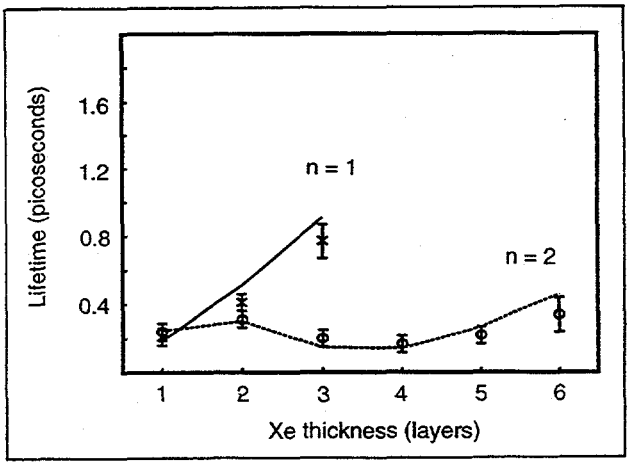

Figure 2. The dynamics of the n = 1 and n = 2 quantum well states of multiple atomic layers of Xe on Ag(111) and comparison to quantum-mechanical model.

accounts for the dynamics as a function of layer thickness and quantum number. These experimental results, conjoined with theory, have contributed to a fundamental understanding of carrier dynamics at interfaces and of the relationship between quantum well electronic structure and bulk band structure.

Experiments on coherence and quantum beats between excited electrons in the higher image potential states are providing important information on two fronts. First, the knowledge gained will benefit studies of magnetic interfaces: these experiments provide a means of studying those small exchange splittings between closely spaced levels that are likely to occur in the conduction bands of many magnetic interfaces. Second, these experiments are enabling us to study electron lifetimes on metal surfaces in the case where the surface state is degenerate with metal bulk bands for bare Ag(111). This is a much more realistic approximation to practical interfaces grown on a metal substrate than can be found in studying interface states in a projected band gap. We should be able to test models of the coupling between interface electronic states and substrate bands that are relevant to metal-polymer device physics.

Publications

R.L. Lingle, Jr., N.-H. Ge, R.E. Jordan, J.D. McNeill, and C.B. Harris, "Femtosecond Studies of Electron Tunneling at Metal-Dielectric Interfaces," *Chem. Phys.* **205**, 191 (1996).

J.D. McNeill, R.L. Lingle, Jr., R.E. Jordan, D.F. Padowitz, and C.B. Harris, "Interfacial Quantum Well States of Xe, Kr Adsorbed on Ag(111)," *J. of Chem. Phys.* **105**, 3883 (1996).

N.-H. Ge, R.L. Lingle, J.D. McNeill, C.M. Wong, and C.B. Harris, "A Time-Resolved Study of the Two-Dimensional Localization of Electrons at Interfaces," in preparation.

J.D. McNeill, R.L. Lingle, Jr., N.-H. Ge, C.M. Wong, and C.B. Harris, "Dynamics of Conduction Band Derived Quantum Well States of Xenon," in preparation.

C.M. Wong, K. Gaffney, R.L. Lingle, Jr., C.B. Harris, "Quantum Beats in the Dynamics of Image States on Ag(111)," in preparation.

Computing Sciences Departments

High Fidelity Simulation of Diesel Combustion

Principal Investigators: John Bell, Nancy Brown, Phillip Colella, and Michael Frenklach

Project No.: 96029

Funding: $ 99,900 (FY96)

Project Description

The design of large diesel engines, such as those used for power generation and for locomotives, is a costly and time-consuming process. A key issue is the tradeoff soot formation and the formation of other pollutants such as NO_x. A computational tool that could accurately model the combustion process in a diesel engine would dramatically reduce costs and enhance the ability of engine designers to improve engine design.

Combustion in a diesel engine is a combination of several complex processes. The fuel is injected in a liquid spray that breaks into droplets and is vaporized. A complete description of the kinetics requires hundreds of species and thousands of chemical reactions. The kinetic process produces soot whose effect on the flow and heat transfer must be modeled. All of these processes occur in an unsteady, fully turbulent flow in a complicated, moving geometry. The full complexity of the underlying physics makes a direct numerical simulation intractable. Our approach will be to model the overall process using high-resolution modeling of the fluid dynamics in a realistic three-dimensional geometry with reduced kinetics mechanisms for droplets and soot. In addition, we will use detailed computational studies of the individual submodels to validate their appropriateness and to calibrate them for use in a full-physics cylinder model.

Accomplishments

We have focused our research efforts on developing modeling capabilities for several components required for modeling diesel engines. We have begun the extension of our adaptive methodology for low Mach number flows to complex engineering geometries. The representation of the geometry in the algorithm is based on a hybrid of the embedded boundary approach developed by Berkeley Lab's Center for Computational Science and Engineering with a conservative component grid algorithm. In this approach, the geometry of the cylinder walls is modeled using a curvilinear body-fitted mesh. This outer mesh is merged with an inner rectangular mesh using a front-tracking algorithm to guarantee conservation at the grid boundaries. The geometry of valves and the motion of pistons are represented as interfaces moving through the fixed, two-component grid systems. During FY96, we completed the initial design of the C++ software infrastructure that is required to represent engineering geometries in this framework and implemented it for problems on a single grid. We are also developing the basic numerical algorithms for solving linear systems on these types of grids.

As well, we are developing computational tools to model coagulation and growth of soot particles in hydrocarbon combustion. A Monte-Carlo simulation is being implemented in C++ to analyze the ballistic model of particle cluster formation. The code is designed to allow simulation of both aggregation and surface growth to occur simultaneously. This has not been studied in the past, but it is of critical importance for predictive modeling of soot formation in practical combustion devices such as diesel engines.

During the reporting period, the first part of the code was completed, which allows simulation of particle aggregation from uniformly distributed spheres. Clusters with up to 20,000 primary particles were constructed. The fractal dimensions obtained in these simulations compare well to the literature.

We are assembling a chemical kinetic mechanism for the oxidation of heptane as a first step in developing a complete mechanism for diesel combustion. To date, three mechanisms have been collected from various groups that specialize in studying combustion chemistry. The mechanisms were constructed using principles established for comprehensive reaction mechanisms, where they are built sequentially upon established sub-mechanisms for simpler fuel molecules. They also consist of empirical reaction rate parameters for reactions that are not yet measured or calculated. Initially, the kinetic schemes are analyzed

using a one-dimensional, laminar, premixed flame code developed at Sandia. The results are then compared to existing experiments. Sensitivity and reaction rate analyses are performed to determine which reactions are critical to the system, and what the principal path of heptane oxidation is, respectively. Once the mechanisms are tested and validated, the chosen mechanism will be reduced by invoking steady state assumptions for intermediate species. This simplified scheme will again be tested against the detailed mechanism so that results are consistent. It will then be incorporated into the soot mechanism we are developing. The final product, describing heptane chemistry complete with a soot submechanism, will then be coupled to the fluids code.

Finally, we have begun a collaboration with the Engineering Research Center at the University of Wisconsin to study spray modeling. Our initial target is to couple R. Reitz's spray model to our adaptive mesh algorithm. It has been conjectured that one of the major limitations in spray modeling is inadequate resolution of the gas phase flow in a neighborhood of the spray. Our goal is to use adaptive mesh refinement to accurately resolve the gas flow and assess the effect on spray modeling.

Characterization and Monitoring of Subsurface Biologic Activity Using Stable Isotope Soil Gas Analyses

Principal Investigators: Mark Conrad, Terrence Leighton, and Bob Buchanan

Project No.: 94003

Funding: $49,600 (FY96)
$82,400 (FY95)
$78,400 (FY94)

Project Description

In situ bioremediation of petroleum hydrocarbon compounds presents a promising alternative to costly "pump and treat" or "burn and bury" techniques that are commonly employed to remove hydrocarbons from contaminated groundwater and soils. Subsurface microbial activity can completely convert toxic hydrocarbon compounds to harmless by products (CO_2, H_2O, etc.) without significant site disturbance or potential for human exposure. However, major difficulties are associated with monitoring the effectiveness of *in situ* bioremediation efforts and determining how these processes can be optimized. Currently available techniques for this purpose involve analyzing the effects of subsurface biologic activity in samples collected from boreholes. Disadvantages of drilling to monitor bioremediation include high cost and site perturbation. In addition, subsurface heterogeneity can significantly compromise the accuracy of borehole data.

Bacterial degradation of petroleum hydrocarbons results in the production of compounds such as CO_2 and CH_4 in soil gases and HCO_3^- in groundwater that can be used to monitor *in situ* microbial activity. There are, however, other sources for these compounds besides subsurface bacterial activity (e.g., root respiration, dissolution of soil carbonates, atmospheric contamination). In addition, bacteria have other substrates to choose from besides contaminants (e.g., soil organic matter). In order to identify the sources of compounds, we use measurements of their isotopic compositions. For many microbial byproducts, there are large differences in the isotopic compositions of compounds produced from bacterial degradation of hydrocarbons and those produced from other substrates, such as soil organic matter. The utility of stable isotope data is limited, however, by a lack of knowledge about the effects of bacterial metabolic activity on the stable isotopic compositions of substrates and byproducts. Most physical, chemical, or biologic processes cause shifts in the isotopic compositions of the materials. The magnitudes of these fractionation effects for processes such as carbonate dissolution or plant respiration have been carefully determined by researchers working in other fields such as botany and oceanography. The importance of bacterial processes in natural systems has only recently been realized, and, as a result, little work has been done in this area.

Accomplishments

The purpose of this project has been twofold:

- to demonstrate the applicability of isotope monitoring at a contaminated site
- to quantify isotopic fractionation effects caused by microbial metabolic processes.

The field demonstration was completed during prior years (leading to several externally funded projects), and research during FY96 was concentrated on fractionation studies.

One series of experiments was run to complete work begun earlier that measured carbon isotope fractionation during microbial metabolism of glucose. Glucose is generally considered a good analog for natural soil organic matter. The earlier work concentrated on shifts in the $\delta^{13}C$ values of CO_2 produced during degradation of glucose and metabolic intermediates (e.g., glycerol, acetate, citrate) by two well-characterized soil bacterium, *Bacillus subtilis* and *Pseudomonas putida*. The culture media used for the previous experiments, however, contained Na-MOPs salt and tricine to buffer the pH of the solutions. Both of these compounds contain carbon, which made it impossible to accurately measure the isotopic composition of the residual substrate and soluble byproducts contained in the culture media at the end of the experiments. Without these measurements, we were not able to determine whether the carbon budget for the experiments was balanced. A carbon-free culture media was used for the follow-up experiments done this year. The $\delta^{13}C$ values of CO_2 and biomass produced

during these experiments were essentially identical to the earlier experiments and the carbon budget was balanced. The combined results of these experiments indicate that CO_2 produced by aerobic degradation of glucose is slightly fractionated (4 to 6‰) relative to the initial substrate.

A second set of experiments to examine isotopic fractionation resulting from microbial oxidation of methane was conducted in collaboration with Prof. Lisa Alvarez-Cohen of the Civil and Environmental Engineering Dept. at U.C. Berkeley. When oxygen in subsurface environments is depleted through aerobic degradation of organic matter (a common occurrence at sites contaminated with hydrocarbons), methane can be formed from anaerobic activity. As this methane diffuses up towards the surface, it is subsequently oxidized to form CO_2 and H_2O. We studied the isotopic fractionation effects of this process by measuring changes in the isotope ratios of methane passed through a continuous-flow fermentor containing a mixed culture of methane-oxidizing bacteria. The $\delta^{13}C$ values of CO_2 and biomass produced in the fermentor were also measured. The carbon isotope results from one experiment are plotted on Fig. 1. Once the culture reached steady state (~Day 10), $\delta^{13}C$ ratios of the residual methane in the effluent gas were shifted to $\delta^{13}C$ values approximately 1.5‰ higher than the initial methane. The CO_2 and biomass produced during the experiment were different by approximately 16‰, with the biomass ~12‰ higher than the original methane and the CO_2 ~4‰ lower.

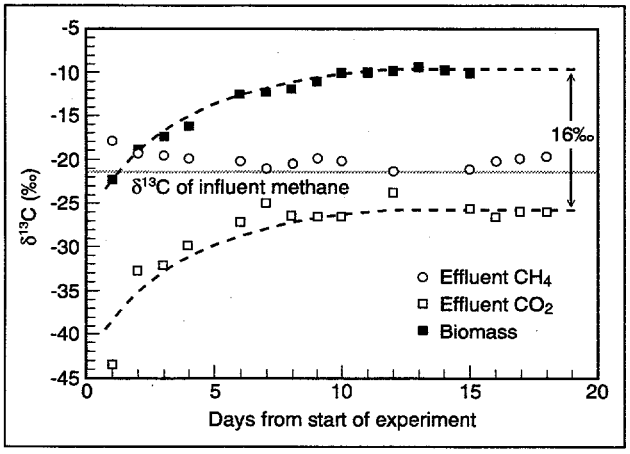

Figure 1. Carbon isotope compositions of CO_2, CH_4, and biomass produced by Type II methanotrophs in CU-free media.

These results differ from those of earlier workers in that the $\delta^{13}C$ ratios of the methane were only slightly shifted by the bacteria, and the biomass has higher $\delta^{13}C$ values than both the methane and the CO_2. The bacterial culture used for our experiments was initially developed to degrade chlorinated solvents (e.g., trichloroethylene). For this purpose, it is preferable that the bacteria produce soluble methane monooxygenase (mmO), the enzyme used to convert methane to methanol. In addition, organisms capable of fixing N_2 (Type II methanotrophs) were selected. Previous workers used Type I methanotrophs under conditions where particulate mmO is expressed by the bacteria. The results of these experiments indicate that the conversion of methane to methanol using soluble mmO causes a much smaller fractionation effect and that biomass produced by Type II methanotrophs will have much higher $\delta^{13}C$ values than that produced by Type I methanotrophs. These findings suggest that isotope measurements may be useful as an indicator of the types of methanotrophs that are present at field sites.

Publications

M.E. Conrad, T. Leighton, and B.B. Buchanan, "Carbon Isotope Fractionation by *Bacillus subtilis*," *Geol. Soc. of Am. Abstracts with Programs* **26** (7), A-510 (1994).

M.E. Conrad, P.F. Daley, M.F. Fischer, B.B. Buchanan, and T. Leighton, "Carbon Isotope Evidence for Subsurface Bacterial Activity at the Naval Air Station, Alameda, California," *EOS, Trans., Am. Geophys. Union* **76** (17), S119 (1995).

M.E. Conrad, P.F. Daley, and M. Kashgarian, "Tracing Subsurface Biodegradation of Hydrocarbons with Radiocarbon," *Am. Chem. Soc., Div. of Geochemistry Abstracts* (1996).

M.E. Conrad, P.F. Daley, M.F. Fischer, B.B. Buchanan, T. Leighton, and M. Kashgarian, "Combined ^{14}C and $\delta^{13}C$ Monitoring of Subsurface Biodegradation of Petroleum Hydrocarbons," *Environ. Sci. Technol.* (in press).

M.E. Conrad, T. Leighton, B.B. Buchanan, and D. Carlson, "Fractionation of Carbon Isotopes by Bacteria During Aerobic Metabolism," in preparation.

A.S. Templeton, M.E. Conrad, K.-H. Chu, and L. Alvarez-Cohen, "Factors Affecting Isotopic Fractionation by Methanotrophic Bacteria," in preparation.

Bioavailability and Degradation of Aromatic Hydrocarbons from Soil

Principal Investigators: Jennie Hunter-Cevera, Hoi-Ying Holman (ESD), and Tamas Torok (LSD)

Project No.: 96004

Funding: $170,300 (FY96)

Project Description

Laboratory and field investigations have demonstrated that the degradation pattern of organic chemicals in soil generally shows a rapid initial phase followed by a period of little or no change in the compounds. This low plateau bioremedial activity is a concern of engineers managing the contaminated sites. Our research examined certain ecophysiological factors that may result in this so-called "hockey stick" phenomenon. One hypothesis is that the weathered material is no longer bioavailable to the microbial community because the level of contamination is at a threshold below the induction level of certain enzymes in the now-adapted community. Hence, one would not expect any sizable biodegradation to occur.

The foundation of this work was based on an ongoing, newly funded project that is assessing intrinsic bioremediation of hydrocarbons and chlorinated solvents located at a variety of sites on the Alameda Naval Air Station in California (ANAS). One of the sites contained p-xylene, a very difficult hydrocarbon to biodegrade. From the records, it was deduced that the contamination had existed for over 80 years. It is not known what the original levels of p-xylene were when the soil was first contaminated. The study focused on three areas:

1. Examining simulated conditions under which the natural microbial community would be exposed to the p-xylene and measuring its biodegradation capability.
2. Examining individual members of the microbial community for their ability to biodegrade p-xylene under stress-related conditions such as those found in a damaged site.
3. Identifying those p-xylene degrading microorganisms via FAME and 16S rRNA analysis.

Moisture was selected as the major ecophysiological parameter for this study since there may be a tidal influence on the sand clay bay-mud profile obtained at ANAS. Both pristine and contaminated soils from different depths at the ANAS were used. Table 1 lists some properties of these soils. A porous disc microcosm was used to measure the p-xylene biodegradation under atmospheric conditions containing between 19 and 22% oxygen. After the microcosm experiments were run for 72 hours, samples were spiked with ^{14}C-labeled p-xylene. Biotransformation of the radiolabeled compound was measured and expressed as cumulative CO_2 (%) production. A variety of media was used to isolate large numbers of

Table 1. A summary of some soil properties from the Alameda Naval Air Station.

		Volume (%)			
Sample	**Depth**	**Sand**	**Silt**	**Clay**	**Moisture (%)**
BK-1	1′3″ – 1′6″	87	10	3	5
BK-2	2′9″ – 3′0″	47	10	34	15
BK-3	5′2″ – 5′5″	34	33	33	21
BK-4	7′3″ – 7′6″	67	3	30	14
BK-5	10′1″ – 10′4″	60	27	13	17
CA-1	1′3″ – 1′6″	67	17	17	4
CA-2	2′9″ – 3′0″	73	7	20	12
CA-3	5′2″ – 5′5″	57	23	20	14
CA-4	7′3″ – 7′6″	47	26	27	12
CA-5	10′1″ – 10′4″	58	4	38	16

aerobic heterotrophic microorganisms. Individual isolates from both the pristine and contaminated sites were then grown overnight, washed, and injected into 40-ml serum vials containing 5 ml of colloidal mineral salt agar with 0.05% yeast extract as the sole carbon and nitrogen source. After 12 hours of growth, p-xylene was injected at the level of 0, 5, and 20 ppm. Headspace gas-chromatography was employed to document any loss of p-xylene due to biotransformation over a five-day period. Any isolate that exhibited biodegrading activity on p-xylene was then identified by fatty acid methylester analysis via FID-gas-chromatography.

Accomplishments

A new microcosm type was designed and its applicability verified. This design, much improved over what is described in the literature, will enable us to obtain more accurate measurements of "real conditions" as they exist in the field. The biotransformation of p-xylene was very slow, as expected. Nevertheless, there was a significant difference between biotic and abiotic changes over the time-period of 45 days. Microorganisms were isolated at around 10^5 and 10^4 cells per gram of pristine and contaminated soil, respectively. The microbial counts were highest near the capillary fringe. Diversity with respect to types and numbers of microbial isolates was less for the contaminated site than the pristine site, and fewer isolates were obtained from samples collected above the capillary fringe. Bench-scale biotransformation experiments were designed using single microbial isolates. Only a few strains biodegraded p-xylene. These isolates, identified using molecular-level identification methods, will be used for further work at ANAS.

Results obtained from the microcosm work correlate with single isolate-biotransformation experiments: i.e., very little biotransformation of p-xylene occurs at ANAS. This may not only indicate that the p-xylene is not readily bioavailable to the resident microbial population in the contaminated soils but that the levels of p-xylene may be below the threshold for enzymatic activity.

Reactive Chemical Transport in Geologic Media

Principal Investigators: Karsten Pruess and George Brimhall

Project No.: 96031

Funding: $16,300 (FY96)

Project Description

The purpose of this project is to develop a detailed three-dimensional simulation of the geologic evolution of an actual ore deposit through reactive porous media flow, subject to unique geologic constraints. The site chosen for the analysis is the El Salvador mine, which is located in the Atacama desert of northern Chile. El Salvador is operated by CODELCO, whose data base of ore grades derived from 11,000 drill holes is available to the project.

The site-specific modeling effort will determine the interplay between paleoclimatic change, hydrogeologic conditions, erosion and uplift, and the mobilization and enrichment of massive amounts of copper-bearing minerals in response to spatially and temporally varying redox conditions. TOUGH2, Berkeley Lab's existing general-purpose, multiphase, multicomponent simulator, will be applied to model the evolution of hydrogeologic conditions over geologic time. The simulator will also be enhanced to describe the transport of chemical species subject to kinetic and equilibrium-controlled reactions, and will be ported to advanced massively-parallel computing platforms. Data from laboratory leach column experiments will be used to determine reaction kinetics, and to test the ability of the simulator to adequately describe reactive chemical transport processes. Existing speciation and reaction path models will be implemented and utilized in the analysis.

Results from the project are expected to aid in future exploration efforts for porphyry copper deposits, and in the management of acid mine waters, leach dumps, and mine tailings. The reactive chemical transport capabilities will also be useful for assessing and remediating environmental contamination at DOE and industrial sites.

Accomplishments

The CODELCO data base has been implemented on a Silicon Graphics workstation. Kriging techniques incorporated in the commercial VULCAN software were used to develop two- and three-dimensional visualizations of the distribution of ore grades. Mass balance calculations were performed to analyze the relationship between the present-day ore body and the distribution of protore from which it originated. This analysis demonstrated the crucial role of faults in the development of a laterally-offset "exotic" ore body (so-called because it occurs several kilometers away from its original source of copper in the primary ore deposit).

Our TOUGH2 simulator was ported to Cray supercomputers at the National Energy Research Scientific Computing Center (NERSC). TOUGH2-CHEM, an enhanced version of TOUGH2 that includes reactive chemical transport, was kindly provided to us by S. White of Industrial Research Ltd., New Zealand, and was implemented on a workstation. We also installed the EQ3/EQ6 speciation and reaction path modeling software.

Development of two-dimensional vertical section models of the hydrogeology at El Salvador was started. Figure 2 shows a computational grid of an east-west cross section for flow simulation with TOUGH2 that was developed with VULCAN software. The zoning is based on our analysis of ore grade data. Simulation of saturated and unsaturated water flow is underway, with one objective being the design of pressure-transient tests for determination of in situ formation permeabilities.

On the institutional side, the project has hired two postdoctoral fellows with experience in mineral reaction kinetics and reactive chemical transport, following an international search. The postdocs will commence work in December 1996 and January 1997, respectively. We have established an information exchange and conducted a site visit with BHP Copper, Inc., of Tucson, Arizona. Our site visit (to the San Manuel mine) has provided valuable insights and data on reactive transport of copper minerals under variable redox conditions in leach heaps as well as laboratory columns. Several small-scale fluid flow and diffusion mechanisms, which will be of use in refining our algorithm for advective and diffusional fluid/rock interaction, were identified. By modeling leach column tests using available time-dependent chemical data, correlated with the observed mineralogical evidence of copper transport, we will be able to improve the accuracy of our simulation of long-term geologic processes.

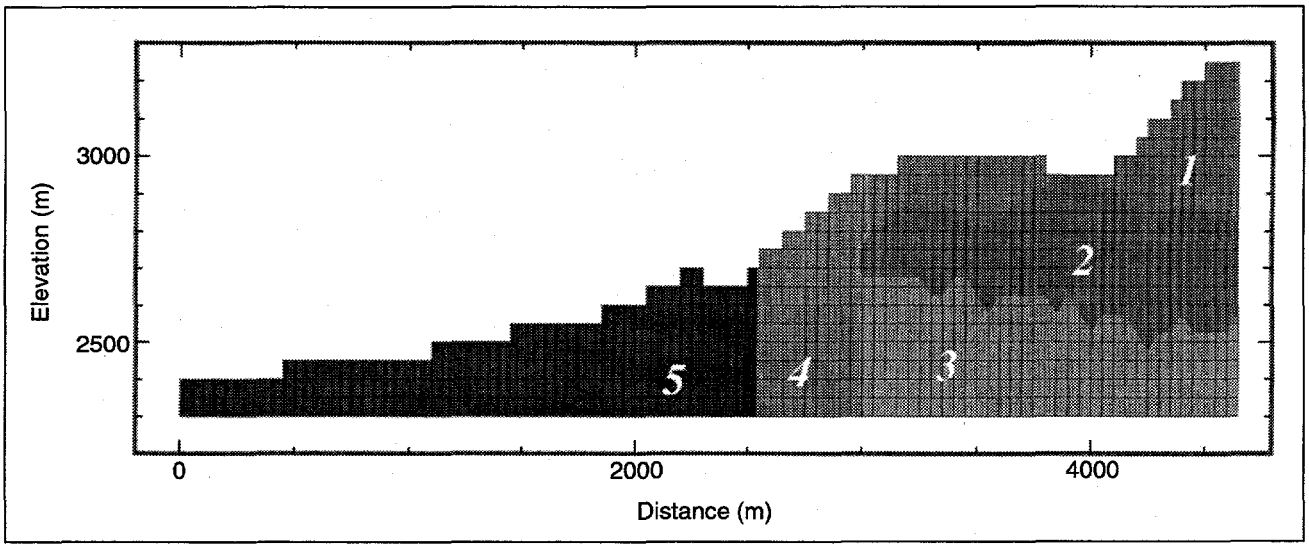

Figure 2. East-west cross section through El Salvador, showing computational grid for hydrogeologic modeling, and zonation based on ore grade data. Zones are: 1 - leached cap, 2 - enrichment blanket, 3 - protore, 4 - transition region, 5 - exotic ore body.

Developing High Resolution Synchrotron X-ray Techniques to Study Natural Porous Media

Principal Investigators: Erika Schlueter and Dale Perry

Project No.: 96005

Funding: $120,300 (FY96)

Project Description

The purpose of this project is to develop synchrotron x-ray techniques with micrometer- and submicrometer-scale spatial resolution to study earth materials. The necessary high-resolution imaging and spectroscopic methods have only become possible with the construction of high-brightness synchrotron radiation x-ray sources such as the Advanced Light Source (ALS). The high-resolution imaging available through ALS presents possibilities for studying soil/rock-fluid interactions on a spatial scale hitherto unattainable. Obtaining microscale geometrical and chemical information from subsurface systems will allow direct modeling and permit—for the first time—the propagation of fluids and contaminants, electricity, sound, and seismic waves through the pore network. This major breakthrough will be the first stage in pursuing fundamental issues such as the scale dependence of transport properties and the influence of heterogeneities. Obtaining microscale geometrical and chemical information from subsurface systems is a much-needed step towards understanding and predicting environmental processes.

High-resolution synchrotron radiation computed microtomography (CMT) was used to obtain direct geometrical information for a given complex microstructure rock/soil. Theoretical investigations and computational approaches are to be used to calculate transport properties—e.g., permeability (single and/or two-phase) and electrical conductivity—from direct measurements of the three-dimensional pore microstructure.

The application of the above techniques to systems of relevance to the earth sciences is entirely new. The thrust of this project was therefore to use optimized experimental systems to assess the potential of the techniques and to predict application areas. CMT was investigated at European Synchrotron Radiation Facility (ESRF). We can make recommendations for future Earth Sciences Division beam lines and end stations to enable study of rock physics and chemistry at the ALS.

Accomplishments

State-of-the-art high resolution (6 μm) CMT experiments on relatively large Berea sandstone cylindrical sample volumes (5 mm diameter) have been successfully accomplished at the ESRF to obtain direct three-dimenstional topological and geometrical information of a rock of complex microstructure (see Fig. 3). State-of-the-art phase contrast imaging experiments on Berea sandstone have also been accomplished at the ESRF to obtain detailed mineral information and distribution (e.g., clay minerals) in the rock (see Fig. 4).

Feasibility Studies: Analytical Phase

Microtomography requires a high energy x-ray source with high brightness (defined as x-ray flux per unit area per unit solid angle). High energy is needed so that x-rays can penetrate the necessary sample thickness—typically, 5 to 20 keV. High brightness is required so that a small spot of light can be focused on the sample while still preserving adequate collimation. The critical energy of a synchrotron source equally divides the power radiated above and below it. This is a useful parameter for thinking about

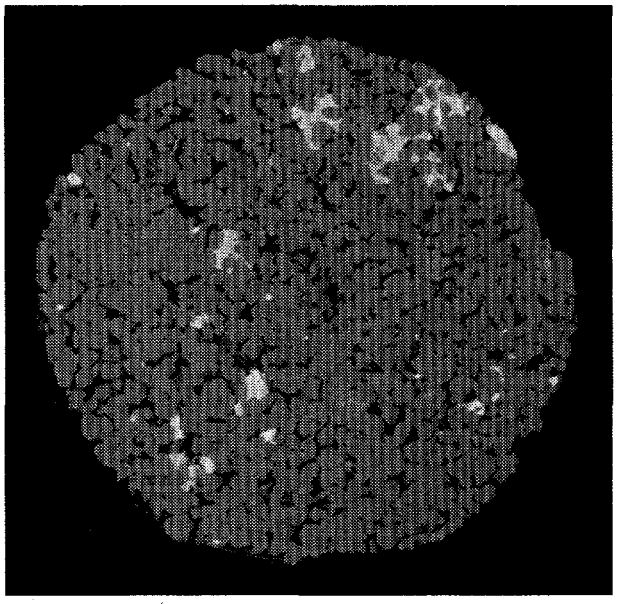

Figure 3. High resolution CMT slice of a 5-mm-diameter Berea sandstone cylindrical sample obtained at 6 μm spatial resolution at the ESRF. The image clearly shows the different minerals present in the rock (quartz, feldspar, iron oxide, and possibly clay), as well as the different pore sizes.

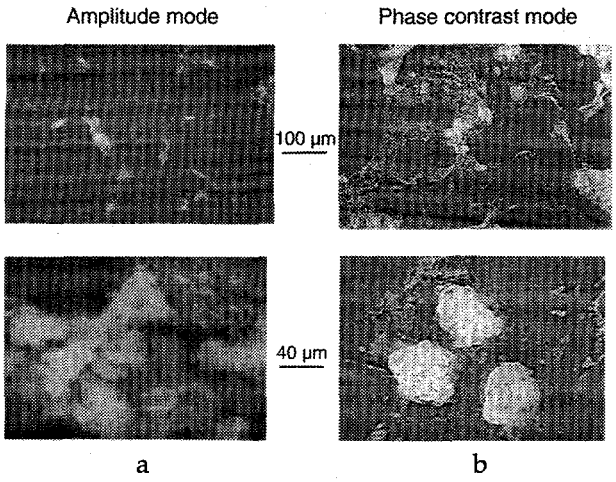

Figure 4. Sample of a Berea sandstone imaged in amplitude mode (a) and in phase contrast mode (b) at the ESRF. Many more fine mineral details (e.g., clay minerals) can be detected in the phase contrast mode.

spectral range because the useful upper photon energy is generally assumed to be about four times as great as the critical energy. For the ALS bending magnet, with the machine set at 1.9 GeV, the critical energy is 3 keV. Therefore, the upper useful energy is 12 keV. Better yet, we could use a higher field device in one of the storage ring straight sections, such as the 2-tesla, 38-pole multipole wiggler already constructed for protein crystallography (W16). The resultant field is 1.6 times the ALS bending magnet field for 1.9 GeV operation, and hence the maximum working photon energy will be 19 keV. And since the device has 38 poles, it is much more intense than a normal dipole source. Also investigated was use of a micro-undulator or a short multipole wiggler or bend in a new low-β section which could produce a very bright high-energy beam.

In addition, computed microtomography is a method well-suited to microscopic nondestructive evaluation (NDE) of materials. The risk of sample-preparation-induced artifacts is minimized because no physical sectioning of the sample is required. The spatial resolution, which can be attained using conventional x-ray tubes, is limited mainly by the source spectral brightness and is generally much greater than 20 µm. The high synchrotron brightness of the x-ray source at ALS is a key parameter for high-resolution CMT.

Feasibility Studies: Experimental Phase

A three-dimensional CMT experiment was done at the ESRF. Five-mm-diameter Berea sandstone samples were scanned in absorption mode with 25 keV photon energy and 6 µm spatial resolution. The absorption gives direct information about the distribution of different minerals present in the rock (Fig. 3). Rock porosity is also clearly resolved in the tomographic slice.

The next area of study concentrated on a CCD-based area detector. In an x-ray CCD detector (consisting in principle of a fluorescence screen to convert x-rays to visible light, a magnifying optical system, and a cooled CCD camera), the limitation in terms of spatial resolution is the fluorescence screen, where scattering inside the phosphor limits the resolution to about the thickness of the phosphor (~4 to 5 µm). A detector system in the three-dimensional CMT instrument at the ESRF uses phosphors such as Gd_2O_2S:Tb that are only a few micrometers thick to get ~6 µm resolution. Further research at the ESRF with fluorescence screens of different materials using ~1-µm-thick monocrystalline phosphors like BGO and YAG:Ce should increase the resolution even further.

Finally, a possibility for improving imaging for low density material (especially biological and organic tissues) is to make use of phase contrast. Figure 4 shows a Berea sandstone thin section imaged in the amplitude and phase contrast modes at the ESRF. Figure 4(a) shows the section imaged in the amplitude contrast mode (the detector is placed directly after the sample). The mineral grains can be localized. Figure 4(b) shows the same region of the sample imaged in phase contrast mode (detector is placed away from the object). Many more fine mineral structures (e.g., clay minerals) can be detected in this image.

The studies completed in the course of this project have immediate implications for synchrotron x-ray techniques, particularly at the ALS. These include:

- Digitizing CMT results for constructing micromodels that replicate exact three-dimensional pore geometry and topology, which could be used in lattice Boltzmann numerical models (based on first principles), and for comparing results with theoretical predictions.
- Establishing that phase contrast imaging could be implemented on an existing beamline.
- Analyzing the use for CMT of an optimal superconducting dipole source, a microundulator, or a short multipole wiggler or bend in a new low-β section which would produce a very bright high-energy beam.

- Establishing that beam fluxes from existing wigglers are sufficient for CMT studies of samples at spatial resolution in the micrometer range for a wide range of materials from water-like to Si-like.
- Establishing that the use of Bragg-Fresnel x-ray optics could reduce the time to scan and increase the spatial resolution.
- Assessing the many potential applications for high resolution phase contrast imaging, including microscopy, tomography, sample alignment, topography, and holography. For medical applications, phase contrast imaging should significantly reduce radiation dose.

Gratitude is expressed to Per Spanne, Anatoly Snigirev, Irina Snigireva, Carsten Raven, and Andreas Koch of the ESRF without whose keen scientific input this project would have not been successfully accomplished. Many thanks are due to Ross Schlueter of the ALS for state-of-the-art high energy source development. Heartfelt thanks are given to Neville Smith, Fred Schlachter, Howard Padmore, Malcolm Howells, and Brian Kincaid of the ALS for their support and continuous encouragement. Thanks are also due to Al Thompson and David Attwood of the Center of X-ray Optics (CXRO), Nancy Johnston and Kevin Campbell (CSD), Tammy Welcome (NERSC), Paul Witherspoon and Robert Zimmerman (ESD), and many others for their encouragement throughout this project.

Molecular Geochemistry of Clay Mineral Surfaces

Principal Investigator: Garrison Sposito

Project No.: 96032

Funding: $25,900 (FY96)

Project Description

This project involves research toward an accurate theoretical model of molecular structure at the surface of hydrated, 2:1 layer type clay minerals (smectites). These minerals are of great importance in nuclear waste containment and contaminant attenuation. Two objectives are to be addressed:

- Monte Carlo and molecular dynamics simulations of interfacial molecular structure on clay minerals adsorbing water and cations, and
- ab initio quantum chemical studies on a variety of hydrated clay minerals, in which the interlayer counter-ions will be lithium, sodium, or potassium.

The results obtained should provide a significantly improved quantitative understanding of clay-clay, clay-water, and cation-clay interactions that will be used to test and, if necessary, improve the potential function models used in our Monte Carlo and molecular dynamics (MC/MD) simulations of hydrated clays.

Computational algorithms for the MC/MD simulations, based on the codes MONTE and MOLDY, have been developed by our collaborators, Dr. N.T. Skipper and Dr. K. Refson. The codes are fully optimized and running well on a Cray C90. Recently, Dr. Refson has produced a fully parallel version of the code MOLDY, which we hope to run on the Cray T3E at NERSC. For the quantum chemical calculations, we employ iterative minimization of the total energy within the framework of density functional theory, using pseudopotentials. This approach will be implemented by the code CASTEP, written by Dr. M.C. Payne, which has also been fully vectorized for use on the C90.

Accomplishments

Molecular structure in the interlayers of swelling lithium-Wyoming montmorillonite with one, two, or three adsorbed water layers was investigated for the first time by concurrent Monte Carlo and molecular dynamics simulation, based on the MCY model of water-water interactions (the first objective listed above). Calculated layer spacings, as well as interlayer-species self-diffusion coefficients, were in good agreement with available experimental data (Table 2). Inner-sphere surface complexes of Li^+ with tetrahedral charge sites were observed in all hydrates, whereas outer-sphere surface complexes of Li^+ with octahedral charge sites, found in the one-layer hydrate, dissociated from the clay mineral basal planes into a diffuse layer in the two- and three-layer hydrates (Fig. 5). This is a signature of the strong interaction between Li^+ and water molecules.

Interlayer water molecules thus tended to solvate adsorbed Li^+, although some were entrapped within cavities in the montmorillonite surface. All of the adsorbed Li^+ and interlayer water species exchanged on the time scale (0.2 ns) of the MD simulations. Comparisons with Monte Carlo results obtained usingthe popular TIP4P model for representing Li-water and Li-clay interactions rather than the MCY

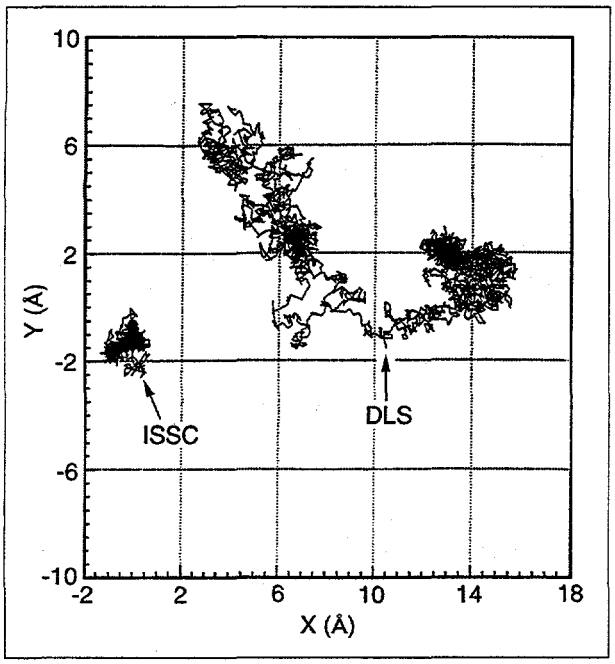

Figure 5. Molecular dynamics simulations of the surface trajectories of Li^+ (during 205 ps) in an inner-sphere surface complex (ISSC) or in the diffuse-ion swarm (DLS) in the three-layer montmorillonite hydrate. Note the restriction of the ISSC Li^+ species to a triangle of surface oxygens and the high lateral mobility of the DLS Li^+ species.

model indicated that both layer clay spacings and interlayer species mobilities tend to be under-predicted by the TIP4P model, probably because of its optimization on the extended, tetrahedral network of hydrogen-bonded water molecules found in the bulk liquid, but not in hydrated 2:1 clay mineral interlayers.

Research underway in the first full year of the project (FY97) includes C90 simulations of Li-montmorillonite hydrates at very low water content (to examine further the accuracy of our intermolecular potential functions), and of K-montmorillonite hydrates, which, by contrast with the Li-montmorillonite case, do not swell in water. In respect to the second objective listed above, we have now purchased a commercial version of the CASTEP code and are arranging to install it on a Silicon Graphics workstation at the Molecular Graphics Laboratory on the Berkeley campus. We also expect to install the parallel version of MOLDY on the Cray T3E at NERSC.

Publications

G. Sposito, F.-R.C. Chang, and N.T. Skipper, "Monte Carlo and Molecular Dynamics Simulations of Interfacial Structure in Li-Montmorillonite Hydrates," to be published in *Langmuir*.

Advanced Computing for Geophysical Inverse Problems

Principal Investigators: Donald Vasco and Lane Johnson

Project No.: 96033

Funding: $34,300 (FY96)

Project Description

The objective of this work is to develop approaches for solving geophysical inverse problems on modern parallel computers. A geophysical inverse problem entails inferring properties of the Earth's interior from data gathered at the surface or from boreholes. There are several impediments to obtaining reliable inferences based upon external measurements. A major problem is the non-uniqueness inherent in almost all inverse problems. That is, many distributions of material properties–often an infinite number–

Table 2. Properties of Li-montmorillonite hydrates (simulated and experimental).

Hydrate	Layer Spacing[a]		Self-Diffusion Coefficient[b]	
	d_{sim} (Å)	d_{exp} (Å)	D_{wsim} (m^2s^{-1})	D_{wexp} (m^2s^{-1})
One-layer	12.27 ± 0.06	12.3	1.3×10^{-10}	$0.5 - 4.0 \times 10^{-10}$
Two-layer	15.1 ± 0.1	15.6	4.5×10^{-10}	$2.6 - 7.0 \times 10^{-10}$
Three-layer	19.5 ± 0.2	19.0	1.4×10^{-9}	1×10^{-9}

[a]Monte Carlo simulation of the c-axis interlayer spacing at 100 kPa pressure.
[b]Molecular dynamics simulation of the water molecule self-diffusion coefficient.

are compatible with a given set of observations. Also, the uncertainties associated with a set of estimates are critical for evaluating the reliability of any proposed Earth structure. A primary goal of this work is to use the power of today's supercomputers to study the non-uniqueness and uncertainty associated with the inverse problem.

Inverse problems divide naturally into linear and nonlinear problems. For linear problems, the observations are linearly related to the unknown Earth structure; for nonlinear problems, the relationship is more complex. Estimating non-uniqueness and uncertainty associated with linear problems is well-established and may be accomplished using techniques from linear algebra. However, the linear systems may be extremely large and ill-conditioned. For nonlinear problems, estimating non-uniqueness and uncertainty is a topic of research. Because most approaches are computationally intensive, use of parallel computers appears promising.

Two applications are currently under investigation: imaging the velocity structure of the entire Earth using seismic travel time observations and determining the permeability variations in a petroleum reservoir based upon oil field production data. The whole Earth-imaging problem is linear but extremely large (1 million travel times and 150,000 unknown parameters). A Lanczos technique is used to solve the linear inverse problem and compute estimates of non-uniqueness and uncertainty. The problem of determining reservoir structure is extremely nonlinear and moderate in size (about 600 measurements and 4000 unknowns). An iterative conjugate gradient method is used to find a solution that is compatible with the observations. The algorithm is implemented in parallel in order to find a large number of solutions that match the data. With this collection of models, the non-uniqueness and uncertainty of the solution to the inverse problem may be estimated using standard statistical techniques.

Accomplishments

We have obtained a preliminary model of the three-dimensional velocity structure of the entire Earth using seismic arrival times. In this model, there are interesting velocity variations in the Earth's outer core (Fig. 6) which have never been observed before. An iterative Lanczos algorithm has been developed and ported to a massively parallel T3D computer. It has also been applied to the whole Earth imaging problem and we have obtained the first estimates of resolution (a measure of non-uniqueness).

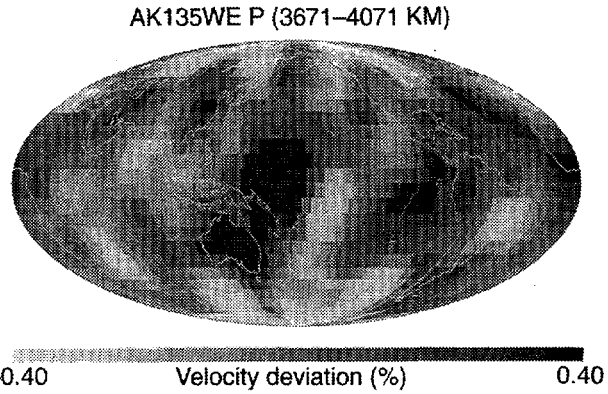

Figure 6. Map of seismic velocity variations in the middle of the Earth's outer core. Lighter tones signify slower velocities and darker tones, regions of faster seismic velocity.

Production data from the North Robertson oil field in the Permian Basin of West Texas is being used to infer the permeability variations in the reservoir (Fig. 7). We have results for a simple three-layer reservoir model (4000 cells) and are currently extending our model to nine layers. A preliminary Parallel Virtual Machine (PVM) code has been developed and will be ported over to the T3D/T3E in the near future. We are also considering developing a parallel conjugate gradient routine for rapid inversions. In this algorithm, which will also be written using PVM, the

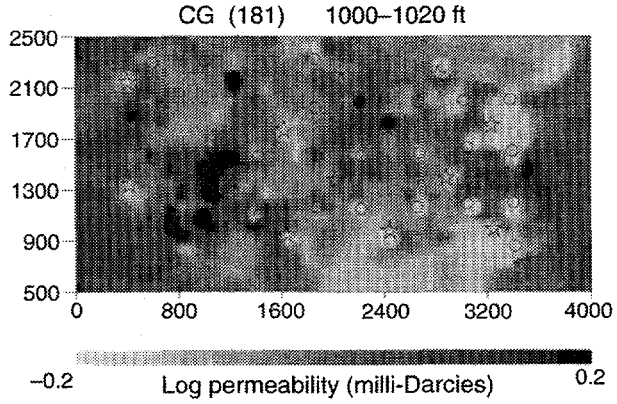

Figure 7. Permeability variations in the uppermost 20 feet of the North Robertson Field, Permian Basin, West Texas. Dark colors denote high permeability regions and light ones correspond to low permeability areas. Injection wells are denoted by stars and production wells by circles.

gradient elements are computed in parallel on various processors.

Some new results have been obtained that will enable us to map nonlinear inverse problems (which are difficult to solve) to linear inverse problems (which are easier to solve). The method is based upon the techniques of continuous (Lie) groups from mathematics. The approach is very powerful and works for general inverse problems. We have applied the method to a set of gravity measurements gathered at Yucca Mountain, Nevada. This work, an outgrowth of our original research, could prove very useful in solving nonlinear inverse problems.

Publications

D.W. Vasco, "Groups, Algebras and the Nonlinearity of Geophysical Inverse Problems," submitted to *Geophys. J. Int.*

D.W. Vasco and L.R. Johnson, "The Seismological Signature of Core Dynamics?" in preparation.

D.W. Vasco, A. Datta-Gupta, and J.C.S. Long, "Integrating Field Production History in Stochastic Reservoir Characterization," submitted to *Soc. Petro. Eng. Form. Eval.*

Microbial Transport and Microbial and Nutrient Delivery in Subsurface Environments

Principal Investigator: Jiamin Wan

Project No.: 95005

Funding: $78,200 (FY96)
$75,100 (FY95)

Project Description

This project was designed to improve our understanding of basic transport processes of colloids and bacteria in subsurface environments through various laboratory experiments. The objectives of this study are to:

- Identify the potential importance of sedimentation on bacterial transport in groundwaters,
- Develop techniques of visually and quantitatively studying water flow and contaminant transport processes, as well as in situ microbial behavior from micrometer to porous medium scales,
- Quantitatively study the dependence of colloid and bacterial transport on water saturation and matric potential in vadose environments, and
- Explore the possibility of injecting foam to deliver bacteria and nutrients to desired locations for enhancing in situ bioremediation.

The approaches taken in this research combine visualization with quantification both in glass micromodels and fractures and in soil columns. This combination permits systematic evaluation of various mechanisms controlling colloid and microbial transport and microbial and nutrient delivery. Mechanisms responsible for microbial transport are studied visually in micromodels subjected to controlling boundary conditions. The observed and measured processes in micromodels are tested in column experiments.

Accomplishments

Task 1: Bacterial Sedimentation Through Porous Medium

This has been a two-year project (1995 to 1996). In the first year, we completed Task 1, bacterial sedimentation through porous medium. In this study, we examined the potential significance of sedimentation as a mechanism for bacterial transport. We developed a model to predict the behavior of bacteria and inorganic colloids sedimenting through granular porous media under hydrostatic conditions. The results suggest that if time scales are sufficiently long, spanning many generations, sedimentation can become a significant mechanism for bacterial transport. This research, summarized in "Bacterial Sedimentation Through Porous Medium," contributes to the field of bacterial transport in both theoretical and practical aspects, and has implications for deep subsurface microbiology and deep subsurface bacterial origins.

Task 2: New Techniques

In the past two years we developed two new techniques for visually and quantitatively studying in situ microbial behavior and small scale flow and transport processes. A submission to *Environmental Science and Technology* discusses these techniques and successfully completes Task 2. One technique is the new method for constructing glass micromodels that permits direct visualization and quantification of flow and transport phenomena in fractured porous media. In the fracture-matrix micromodels, a sequential etching procedure was developed in order to provide the

necessary contrast of depths between matrix pores and fracture apertures. This high contrast in etching depths ensures that very different capillary properties are associated with micromodel fractures and matrix blocks.

Improved techniques were also developed for reducing the pore sizes of the matrix to a natural fine-grained sandstone pore-scale. The improved micromodel pattern designs allow for previously unachievable control of boundary conditions. Various saturated and unsaturated fracture flow and transport processes can be visually and quantitatively studied with these micromodels. In general, the improved micromodel method provides a unique tool for exploring some of the previously unrecognized flow and transport processes in fractured porous media. This research is directed at providing microscale explanations to some currently unresolved flow and transport issues important in predicting larger-scale flow processes. "Improved Glass Micromodel Methods for Studies of Flow and Transport in Fractured Porous Media," describing the technique and giving examples of applications, has been published recently in *Water Resources Research*.

Another technique we developed in the past two years allows the fabrication of casts of fractured rock pairs with glass. "Glass Casts of Rock Fractures: A New Tool for Studying Flow and Transport," submitted to *Water Resources Research* a few months ago, summarizes our work in this area. These glass casts provide accurate reproduction of aperture structure and fine-scale surface roughness of natural fractures, good optical clarity, and representative wettabilities of mineral surfaces. The surface of a clean glass fracture wall has zero contact angle, and wettability of the glass fracture surfaces can be intentionally altered with chemical treatment. Glass casts of fracture surfaces will be useful tools for visually and quantitatively studying various physical, chemical, and microbial processes occurring in rock fractures. The experiments conducted in glass fracture casts will be more relevant to water-wettable rock systems.

Task 3: Unsaturated Transport of Colloids and Bacteria

The most recent achievement is on unsaturated transport of colloids and bacteria (Task 3). In this work a conceptual model for "film-straining" is proposed to predict the effect of partial saturation on subsurface colloid transport. In the vadose zone, local thinning of water films can strongly hinder colloid transport. The concepts of a "critical matric potential" and "critical saturation" are introduced, below which pendular rings of water disconnect and film-straining of colloids becomes important. The modeled magnitude of film-straining depends on the ratio of colloid size to film thickness as well as on flow rate. The model was calibrated with experiments on transport of hydrophilic latex particles (four sizes from 0.01 to 1.0 μm), in sand columns of three different grain-size ranges (150 to 212, 212 to 425, and 425 to 500 μm), at flow rates spanning four orders of magnitude. Good agreement was obtained between the wide range of experiments and model predictions fit with only two adjustable parameters. This work revealed for the first time a basic mechanism controlling colloid transport in unsaturated porous media, and proposed and tested a conceptual model describing the process. A manuscript about this work ("Film-Straining of Colloids in Unsaturated Porous Media: Conceptual Model and Experimental Testing") has just been submitted to *Environmental Science and Technology*.

Task 4: Injecting Foam for Enhanced Bioremediation

The fourth task will be developed in 1997, under funding support from Office of Environmental Management, DOE. Two three-year proposals, largely using the above results as supporting materials, have been funded starting from 1997.

Publications

J. Wan and T.K. Tokunaga, "Film-Straining of Colloids in Unsaturated Porous Media: Conceptual Model and Experimental Testing," submitted to *Environmental Science and Technology*, November 1996.

J. Wan, T. Orr, J. O'Neill, and T. Tokunaga, "Glass Casts of Rock Fractures: A New Tool for Studying Flow and Transport," submitted to *Water Resources Research*, May 1996.

J. Wan, T.K. Tokunaga, C.F. Tsang, and G.S. Bodvarsson, "Improved Glass Micromodel Methods for Studies of Flow and Transport in Fractured Porous Media," *Water Resources Research*, **32**, 1955-1964 (1996).

J. Wan, T.K. Tokunaga, and C.F. Tsang, "Bacterial Sedimentation Through Porous Medium," *Water Resources Research*, **31**, 1627-1636 (1995).

J. Wan and T.K. Tokunaga, "A New Method for Constructing Glass Micromodels Resulting in a Wide Distribution of Pore Sizes," *Patent Disclosure*, LBNL 1162-IB (1995).

J. Wan, T.R. Orr, and J. O'Neill, "Glass Casting of Rock Fractures," *Patent Disclosure*, LBNL 1171-IB (1995).

Energy and Environment Division

Sediment Toxicity and Site Restoration at the Mare Island Naval Shipyard

Principal Investigator: Susan Anderson

Project No.: 95006

Funding: $60,200 (FY96)
$78,000 (FY95)

Project Description

We had two primary objectives. The first was to assess the feasibility of using estuarine fish embryo species to conduct marine and sediment toxicity tests with minimal manipulation of the test substrate. The second was to compare standard sediment toxicity tests to *in situ* field testing using these same species. This work will advance the application of ecological hazard assessment techniques to the important problems of wetland restoration and military base closures.

In accordance with our first objective, temperature, salinity, and reference toxicant studies were conducted with two fish embryo and one amphipod species (*Atherinops affinis, Menidia beryllina*, and *Eohaustorius estuarius*, respectively) to determine their physio-chemical tolerances to estuarine conditions. Successful hatching of the embryos and survival with the amphipods were the final endpoint estimates. These studies were used to evaluate the tolerances of these species to estuarine conditions.

Once the physical tolerances of these species were established, comparisons between standard laboratory toxicity tests and *in situ* toxicity tests were conducted. Standard laboratory tests using both pore-water and sediment-water-interface-corers (SWIC) were compared to *in situ* field tests at the pier pilings site in the Mare Island Naval Shipyard (MINSY) using these same species. In addition, these tests were also compared to a known contaminated site in the San Francisco Bay. At each site, a reference and contaminated station was sampled and both seawater and sitewater controls were implemented.

Accomplishments

Salinity and temperature tolerance experiments revealed that *M. beryllina* embryos can tolerate temperatures between 16 and 24°C and salinities between 5 and 20 ppt, whereas *A. affinis* has a temperature range between 16 and 20°C and salinity tolerance of 10 to 25 ppt. In addition, both species exhibited an LC50 to un-ionized ammonia at approximately 5 mg/L, which is comparable to the amphipod. The results show that these species can be used in a variety of wetland habitats with little or no test manipulations: they are ideal for conducting *in situ* toxicity tests.

Comparisons between pore-water, SWIC, and *in situ* exposures were conducted at both the pier pilings site within MINSY and at Islais Creek in the San Francisco Bay. At Islais Creek, the salinity range for *M. beryllina* was too high and the controls did not meet acceptable criteria. However, *A. affinis* embryos exhibited excellent hatching success in both of the controls and the reference site, and showed significantly lower hatching success at the contaminated site for all test exposure scenarios (Fig. 1). These results were similar to *E. estuarius* survival data at the same sites (Fig. 1).

At the pier pilings site, two experiments were conducted. Both experiments exhibited excellent hatching success in both the controls and the reference site for all test types. At the contaminated site (Launch Ramp), *A. affinis* showed significantly lower hatching success in both *in situ* tests and the second pore-water test. However, there were no significant differences for the SWIC exposures. *M. beryllina* exhibited lower hatching success in the second *in situ* test only. For *E. estuarius*, there were no significant differences among any of the test types or treatments.

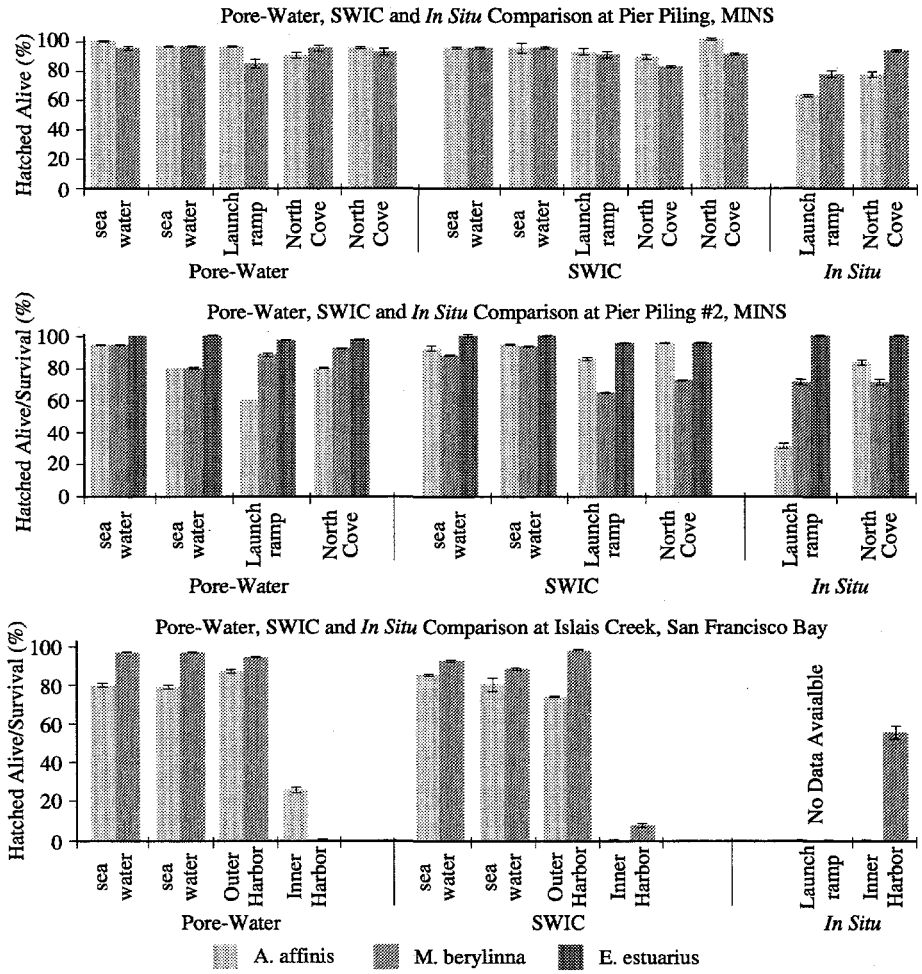

Figure 1. Pore-water, SWIC, and in situ *comparison for selected estuarine species at two sites in the San Francisco Bay.*

The results of this study show that both *A. affinis* and *M. beryllina* are ideal test organisms for assessing toxicity in estuarine environments. Furthermore, *in situ* toxicity tests using these species provide a valuable site-specific approach to ecological risk assessment. *In situ* toxicity testing is comparable to and in most cases more sensitive than traditional laboratory testing techniques, and serves as a useful complementary tool in assessing sediment toxicity.

Publications

S. L. Anderson and J. A. Jelinski, "Pore-Water and Epibenthic Exposures in Contaminated Sediments Using Embryos of Two Estuarine Fish Species," presented at the 1996 National Society of Environmental Toxicology and Chemistry (SETAC) conference, Washington DC, November, 1996 and in draft.

Instruments for the in situ Detection of NO and NO_2 and Their Precursors

Principal Investigator: Ronald Cohen

Project No.: 96006

Funding: $129,800 (FY96)

Project Description

Defensible public policy concerned with global warming and with urban pollution requires that we understand the sources, chemical transformations, and sinks of trace atmospheric constituents. Recent observational evidence has reinforced the view that many such policies are based on assumptions that have never been tested. For example, Blake and Rowland used observations from Mexico City to show that the predominant hydrocarbons there are derived from liquid petroleum gas used for heating and cooking and not from automobiles. Thus the expensive campaign to reduce auto emissions in Mexico City is likely to be much less effective at reducing air pollution than previously expected. In another study of urban air, Beaton et al. showed that poorly maintained new-model cars in California were responsible for considerably more emissions than well-maintained 20-year-old cars. On the basis of this data, Beaton et al. conclude that pollution control strategies aimed at old cars in California are likely to be much more expensive (and possibly less effective) than strategies aimed at controlling emissions of the worst 10% of cars of all model years. These examples of observational data forcing reevaluation of policy options serve to emphasize the need for more accurate atmospheric observations. Accurate instrumentation is needed for observations over a wide range of spectral and temporal scales.

This project focuses on designing, building, and calibrating the first of a new generation of optical sensors for nitrogen oxide radicals and their precursors. The new instrument will be used to make spatially and temporally correlated measurements of the concentrations of NO and NO_2. It will be unambiguously specific, sensitive (<10 parts per trillion/s), fully robotic, compact (<0.5 cubic meters), lightweight (<100 lbs), designed to make observations over the full six orders of magnitude of NO_2 concentrations observed in different regions of the atmosphere (0.1 ppt in the remote marine boundary layer and as much as 100 parts per billion in urban environs), and capable of nearly continuous observations over a period of months to years.

This instrument will be used to test assumptions about the chemical transformations within the nitrogen oxide family leading to production of the oxidizing species OH and O_3 in urban and remote environments. OH and O_3 are the primary agents of chemical change on regional and global scales. Understanding the role of NO_X in controlling production of these species is fundamental to reliable climate and air quality modeling.

Accomplishments

We have assembled and tested a compact, highly efficient, solid-state, pumped dye laser design (0.5 W, 5000 Hz, 0.07 cm^{-1} linewidth, 585 nm). The laser will be used as a source for fluorescence spectroscopy of NO_2. We are developing new technology for single photon counting with a large area (64 mm^2) silicon avalanche photodiode to enhance the sensitivity of this instrument by a factor of five to ten over what is possible with commercially available GaAs photomultipliers. Initial results are encouraging. A chamber has been designed to allow direct comparison of the NO_2 signal using PMT (Photomultiplier Tube) and APD (Avalanche Photodiode) technologies. Ongoing efforts to integrate and automate this instrument are expected to lead to an operational field instrument by the fall of 1997.

Mechanism and Modeling of Soot Formation in Hydrocarbon Flames

Principal Investigator: Michael Frenklach

Project No.: 96007

Funding: $75,000 (FY96)

Project Description

Soot formation is one of the key environmental problems associated with the operation of practical combustion devices. The goal of the project is to develop reliable models of soot formation that can be used in numerical simulation and optimization of combustion devices. The specific goals are fundamental understanding and modeling of gas-surface

processes; development of a model for fractal growth of soot particles; and modeling approaches to turbulence-chemistry interactions.

The project is theoretical/computational and experimental in nature and is focused on the development and testing of chemical and physical models of soot particle formation and growth. The research will involve theoretical exploration of reaction mechanisms via quantum chemistry, chemical kinetics, numerical simulation of flames, aerosol dynamics, Monte Carlo and molecular dynamic simulations, and shock-tube experiments.

Accomplishments

Preparation, Testing, and Calibration of Soot Formation Model

The soot formation model developed in the past was updated with new kinetic data and submodels:

- mutually consistent new PAH (Polycylcic Aromatic Hydrocarbon) thermochemistry, new main-combustion-zone reaction mechanism, and new rate coefficients for PAH reactions,
- new transport data,
- coagulation model for all pressure regimes,
- newly developed kinetic model for agglomeration of soot particles.

The work continues with the addition of a physically more realistic surface growth model, and will follow with extensive testing of the combined new model.

Stochastic Modeling of Soot Particle Aggregation

A new Monte Carlo computer code in C++ is being written for simulation of primary particle collisions with simultaneously occurring surface growth of the forming aggregates. The initial part of the code, for aggregation of equal-size particles, has been completed and tested. Results show good agreement with available literature data. Future work will include programming and simulation of surface growth along with the particle aggregation.

Manganese Oxide Aerogels for Lithium Batteries

Principal Investigator: Arlon Hunt

Project No.: 96034

Funding: $75,100 (FY96)

Project Description

The goal of this project is to develop new manganese oxide aerogel materials for use in lithium batteries. It has been shown that lithium can be intercalated into a variety of host materials without causing significant structural changes. Reversible intercalation into those materials forms the basis for high-performance, rechargeable lithium batteries. The host materials may take up lithium in layers, channels, or into amorphous solid phases. Energy storage capacity of batteries made in this way depends on the total amount of lithium per mole of host material and the volume density of the host. Power delivered by the battery depends on the rate of lithium transport to and from the host material.

Previous research established that MnO_2 is an excellent intercalation medium for lithium insertion in battery applications. This earlier research explored battery materials based on manganese oxide powders. Until now there has been no reported research into the use and properties of manganese oxide aerogels. Potential advantages of MnO_2 aerogel for this application include high lithium storage capacity; greater power delivery due to the ease of lithium transport in the controllable, open pore nature of a MnO_2 aerogel; and simplified processing and manufacturing. MnO_2 powders and monoliths will be prepared using sol-gel processing and dried using carbon dioxide substitution and supercritical extraction techniques developed at Berkeley Lab. These substitution and extraction techniques provide an alternative to conventional powder processing of MnO_2, which involves grinding, the use of polymer binders, and incorporation into an electrode system.

Sol-gel processing is well-suited to forming materials with controllable pore size distribution and surface. Additionally, aerogel primary particles are extremely small, and therefore show a low free energy of crystallization. This results in an amorphous-to-crystalline phase transition at somewhat lower temperatures than materials prepared by classical methods. Other advantages of the sol-gel/aerogel processing include near-ambient temperature processing. The optimum order of crystallinity for lithium intercalation of these materials is not well-understood and will be explored in this research.

Accomplishments

The major tasks for this project were preparation and characterization of manganese oxide-based aerogels with suitable composition and structure for use in lithium-ion batteries. The synthesis of these materials drew on previous work in which various manganese oxides were prepared using a modified sol-gel approach. MnO_2 (or $Li_xMn_2O_4$) aerogels were synthesized to produce a high-surface-area material suitable for use in lithium-ion batteries. As there are no Mn^{IV} salts stable in aqueous solution, nor available Mn^{IV} alkoxides, their preparation involved the reduction of an aqueous permanganate solution by an organic acid. Ammonium permanganate produced α- or γ-Mn_2O_3 while the alkali permanganates formed mixed oxides such as $Li_xMn_yO_z$, which crystallize to a spinel phase at 500°C. Various approaches to produce these sol-gel compounds were explored until methods to produce suitable monolithic gels were established. Solvent substitution and carbon dioxide supercritical extraction were then used to produce the corresponding aerogels. After the aerogel materials were prepared and characterized, colloidal carbon was added during processing to improve the conductivity of the films. Properties evaluated include pore size distribution, specific surface area, phase and level of crystallinity, and ability to repeatedly intercalate lithium.

Characterization of the Aerogel Materials

X-ray diffraction analysis of fresh aerogels showed two broad, weak diffraction peaks at $2\theta = 37$ and 66 degrees. This did not give a satisfactory match with standard x-ray diffraction patterns for the target phases, but most closely matched $Li_{1-x}Mn_2O_4$. A sample of the aerogel that had been heated to 600°C in air for 18 hours gave a strong pattern that closely matched the standard x-ray diffraction file for Mn_2O_3 (bixbyite). However, this thermal treatment sintered the aerogel to ~20% of its original volume. Chemical analyses determined that the typical composition was 52% Mn, 4.2% C, 2.4% H, and 0.12% Li. This corresponds to a molecular formula of $Li_{0.02}MnO_{2.73}C_{0.37}H_{2.42}$. The presence of carbon is most likely due to oxalates (the oxidation product of fumaric acid), residual fumaric acid, or surface carbonates from the CO_2 drying process. The low level of lithium suspected from the x-ray results was confirmed by this analysis. The $LiMnO_2$ reported in earlier sol-gel research may have resulted from insufficient removal of lithium-containing products from the gel prior to drying and the ensuing incorporation of this gel into the manganese oxide phase during firing. TEM analysis showed a typical aerogel microstructure for this material with a three-dimensional connected network of very fine particles of ~ 100 Å in diameter. Nitrogen adsorption analysis yielded single point BET surface areas of 400 m^2/g. Multipoint nitrogen adsorption revealed material with total pore volume of 5.7 cm^3/g, and average pore diameter of 570 Å. The high surface areas and pore volumes are favorable for aerogel-based battery materials.

Test electrodes based on manganese oxide aerogels were prepared by mixing the aerogel with carbon powder (10/90%) and a small amount of PTFE binder. The mixture was mixed thoroughly with isopropanol, and pressed on to a thin nickel mesh. The electrode was then dried to remove the isopropanol and filled with a standard electrolyte, consisting of lithium hexafluorophosphate in propylene carbonate. Standard cyclic voltametry studies were then performed using a lithium metal anode. The initial charge cycle showed an unusual negative slope that was presumed to be caused by parasitic reactions at the aerogel surface. Subsequent cycles did not show this behavior. The same lithium metal anode acted as a battery for the next seven test cycles. The results suggest that this material could be improved by increasing lithium content in the fresh aerogel and by increasing the crystallinity of the aerogel (if this could be accomplished without significantly reducing the aerogel's surface area). Limited material preparation and evaluation will be continued to establish a firm basis for more extensive investigation of aerogel-based manganese oxide materials for rechargeable batteries.

Kinetics and Modeling of Anaerobic TCE Degradation for in situ and ex situ Applications

Principal Investigator: Jay Keasling

Project No.: 96008

Funding: $60,500 (FY96)

Project Description

Halogenated hydrocarbons are widely used as industrial solvents and are the most common contaminant of ground water aquifers. Trichloroethene (TCE), a volatile chlorinated organic compound, has been used extensively in metal and glass industries as a solvent and degreasing agent and in household products such as spot removers, rug cleaners, and air fresheners. The U.S. EPA has classified TCE as a priority pollutant on the basis of its widespread contamination, its possible carcinogenicity, and its anaerobic bioconversion to the more potent carcinogen vinyl chloride (VC). Due to its widespread use, many groundwater aquifers and waterways are contaminated with TCE. A large number of TCE-contaminated sites exist in Northern California, primarily at locations where silicon wafers were manufactured and at military air bases. Chlorinated hydrocarbons are the most frequently occurring contaminant of ground water at DOE facilities and waste sites. The DOE has reported that the ground water at 14 of its 18 facilities are contaminated with TCE at 0.2-to-980,000-mg/L levels and with tetrachloroethene (PCE) at 0.18-to-272,000-mg/L levels. The DOE spends approximately $330 million per year on cleaning sites contaminated with chlorinated hydrocarbons.

There are a number of methods to alleviate contamination of ground water by organic pollutants. These include physical containment; in situ treatment with chemicals or microorganisms; and withdrawal prior to physical, chemical, or biological treatment. One form of biological treatment of halogenated hydrocarbons, aerobic biodegradation, has been well studied and applied with limited success at a small number of sites. However, aerobic degradation is not always possible due to toxicity of intermediates, possible inhibitory levels of copper in the contamination site, inability to dechlorinate PCE, need to oxygenate the aquifer and the difficulty of doing so, and need to induce degradative pathways with toxic substances.

Anaerobic degradation of halogenated hydrocarbons may be more practical in some situations. Unfortunately, anaerobic degradation rates are several orders of magnitude lower than aerobic rates. Early work on anaerobic PCE and TCE biodegradation reported the accumulation of vinyl chloride, dichloroethene (DCE), and TCE under methanogenic conditions in batch cultures and in a continuous-flow fixed-film laboratory-scale column. Recently, complete dehalogenation of PCE to ethene by methanogenic cultures enriched from a wastewater treatment plant has been reported. We report here the complete reductive dehalogenation of PCE and TCE by anaerobic groundwater microorganisms.

Accomplishments

Degradation of Subsaturating Concentrations of Chlorinated Hydrocarbon

Recently, we enriched microorganisms from a TCE-contaminated aquifer to reductively dechlorinate TCE and PCE to ethene. These organisms were cultured on mineral medium containing yeast extract and glucose, acetate, formate or methanol. In 20 days, the culture grown in glucose degraded 0.5 µg/ml TCE to below detectable limits. In the three-month monitoring period, the intermediate product, *cis*-DCE, was degraded to VC and then to ethene. The cultures grown in acetate, formate, and methanol incompletely degraded TCE, resulting in the products DCE, VC, and ethene. The culture grown on glucose was later enriched on TCE to increase the degradation rates (Fig. 2). This enriched culture degraded 33 µg of TCE in 12 days with an apparent TCE degradation rate of 20 µg/L/day. This rate compares to the TCE degradation rate of the unenriched culture. However, the time required for complete conversion of TCE to ethene was significantly less. In separate experiments, we have shown that anaerobic TCE degradation will not occur in medium not inoculated with ground water samples (data not shown).

Degradation of Saturating Concentrations of Chlorinated Hydrocarbons

To examine the degradation of chlorinated hydrocarbon DNAPLs (Dense Non-Aqueous Phase Liquids), saturating amounts of the chlorinated hydrocarbon were maintained by ensuring that a separate organic phase of TCE or PCE remained in the bottom of the bottles. In contrast to the subsaturated

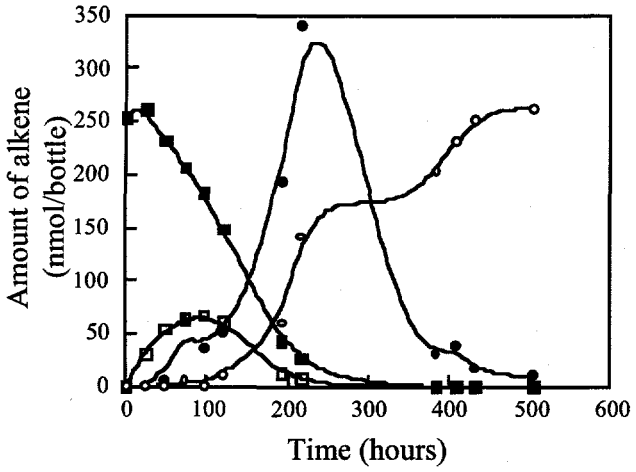

Figure 2. TCE degradation by enriched, groundwater microorganisms. Cultures from a groundwater microcosm were enriched in medium containing TCE and glucose. Filled squares: TCE. Open squares: cis-1,2-DCE. Filled circles: VC. Open circles: ethene.

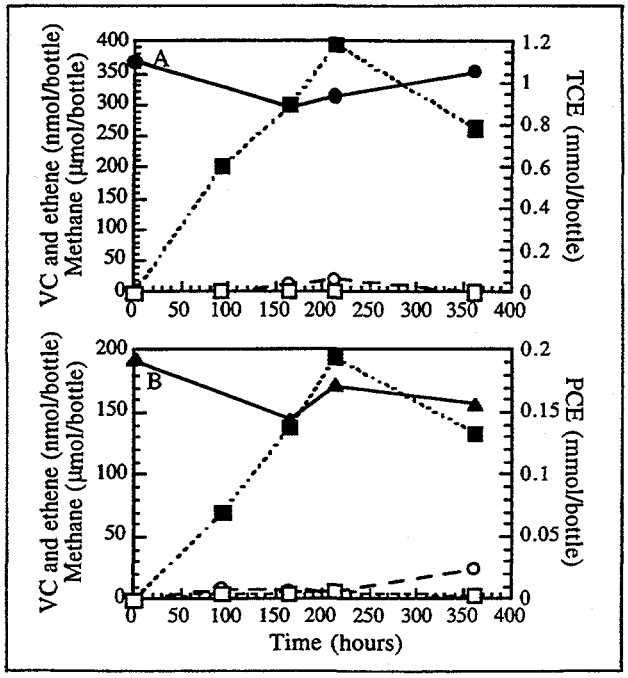

Figure 3. Reductive dechlorination of PCE and TCE and methane production under saturating conditions. (a) Degradation of PCE. (b) Degradation of TCE. Filled circles: TCE. Open circles: VC. Filled squares: ethene. Open squares: methane. Filled triangles: PCE.

cultures, cultures grown in the presence of saturating concentrations of TCE or PCE showed a rapid dechlorination to ethene with little or no VC detected (Fig. 3). Further, relatively little methane was produced, indicating that methanogenesis was inhibited.

The initial rates of VC and ethene accumulation vary significantly between the saturating and subsaturating cases. Accumulation of VC refers to the change in VC with time and is equal to the difference between the rate of production of VC from TCE or PCE ($V_{PCE \rightarrow VC}$) and the rate of degradation of VC to ethene ($V_{VC \rightarrow Ethene}$):

$$\frac{d(VC)}{dt} = V_{PCE \rightarrow VC} - V_{VC \rightarrow Ethene}.$$

For ethene, there is no consumption term. The initial rate of VC accumulation from subsaturating concentrations of TCE was eighteenfold higher than from saturating concentrations, whereas the initial rate of ethene accumulation under saturating conditions was over 100 times the initial rate under subsaturating conditions (Table 1). A similar relationship was observed for saturating and subsaturating concentrations of PCE. The rates of TCE or PCE disappearance for the saturating case could not be measured, since their concentrations in the headspace of the bottle did not change (Fig. 3).

However, the generation of VC and ethene is a goodindication of TCE and PCE degradation rates: the sums of the VC and ethene accumulation rates were approximately the same in the presence of saturating or subsaturating concentrations of TCE and were very similar in the presence of PCE.

Implications of Research

The results presented here have important implications for the treatment of highly-contaminated groundwater aquifers. Being more dense than water, chlorinated ethenes sink to the clay-containing aquitard at the bottom of groundwater aquifers, where they accumulate as DNAPLs. This aquitard region may be highly anaerobic and conducive to anaerobic bioremediation strategies. Although the anaerobic remediation of subsaturating amounts of chlorinated ethenes is known to produce nearly stoichiometric amounts of VC, the results from this work demonstrate that a microbial consortium enriched from TCE-contaminated groundwater can dechlorinate saturating concentrations of TCE or PCE

Table 1. Initial rates of VC, ethene, and methane accumulation during the reductive dechlorination of TCE and PCE under saturating and subsaturating conditions. For the TCE and PCE cases, the units are nmol/hr/mg protein for the VC and ethene accumulation rates and μmol/hr/mg protein for the methane production rates.

	VC accumulation rate	Ethene accumulation rate	Methane production rate
	(nmol/hr/mg protein)	(nmol/hr/mg protein)	(μmol/hr/mg protein)
TCE			
subsaturation	3.66	0.03	1.47
saturation	0.20	3.67	0.02
PCE			
subsaturation	0.71	0.06	1.30
saturation	0.06	1.80	0.05

to ethene directly (or very quickly) with little or no detectable VC. These results imply that a suitable electron donor added to groundwater aquifer contaminated with TCE or PCE DNAPLs could directly convert most of the TCE or PCE to ethene while the DNAPL is still present. Only a small fraction of the TCE or PCE originally present would be converted to ethene through VC after the DNAPL disappeared.

Publications

R.B. Nielsen and J.D. Keasling, "Reductive Dechlorination of Chlorinated Ethene DNAPLs by a Culture Enriched from Contaminated Groundwater," submitted to *Appl. Environ. Microbiol* (1996).

D.G. Bolesch, R.B. Nielsen, and J.D. Keasling, "Complete Reductive Dechlorination of Trichloroethene by a Groundwater Microbial Consortium," *Ann. New York Acad. Sci.*, in press (1996).

Decontamination Technology for Marine Sediments

Principal Investigator: Rolf Mehlhorn

Project No.: 96035

Funding: $5,900 (FY96)

Project Description

The purpose of this project is to acquire data for a novel decontamination technology for marine sediments. The technical approach consists of synthesizing contaminants labeled with paramagnetic "reporter groups" to trace the binding and release of broad classes of contaminants and using the labeled compounds to further test a decontamination scheme based on surfactant-mediated release of insoluble compounds from sediments. A significant element of the proposed decontamination scheme is the recovery of contaminants and surfactants in concentrated form, which offers advantages of facilitated disposal or reuse of both contaminants and surfactants. Specifically targeted contaminant classes include heavily chlorinated hydrocarbons (PCBs) and toxic heavy metals. Both have been identified as priority pollutants, and are of particular concern in harbors that require periodic dredging.

The initial focus was to be on using fatty acids to solubilize hydrophobic contaminants in seawater and separate them from sediments by a simple settling out of the sediments, which would cause the contaminants to remain suspended in the water. Based on our studies of the interactions of inorganic mercury with algae, we anticipated that toxic heavy metals would selectively bind to the fatty acid micelles under appropriate pH manipulations. Another aspect of the envisioned process was to separate the contaminants from the seawater by manipulating the surfactant charge and causing it to aggregate along with the contaminants. Finally, contaminants were to be separated from the surfactant so that the surfactants could be re-used. This aspect of the project was acknowledged to be more challenging and was to be conducted after the requested funding period, assuming that followup funding from extramural sources could be obtained. However, even in the absence of further research funding, it was felt that the data acquired during a

one-year effort would be adequate to define this sediment decontamination process.

Accomplishments

The major accomplishments of this project were:

- Synthesis of new paramagnetic tools for analyzing the interaction of contaminants with sediments or soils and for developing decontamination procedures.
- Surprising discovery that these tools could be used to discriminate between biotic and abiotic processes, including redox reactions.
- Discovery that hydrophobic contaminants modeled by our compounds rapidly partition into marine sediments, forming aggregates that become increasingly difficult to remove with surfactants as a function of time.
- Discovery that weak acid- and primary amine-containing surfactants are ineffective for stripping contaminants out of sediments, but that other surfactants with more strongly acidic or basic charge groups are highly effective in completely removing such contaminants under appropriate conditions.
- Development of a novel procedure for separating surfactant-mobilized contaminants from water, allowing for recovery in concentrated form of both contaminants and surfactants.

One highlight of the work was the introduction of a new methodology for environmental studies. The attachment of paramagnetic reporter groups to organic pollutants allows for a considerably more detailed analysis of molecular interactions governing the retention and mobilization of such compounds in particulate matrices (e.g., in soils, humic materials, and sediments as well as in the tissues of plants and animals) than is afforded by more conventional methodologies. Simple ESR measurements allowed us to demonstrate that the hydrophobic contaminants modeled by our probes partition into sediments in aggregated form, and that aggregation increases with time and correlates inversely with the effectiveness of surfactants as solubilizing agents. Moreover, we observed a potent reducing activity in sediments obtained from San Francisco Bay and could ascribe the bulk of this activity to living organisms by comparing the behavior of different probes. We conclude that the new methodology has great potential in the environmental management area.

Publications

R.J. Mehlhorn and C. Feliciano, "Synthesis of Paramagnetically-Labeled Chlorinated Aromatic Hydrocarbons for Environmental Studies," at the following URL: **`http://csee.lbl.gov/isolation/Feliciano/index.html`**. This Web page describes synthetic procedures for attaching paramagnetic report groups to pentachlorobenzene moieties.

Composition and Sources of Marine Cloud Condensation Nuclei

Principal Investigator: Tihomir Novakov

Project No.: 96036

Funding: $74,900 (FY96)

Project Description

The objective of this project is to experimentally determine the role of organic aerosol components in determining the optical properties and cloud condensation nucleus (CCN) activity of atmospheric aerosols. Particular emphasis is on testing the possibility that background oceanic aerosols have a large organic—possibly natural—component. Knowing the composition of background aerosols and CCN is crucial for assessing anthropogenic influences on radiative transfer and cloud microphysics.

Our approach to this research involves measurement and interpretation of physical and chemical properties of aerosols at two marine sites, and chemical analysis of airborne samples collected off the polluted eastern coast (onshore and offshore) of the United States. The two marine sites are Point Reyes, California, and Cape San Juan, Puerto Rico, complemented by recently initiated shipboard measurements in the tropical trade wind air masses. The Caribbean studies are conducted in collaboration with Professor O. Rosario of the Chemistry Department, University of Puerto Rico. Model interpretation of results was performed at LLNL by Drs. J.E. Penner and C. Chuang. The airborne study was performed in collaboration with Professors P.V. Hobbs and D.A. Hegg of the Department of Atmospheric Science, University of Washington.

Accomplishments

Marine Aerosols

Analyses of Cape San Juan samples show that:

- Submicron particulate organic aerosol material, OC_p, (average about 400 ng m^{-3}) exceed sulfate concentrations (average about 250 ng m^{-3}).
- This organic aerosol material is water soluble (i.e., cloud condensation nucleus active).
- Primary combustion aerosol does not appear to be a major contributor to OC_P.

The fact that OC_P concentrations measured at the coastal site are similar to OC_P concentrations (330 to 400 ng m^{-3}) measured at the Atlantic Ocean site removed from the coast suggests that a substantial fraction of the OC_P in the Caribbean trade winds may be associated with oceanic background aerosol. A model was used to estimate how much of the effect on cloud albedos was due to the addition of anthropogenic sulfate aerosol to this marine background aerosol. Results imply that the indirect forcing of climate that results from anthropogenic sulfate aerosol could be substantially overestimated if background organic marine aerosol are not included.

Anthropogenic Aerosols

Airborne measurements over the polluted eastern coast of the United States, of total aerosol and carbonaceous mass, together with concurrent measurements of aerosol light-absorption and light-scattering coefficients, reveal an important role for carbonaceous particles in both light-absorption and light-scattering. The carbon mass was, on average, 50% of the total aerosol mass—significantly higher than has been previously found. The carbon mass fraction tended to increase with altitude, suggesting that ground-based measurements can significantly underestimate the importance of carbon species in the aerosol mass budget. The aerosol carbon mass was significantly correlated with both aerosol light absorption and light scattering. The high correlations between the total carbon mass and aerosol light-scattering coefficient clearly establish the importance of carbon species in aerosol light-scattering and absorption on the East Coast of the United States.

Publications

T. Novakov, C.E. Corrigan, J.E. Penner, C.C. Chuang, O. Rosario, and O.L. Mayol Bracero, "Organic Aerosols in the Caribbean Trade Winds," accepted by *J. Geophys. Res.* (1996).

T. Novakov, D.A. Hegg, and P.V. Hobbs, "Airborne Measurements of Carbonaceous Aerosols on the East Coast of the United States," submitted to *J. Geophys. Res.*

Metal-Specific Chemical Sensors Using Polymer Films for Non-Proliferation and Environmental Applications

Principal Investigators: Richard Russo and Richard Fish

Project No.: 96009

Funding: $81,100 (FY96)

Project Description

This project was to demonstrate a prototype metal-specific optical-fiber sensor using Berkeley Lab-patented functionalized polymer technology. The goal was to establish system characteristics that would achieve the sensitivity and selectivity necessary for monitoring contaminants in aqueous environments. Such a sensor would have application within DOE non-proliferation and environmental waste management programs. A computer-based optical-fiber spectrometer system was developed and used to study the behavior of this sensor technology for a model heavy metal toxic chemical species. A transmission and reflection optical fiber system was developed and tested.

A critical technological area facing DOE is in-situ, real-time detection of chemical species in the environment. Such detection has waste management and non-proliferation applications. Some chemical species of concern include uranium, plutonium, lead, cadmium, chromium, and other toxic elements. For non-proliferation, requirements include ultra-sensitive chemical detection of fission products, activation products, and actinides. The DOE needs small, rugged, inexpensive sensors to measure these chemical species at concentration levels too minute for existing technologies. The research goal was to demonstrate sensors for these chemical species using a new (patented) polymer-pendant ligand technology that is unique to the Berkeley Lab. The polymers were invented here in the Energy and Environment Division and can be tailored to monitor any toxic element. Importantly, the polymer-pendant ligands

change color as the specific chemical of interest is incorporated into the matrix. Another unique property of the functionalized polymers is that they exhibit wavelength shifts in their absorption and emission spectra as the metal is incorporated, and the wavelength shift is specific for the individual metals. These characteristics of element specificity and wavelength identification are ideal for optical fiber sensors, and have not been previously available. The color change can be used to indicate presence of a toxic element and its concentration. The selected polymers were previously developed as bulk materials and have never been tested as chemical sensors. In this research effort, these polymers were employed in several model toxic solutions and an optical fiber spectrometer was developed to study/monitor the color change.

Accomplishments

A handheld computer-card spectrometer was purchased and developed into a reflectance and transmission probe using optical fibers. A small incandescent light source was coupled to the spectrometer also using optical fibers. Several months were devoted to developing this spectrometer system, including establishing software support. By using this optical fiber spectrometer, our research represented the first investigation of chemically-modified functionalized polymers as chemical sensors. The Fe-specific polymer PS-3,3-LICAMS was tested for sensitivity and kinetics of response. We proved that reflectance could be used to monitor the color change of the polymer bead as Fe(3+) was extracted from the aqueous solution. Sensitivity was not accurately determined but was estimated to be at the 100 ppm level. This detection level is much greater than that required for environmental and non-proliferation applications, and was limited by the low diffuse reflectance light levels. An alternate optical absorption approach was tested in which the solution color change was monitored as the polymer-pendant ligands removed species from solution. This absorption approach was also only sensitive in the part per million range. Based on this research, we proposed that a direct fluorescence approach would be necessary to achieve the sensitivity levels required for environmental and non-proliferation applications. Fluorescent dyes would have to be attached to the polymer-pendant ligands to achieve this detection capability.

An alternate approach to achieve improved sensitivity would be to coat the polymer pendant ligands as thin films on optically transparent substrates. Preliminary chemistry for achieving this coating was tested and found to be unsuccessful. An in-depth research effort would be necessary to convert the polymer pendant ligands into thin-film form.

This research was successful in demonstrating the coupling of polymer-pendant ligand metal specificity with optical fiber spectrometer as a potential chemical sensor, and in identifying the necessary improvements to achieve better sensitivity. However, because of the poor sensitivity levels achieved with the initial system, this work has not been submitted for publication.

Building Performance Assurance with Building Life-Cycle Information Systems

Principal Investigators: Stephen Selkowitz, Mary Ann Piette, Frank Olken, and Max Sherman

Project No.: 95009

Funding: $278,800 (FY96)
$369,800 (FY95)

Project Description

Despite significant advances in building technology and the promulgation of tighter building standards, buildings still consume one third of all U.S. energy, at a cost of $200 billion per year, with $85 billion used in commercial buildings. Half of this consumption is very likely wasted, compared to what could be achieved. The goal of this project is to explore technical underpinnings of a new approach to life-cycle intervention that can increase building resource efficiency. The long-term goal is not only to capture wasted energy in the commercial building sector, but to provide even greater financial savings for building owners by improving comfort and productivity in conjunction with energy-related workplace improvements.

Our activities in the second year of this project continued along the three parallel tracks developed in the first year:

- First, we used our understanding of building physics and decision-making needs and the Berkeley Lab's computer science and information systems expertise to develop the conceptual framework for a life-cycle building information

system. This information system—which represents both the decision-making process and physical building elements, and all their performance attributes over time—must accommodate the needs of many different simulation tools and users. It must be sufficiently robust to adapt to growth and expansion as well as to inevitable changes in computer hardware and software over time.

- Second, we demonstrated the specific benefits of using such an approach by developing several new tools and building assessment procedures that: utilize the new information system, capture new data from the building, and add value for building owners and occupants (for example, by tuning building performance in the commissioning phase and tracking performance over time). This work took place in an occupied testbed (Soda Hall at UC Berkeley) and involved investigations of sensor needs and data-acquisition systems.
- Finally, we continued to develop partnerships with key building industry decision-makers for continuation of our research and implementation efforts.

Accomplishments

During the second year of the project, we made substantial progress developing and demonstrating prototype software, and increasing industry interest in these new approaches to building energy management. One example is Building Life-Cycle Information Systems (BLISS), which is intended to provide a distributed computing environment for managing, archiving, and providing access to a wide variety of data generated across the complete life cycle of a building project. BLISS requires standardization both in a common building database model and in the mechanisms for transferring data and information between tools. Several components are considered to be necessary in order to achieve the desired functionality of BLISS, including a common information repository, a data exchange mechanism, process and work flow management, and a user interface. We are developing an object-oriented data model for managing component-based building information, and a time-series database for managing performance measurements from an occupied building. The integration of these models will serve as our common information repository. We are continuing to work with the International Alliance for Interoperability (IAI) to develop a STEP-based standard building model; we will incorporate this work, as it becomes viable, into our model.

A principal goal of the project is to provide decision-makers with the information needed to cost-effectively assure desired performance of a building across its life cycle. A fundamental requirement for achieving this goal is the explicit specification of performance objectives to define the functional and operational needs of the building's owners and occupants. Performance objectives provide benchmark metrics that can be used to evaluate: alternative solutions during design, as-built performance during commissioning, and day-to-day performance during occupancy. Specification of performance objectives thus needs to be documented in a manner that can be tracked across the building life cycle. We have developed a prototype design intent tool for specifying and tracking performance objectives.

Following construction, buildings should be carefully commissioned to ensure that the systems and components function in accordance with the design intent. During 1996, we finalized and tested the Chiller Commissioning Toolkit at Soda Hall to demonstrate how design and as-built equipment specifications differ. This software also serves to archive commissioning tests and test results, serving as the starting point for ongoing performance tracking.

The Performance Evaluation and Tracking Tool compares measured performance of the HVAC system to emulated performance with the objective of either identifying deviations from expected performance or suggesting better control schemes. The tracking tool has capability to manipulate measured data or instigate emulation runs as required. Measured data collected during commissioning and early operation is used to calibrate the component models, which set the standard for expected performance. The need for such calibration is illustrated by Fig. 4 which compares measured performance to calculated performance. The initial calculations use data supplied by the manufacturer, illustrating the inadequacy of relying on manufacturers' data for an accurate tracking tool. We recalibrate the chiller performance model using measured data ensuring that simulated performance will closely match actual performance. We extended chiller models to include cooling towers and performed detailed error analysis. These models illustrated that optimal control of chillers and towers could result in thousands of

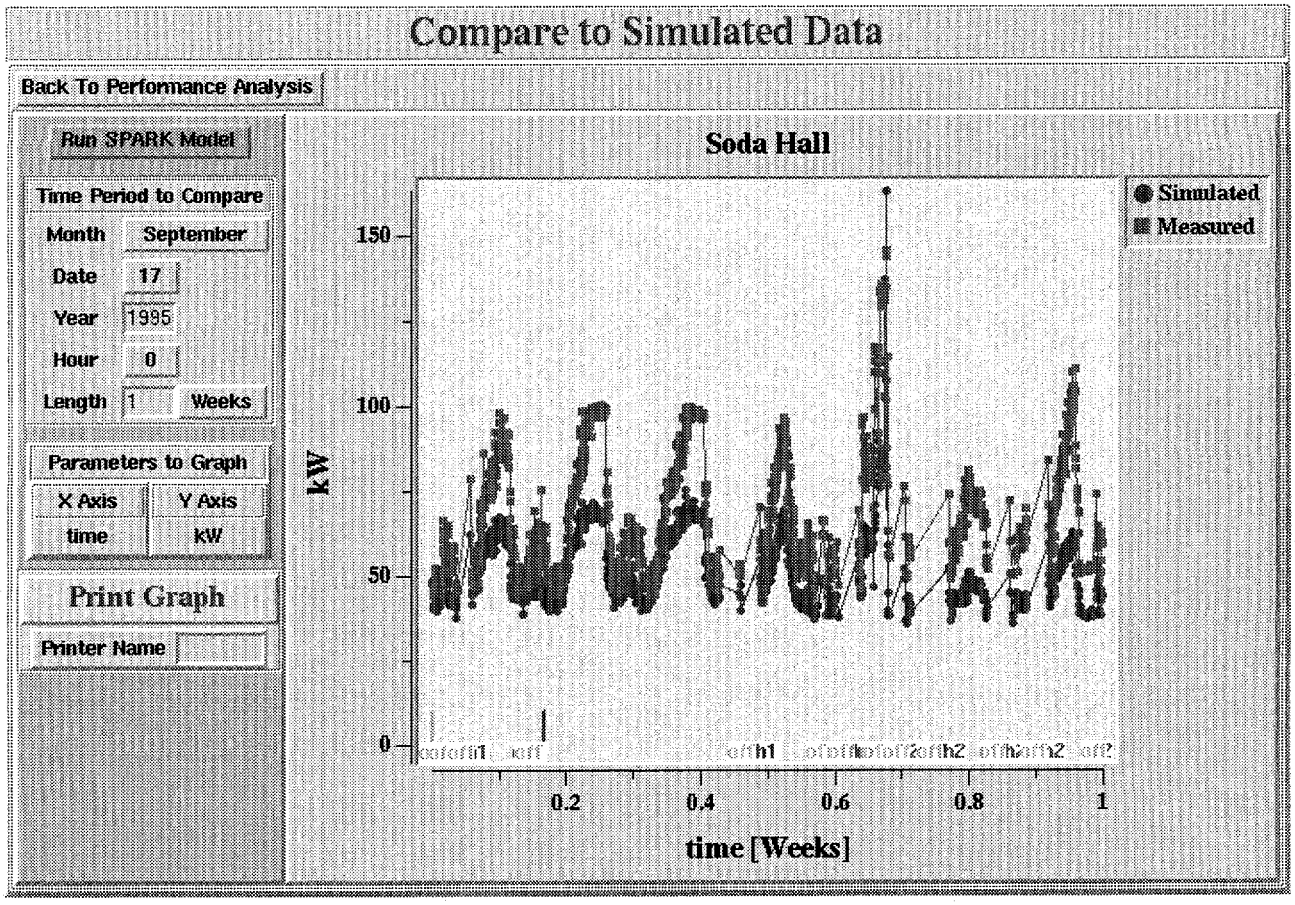

Figure 4. Comparison of measured chiller data to simulations based on manufacturer's data. The discrepancy between the two illustrates the need for new calibrated chiller performance models.

dollars of energy savings at Soda Hall. (Several recommendations from our studies have been adopted by its building operators.) We also have demonstrated that the as-built design for this campus building has a cooling capacity that is 250% greater than actually required, a vivid illustration of the value of our research. Incorporation of our findings into standard building practice thus has many potential benefits.

In order to explain the overall building performance concept to potential industrial partners, we created a computer tool demonstration package using our prototypes and a related videotape of its operation. This collapses 2 to 3 years of the building life cycle into a 20-minute sequence and has proved very valuable in explaining our concepts to others.

Publications

R.J. Hitchcock, "Improving Building Life-Cycle Information Management through Documentation of Project Objectives and Design Rationale," Ph.D. dissertation, University of California at Berkeley, December 1996.

R.J. Hitchcock, J. Thorpe, "Building Performance Assurance: Building Life-Cycle Information Systems," a promotional video tape showing the BPA software mockup, 1996.

R.J. Hitchcock, S.S. Selkowitz, J. Thorpe, "Building Life-Cycle Information System Prototype," poster presentation at ACEEE Summer Study on Energy Efficient in Buildings, Pacific Grove, California, August 25–31, 1996.

M.A. Piette, "Commissioning Tools for Life-Cycle Building Performance Assurance," LBNL 38979, *Proceedings of the Fourth National Conference on Building Commissioning*, St. Petersburg Beach, Florida, April 1996.

S.R. Meyers, "Chiller Modeling Error Analysis: Implications for Energy-Saving Retrofits and Control Strategies," Masters' thesis, University of California at Berkeley, Mechanical Engineering Department, May 1996.

Engineering Division

Development of Next-Generation Detectors for Use at the Advanced Light Source

Principal Investigators: Eugene Binnall, Joseph Katz, Charles Fadley, Helmuth Spieler, and Jorge Zaninovich

Project No.: 96010

Funding: $119,800 (FY96)

Project Description

The purpose of this project is to develop a next-generation high-spatial-resolution and high-speed detector for electrons, photons, and ions that will be of use in various advanced spectroscopies. Such a detector will permit taking full advantage of the high-brightness radiation that is now available from the Advanced Light Source (ALS). It is clear that such detectors are crucial to the science that will be carried out there. More specifically, a high fraction of the spectroscopy that will be done at the ALS will involve the photoexcitation of electrons (e.g., photoelectrons, Auger electrons, or some form of secondary electrons) and their ultimate resolution in energy. Other important studies will measure x-ray emission following photoexcitation, absorption, or scattering by ALS radiation, again resolved in energy. In both cases, the highest-resolution spectra are obtained by using some sort of spectrometer to disperse the electrons/photons over a spatial coordinate that is nearly linear in energy. Being able to detect spectra dispersed over the focal plane in a multichannel mode vastly increases data acquisition rates, provided that the physical width of each counting channel is sufficiently narrow (to avoid undesirable loss in energy resolution), and that each channel can count at a high enough rate (to avoid nonlinearity and saturation effects). Working in a pulse-counting mode rather than a current-integrating mode (as might be appropriate with charge-coupled devices) is also important because of the broad dynamic range that may be encountered from one spectral peak to another or from one type of experiment to another. Such detectors will find wide use at the ALS and elsewhere in fields such as photoelectron spectroscopy, diffraction, and holography; x-ray absorption and fluorescence spectroscopy; mass spectrometry and surface analysis using electron and ion probes; laser spectroscopy; and atomic and molecular physics.

At present, no multichannel detectors will count at rates sufficiently high enough to accommodate the fluxes expected from various experiments at the ALS (or indeed even those using various laboratory photon, electron, or ion sources). For many experiments, without faster detectors we are therefore in the situation of having to close down the slits to reduce effective ALS source brightness and avoid detector saturation. To illustrate the nature of the multichannel counting problem, it is a simple matter to calculate the photoelectron intensities that will be emitted from a solid sample by the radiation from an undulator at the ALS. With a total incident flux of 6×10^{12}/s and after passage through a high-transmission electrostatic deflection analyzer, the total counts in a typical core- or valence-level peak (e.g., C 1s or Fe 3d) will be in the 10 MHz to 1 GHz range. To this is usually added an inelastically-scattered background that would lead to even higher overall rates on the detector. It is necessary to spatially resolve this spectrum-plus-background into 100 to 1000 channels, with each channel then corresponding to a different kinetic energy value. The optimum present technical approach to such a system is to use a microchannel-plate (MCP) electron multiplier as the first stage and then a series of discrete line collectors behind this, each of which has its own integrated-circuit preamplifier and counter. The best commercially available detector of this type is from Integrated Sensors in the U.K. It has 116 separate collectors, each of which can count at a rate of 100 kHz, thus yielding a total of only about 12 MHz overall. The individual collector channels in this detector are also too wide, at 160 microns, to avoid significant resolution loss in energy; collectors of 50 microns or less are needed to achieve the overall energy resolutions of $1:10^4$ that are desired in a typical high-resolution analyzer of ~20 cm radius. Our goal in this project has been to develop a higher-spatial-resolution multichannel detector with GHz count-rate capability.

This project combines integrated-circuit technology developed at Berkeley Lab for the SDC (Silicon Detector Collaboration) particle physics detector with a specially-designed counter IC (integrated circuit) to create a next-generation multichannel detection system that will be significantly superior to any currently available. The Berkeley Lab detector makes use of 12 64-channel sets of two ICs. The first IC in each set provides a fast, low-noise preamplifier-shaper-discriminator for each channel, and was originally developed for the SDC silicon tracker at the Superconducting Super Collider (SSC). The second IC is a double-buffered counter (DBC), specifically developed in this project, but also potentially useful for particle physics applications. This IC includes 64 16-bit counters with a buffered multiplexed readout. The 16-bit counters allow for over 20 ms of data accumulation before overflow at a maximum input rate of 1.5 MHz per channel. Transferring data after this counting interval requires only 100 ns, leading to a deadtime fraction of $<1{:}10^5$. The channel widths are only 50 microns, and thus are compatible with measuring at overall resolutions of $1{:}10^4$ in systems such as those now in use at the ALS. The overall count-rate capability of ~1.2 GHz over our 768 channels at 1.5 MHz will thus be a hundred times better than that of the best commercially available counter–and the new detector also has approximately seven times more channels. For many cases, this will permit the taking of spectra in a single rapid "snapshot" approach without any scanning of the analyzer deflection parameters; e.g., a single photoelectron spectrum could thus be obtained in as little as 10^{-2} to 10^{-3} second, compared to the minutes that are often now required.

Accomplishments

Several things have been accomplished over the past year, including:

- A complete set of electronics support systems has been debugged and shown to work. This included the MCPs (microchannel plates), power supplies, and the computer interfaces designed to monitor the system performance.
- A microchannel plate characterization and test vehicle has been assembled. A new clamp-heat sink was designed and installed to cure MCP thermal runaway problems found in the original design. This test device provided the means to test the MCPs, enabling the measurements of wall current, temperature stability, modal gain (see Fig. 1), dark noise count, etc.
- The Digital Signal Processor (DSP) hardware interface was debugged, and the DSP assembly and associated personal computer (PC) C-codes were designed and tested. These codes manage the transfer of information between the detector counters and the PC for display.
- A second generation alumina substrate was designed, fabricated, and fully populated with active and passive devices. The new thinner substrate provides a reduced thermal impedance while still providing the required mechanical support. Electronics redesign solved some interface problems. This newly assembled hardware is ready for testing. (See example of substrate with mounted components in Fig. 2).
- A new vacuum pumping system was installed, providing for a much faster turnaround operation mode. The vacuum can now be broken and the system pumped down to operational vacuum within the same day.

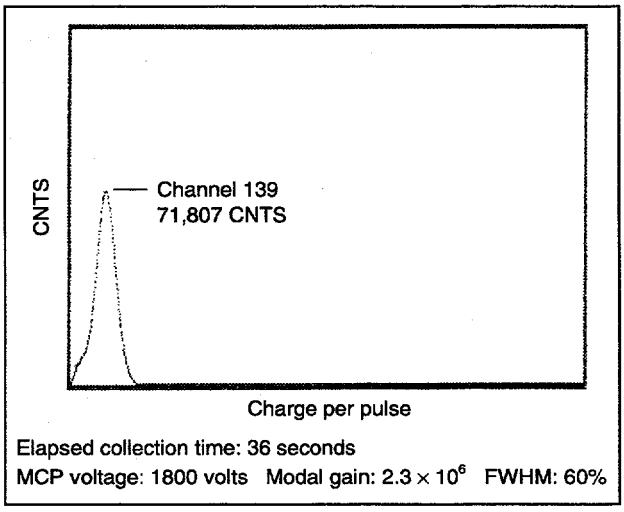

Figure 1. MCP output pulse height analysis.

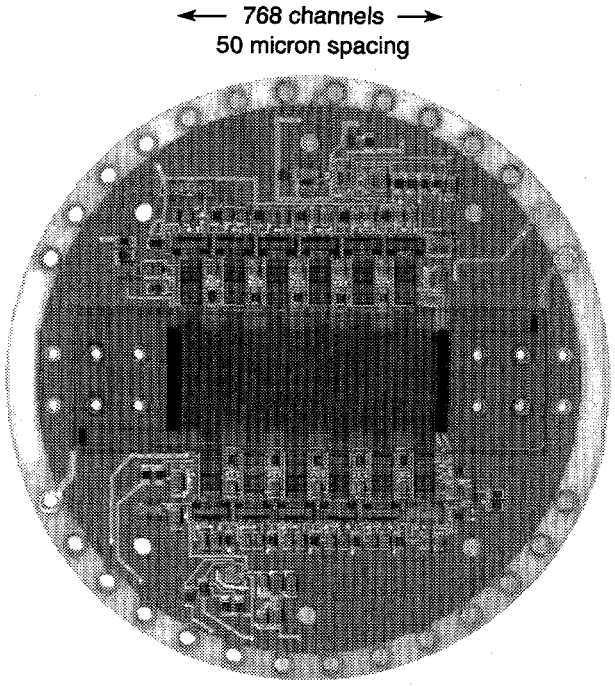

Figure 2. Next-generation high-speed multichannel detector.

Non-Destructive Evaluation and Testing of Vehicle Bodies and Components

Principal Investigators: Deborah Hopkins, Bill Edwards, and Carol Corradi (Engineering Division); Kurt Nihei, Larry Myer, and Seiji Nakagawa (Earth Sciences Division)

Project No.: 96011

Funding: $50,100 (FY96)

Project Description

The purpose of the project is to determine the ability of non-destructive acoustic wave techniques to characterize and evaluate adhesively-bonded joints in automotive structures. Laboratory experiments were performed on six test specimens supplied by the Ford Motor Company: three aluminum and three steel samples, all with adhesively-bonded lap joints.

The samples were identical except for the properties of the joint. For both the steel and aluminum samples, one specimen had a *perfectly* bonded joint, one had a three-inch gap in the joint with no adhesive, and one had a three-inch piece of slip-paper in the joint.

Accomplishments

The samples were evaluated using three acoustic wave techniques: pulse transmission using P-wave contact transducers, global resonance, and local resonance using an acoustical hammer (see Fig. 3). As shown in the figure, the defects in the joints were easily detected by all three methods. The effect of the defects on acoustic wave properties included a loss in amplitude and change in frequency content for propagating waves, a shift in resonance peaks, and a change in the amplitude response of the samples.

In conjunction with the laboratory experiments, the resonance properties of the samples provided by Ford

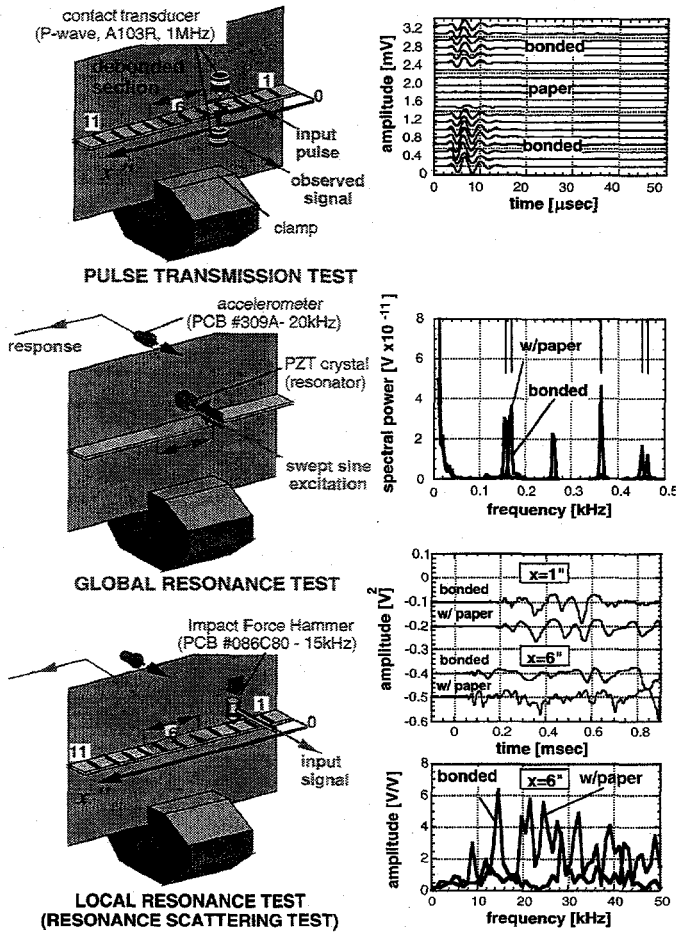

Figure 3. Aluminum and steel specimens provided by the Ford Motor Company were evaluated using pulse transmission, global resonance, and local resonance techniques. As shown in the plots, defects in the joints were easily detected by all three methods. Results shown are for steel samples.

were evaluated using finite-element modeling (see Fig. 4). The modeling results were used to provide guidance in the design of laboratory experiments, and to help in the interpretation of results from laboratory resonance experiments. Four cases were evaluated:

1. Solid aluminum structure with no joint,
2. Continuously bonded epoxy joint,
3. Continuously bonded epoxy joint with half the modulus of Case 2, and
4. Epoxy joint with a three-inch gap with no adhesive.

The finite-element model analysis showed a change in the resonance frequencies for the case of an epoxy joint with a gap in the adhesive (Case 4). The mode-shapes for the three cases with epoxy joints were all similar (Cases 2, 3, and 4), but were different from the mode-shape for the baseline case of a solid aluminum structure with no joint (Case 1).

In summary, acoustic wave propagation and global and local resonance techniques were all demonstrated to be feasible non-destructive test methods for evaluating adhesively-bonded joints (see Fig. 3). In addition, finite-element modeling of the test specimens supplied by Ford was performed, and was shown to be a valuable tool in providing guidance in laboratory experiments and helping in the interpretation of laboratory results (see Fig. 4).

This effort generated significant interest. Follow-on funding was obtained from the Office of Transportation Technologies (OTT), DOE. Next, based on project results presented to the Ford Motor Company in Detroit in February 1996, Ford actively supported LBNL efforts to obtain long-term DOE funding by

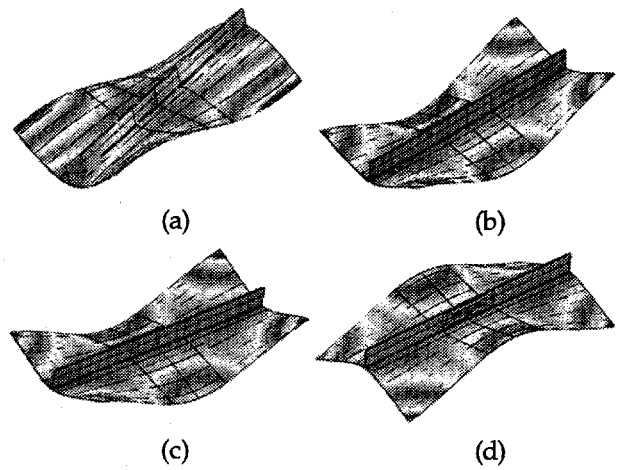

Figure 4. Finite-element modeling of the test specimens provided by Ford was performed to guide laboratory experiment design and to help in the interpretation of experimental results. The pictures above show contours of displacement superposed on mode-shape plots for the same resonant mode for four cases: a) Solid aluminum structure with no joint. Frequency: 235 Hz. b) Continuously bonded epoxy joint. Frequency: 234 Hz. c) Continuously bonded epoxy joint with half the modulus of Case b. Frequency: 233 Hz. d) Epoxy joint with a three-inch gap with no adhesive. Frequency: 220 Hz.

securing the support of GM and Chrysler as required by DOE for proposals submitted under the auspices of the Partnership for New Generation Vehicles. Ford also has promised technical support, including fabrication of test specimens, for experiments at LBNL. Finally, a collaborative effort was initiated with researchers at NIST and the University of Colorado to develop non-contact sensors for manufacturing applications.

Information and Computing Sciences Division

High-Speed Distributed Data Handling

Principal Investigators: William Johnston, William Greiman, and Brian Tierney

Project No.: 96012

Funding: $216,800 (FY96)

Project Description

Large-scale science collaborations are global in extent. Because scientific laboratories are becoming "virtual" laboratories (collaboratories), large-scale, high performance computational and data storage systems will have to be widely distributed in order to achieve the necessary parallelism. All of these circumstances argue that data-intensive, computational-intensive, and collaboration-intensive activities will, in the future, always be supported by wide area network-based resources. The RHIC-STAR experiment clearly fits into this model, and the emerging technology of widely distributed computing and storage systems will be needed to support this activity. We propose to design, document, and construct prototype distributed computing and storage systems that will demonstrate the capability of supporting large-scale, widely dispersed experiments like RHIC-STAR.

Based on the currently available research results on tightly coupled distributed systems, we will:

- Design and implement a prototype, configurable, wide area network-based computational environment.
- Establish the design parameters for distributed access to STAR data.
- Construct and demonstrate a network-distributed storage system that will use the new high speed ESNet backbone to give high speed access to large quantities of data from many ESNet sites (i.e., potential STAR data analysis sites).

Accomplishments

Several configurations of OC-3 (155 Mb/s) ATM networks, a distributed-parallel storage system, and a simulated "detector" with local buffering were used to feed data to the distributed storage system. A variety of tests exercised the configurations for high-speed data stream experiments. Multimegabyte data rates were obtained, together with the information needed to go to the multiple tens of megabytes level.

The XDR data access modules for the STAR analysis code were enhanced to incorporate the distributed storage system as a data source. Early experiments were conducted, and the knowledge needed to use this prototype with the production analysis code was obtained.

Scientific Computing on Networks of Workstations

Principal Investigators: William Johnston and Horst Simon

Project No.: 96037

Funding: $129,200 (FY96)

Project Description

We propose to implement a prototype-production Network of Workstations (NOW) computing architecture to uniformly address the three aspects of computational science: numerical simulation, real-time experiment control, and large-scale data analysis. We propose an evaluation methodology that involves identifying a set of problems from each of the aforementioned areas, and then implementing each in a prototype-production NOW environment. In addition to providing the computation requirements and integration for each of these problems, we will

evaluate the difficulty and effectiveness of the NOW approach in the scientific environment. Our goal is to install a NOW cluster at Berkeley Lab and evaluate its utility to the scientific community by carefully examining the issues encountered during its use as a "prototype" production facility.

Accomplishments

Although this project nominally started in FY97, most of the hardware platform was obtained in FY96. The two donated Sun E-4000 8 CPU servers were installed and configured. The disk arrays were configured, and the systems were configured onto both Ethernet and OC-3 ATM networks. The OS-12 ATMc network equipment was obtained and assembled. MPI was installed and tested, and initial performance tests were conducted.

Life Sciences Division

Computational Investigation of Chromatin Structure

Principal Investigators: Aloke Chatterjee, William Holley, Saira Mian, and Björn Rydberg

Project No.: 96013

Funding: $80,000 (FY96)

Project Description

Information in DNA is not limited to sequence information. Many current models for eukaryotic gene activation and regulation postulate that higher order chromatin structures act as major modulators of gene function. The association of specific proteins with eukaryotic DNA leads to the formation of nucleosomes, the unit particles of chromatin. Nucleosomes are packed upon one another to generate regular arrays, and chromatin is often seen to be in the form of ~30-nm-diameter fibers. Electron microscopic studies of intact chromosomes suggest that the 30 nm fiber is further folded and organized into a series of subdomains of distinct character. The primary aim of the proposed research is to explore different models for this fiber and examine its higher order organization to gain a more coherent view of the complex global structure of chromosomes.

At present, several models describe nucleosome and linker DNA organization within the basic chromatin fiber. The commonly accepted model is known as the 30-nm-solenoidal model. In our version of this model, the solenoid consists of 20 helical turns with six nucleosomes per turn organized in a manner to be contained within 30 nm. Each nucleosome-linker unit contains 171 base pairs (bp) of B-form DNA wound in a left-handed helix; the whole fiber contains more than 20,000 bp. We have used this model to study DNA radiation damage induced by heavy charged particles.

In an unexpected spin-off from this research, we predicted the phenomenon of short DNA fragment formation (up to a few thousand base pairs long). The calculated fragment length distribution reflected closely the symmetries and near-symmetries in the underlying structure of the 30-nm-solenoidal chromatin fiber. This prediction initiated experimental measurements with human fibroblasts, the results of which support the general theoretical prediction of fragment production. The experimental spectra are qualitatively similar regardless of the type of radiation. Importantly, the presence of a strong peak at 85 bp, corresponding to one full turn of DNA on the nucleosome, confirms the theoretical model calculations. However, contrary to the theoretical prediction of a distinct peak near 1,000 bp, experimental data show the presence of several peaks in the 185-to-450-bp range and the complete absence of any peak at or near 1,000 bp. Since the experiments are reproducible, we have concluded that solenoidal models are not consistent with the experimental data.

Theoretical and electron tomographic studies of the three-dimensional structure of chromatin fibers have suggested a unifying structural motif comprised of a two-nucleosome-wide ribbon, variably bent and twisted, in which there is little face-to-face contact between nucleosomes. This asymmetric three-dimensional zigzag of nucleosomes and linker DNA may represent the basic chromatin structure (the simplest form) determined by the properties of the nucleosome-linker unit. In this project, we perform detailed calculations of the production of radiation-induced DNA fragments and their size distributions for this class of zigzag models. By comparing with experimental data, we are able to determine detailed parameters for this model.

The 30 nm chromatin fibers observed in eukaryotic nuclei form the basic structures in a hierarchy of DNA folding. At the next level of organization, the chromatin fibers are hypothesized to be arranged in a series of looped domains, each containing perhaps 20,000 to 100,000 bp extending from the main chromosome axis. Experimental tests of the looped domain model will be carried out using ionizing radiation as a probe. Depending on the spatial organization of the loops, single ion traversals of the cell nucleus may generate an excess of DNA fragments in the 20,000-to-100,000-bp range from correlated breaks. After cells are irradiated with accelerated ions, enhancements in the fragment distributions will be determined using pulsed field gel electrophoresis. The distributions of fragment lengths obtained experimentally will be compared to theoretical distributions obtained under various assumptions of domain loop configuration.

This work lays the foundation for modeling whole chromosomes and even whole cellular nuclei. It will be possible not only to study structure averaged over the whole cell, but to look in detail at specific chromosomal compartments such as active and inactive regions, centromeres, and telomeres. In the future, it may also be possible to study the three-dimensional organization of specific genes.

Accomplishments

As a first step, we have developed a preliminary version of a computer program, cbuilder (for chromatin/chromosome builder), to assist in generating, modifying, and visualizing coordinate models of candidate chromatin fiber and eventually chromosome structures. Currently, cbuilder has been employed to create a number of zigzag ribbon fiber models. The theoretical fragment spectra obtained using these models and our Monte Carlo calculations are in better agreement with the experimental fragment spectrum from human fibroblasts than those obtained using the classical solenoid fiber model. In the theoretical fragment spectrum for a twisted planer zigzag ribbon fiber model, the 85 bp nucleosome peak is present along with significant structure near 185 bp and additional peaks up to ~ 500 bp. For none of the ribbon models studied is there any suggestion of significant enhancements in the spectra near 1000 bp. In the experimental spectra obtained by Björn Rydberg, peak locations and relative amplitudes are in good agreement with the zigzag model. Similar experimental spectra have been obtained for a wide range of incident radiation qualities for both interphase DNA (confluent cells in G0) and highly condensed mitotic chromosomes.

Measurements of large fragment distribution (in the 10-to-500-kbp size range) have also been made. Preliminary results indicate that there are significant enhancements in the production of fragments in this size range over that expected for random generation of double strand breaks, especially for densely ionizing radiation. Preliminary theoretical investigations also suggest that these enhancements may not be consistent with those expected for interaction of ionizing radiation with randomly coiled fibers. These results support the hypothesis that information on the structure of chromatin at this level of organization may be obtained from fragment distributions.

Publications

B. Rydberg, "Measurement of Chromatin Conformation in Living Cells: Support for a Zigzag Model of the 30 nm Chromatin Fiber," in preparation.

M. Löbrich, P.K. Cooper and B. Rydberg, "Non-Random Distribution of Double-Strand Breaks Induced by Particle Irradiation," *Int. J. Radiat. Biol.* **70**, 493–503 (1996).

W.R. Holley and A. Chatterjee, "Clusters of DNA Damage Induced by Ionizing Radiation: Formation of Short DNA Fragments. I. Theoretical Modeling," *Radiat. Res.* **145**, 188–199 (1996).

B. Rydberg, "Clusters of DNA Damage Induced by Ionizing Radiation: Formation of Short DNA Fragments. II. Experimental Detection" *Radiat. Res.* **145**, 200–209 (1996).

Techniques for Discovery of Disease-Related Genes

Principal Investigator: Joe Gray

Project No.: 96014

Funding: $457,100 (FY96)

Project Description

The purpose of this project is to stimulate basic genomic knowledge and technologies developed in the Human Genome Center and the Resource for Molecular Cytogenetics to analysis of the genetic basis of cancer and other diseases by supporting development of technologies needed for these studies. This will be carried out in collaboration with projects in the Life Sciences Division, the UCSF Cancer Center, and other Bay Area institutions.

Accomplishments

Several technical capabilities have been developed or made available under this program. These include: contig assembly, DNA sequencing, and gene identification and functional analysis, all of which are detailed below.

Contig Assembly

Fiber FISH has evolved into a useful quantitative procedure for physical map assembly and has been applied in assembly of sequence-ready genomic maps at 20q13 and 5q31. With this technique, it is now possible to map P1, BAC, and PAC clones onto each other or onto YACs. Recent advances have obviated the need to linearize P1, BAC, or PAC substrates: it is now possible to map onto open circles *and* to determine insert orientation relative to the vector. Only three days are required to determine if two or more clones overlap. Determining the degree of overlap is done with kilobase resolution, permitting true minimum tiling paths to be selected for sequencing or exon trapping. This project also has acquired genomic P1, PAC, and BAC libraries to facilitate physical map assembly in mice and humans. These libraries are available to all Berkeley Lab (LBNL) and UCSF Cancer Center investigators. Efforts are now beginning to extend this approach to identify cancer genes located at 7q (several locations), 8q22, and 3q26.

DNA Sequencing

The LBNL Genome Center has developed a highly efficient approach to directed genomic sequencing. However, the efficiency of the approach comes from sequencing many regions of the genome in parallel. As a result, it does not yield complete sequence information quickly about specific regions of the genome. We have collaborated with the Genome Center to overcome this limitation by combining high-resolution DNA fiber mapping with genomic sequencing. This approach allows several non-overlapping contigs to be sequenced in parallel, thereby substantially increasing the rate at which a specific clone can be sequenced. All positional cloning efforts at LBNL should benefit from this capability. In addition, we have collaborated with the Genome Center to develop informatics techniques for efficient assembly and annotation of genomic sequence, and we are beginning to address the issue of efficient DNA sequence closure (i.e., generation of complete contiguous genomic sequence across regions of biological interest).

Gene Identification and Functional Analysis

Exon trapping and cDNA selection are now being used to identify putative oncogenes located at chromosome 20q13 that are hypothesized to contribute to cancer progression in several solid tumors (breast, bladder, colon, brain, ovarian, and head and neck) when overexpressed. In addition, 365 kb of the 600 kb interval believed to encode the putative oncogene have been sequenced. To identify genes in the genomic sequence, we utilize the exon prediction and gene modeling software GRAIL, XGRAIL, and SORFIND. These are compared weekly against nucleic acid and protein sequence databases to identify informative homologies. Interestingly, a number of our cDNA clones have significant DNA and/or protein sequence homology to zinc finger-containing genes, suggesting that they may encode transcription factors. In addition, cDNA fragments and trapped exons and oligonucleotides for predicted exons have been used to probe Northern blots containing RNA from multiple tissues and breast cancer cell lines. To date, this effort has resulted in the identification of at least 10 transcripts. At least two of these genes are overexpressed in breast cancer cell lines having 20q13.2 amplification and in primary breast cancers.

We also are using FISH with gene specific probes to analyze mRNA levels in cells, tissues, and primary tumors. This approach allows assessment of transcription level, subcellular transcript localization, and intratumor expression heterogeneity, and can be applied to small primary tumors. In addition, we are developing polyclonal antibodies to candidate oncoproteins in order to assess the expression level and subcellular localization of these proteins. In an effort to make our data widely and immediately available to our collaborators at LBNL and UCSF, we have created a password-protected Web page that contains all data concerning the physical map, cDNAs, exons, genes, ESTs, STSs and genomic sequence. In this graphical environment, we are able to "click" on an exon or genomic sequence and display its annotated sequence, the gene to which it belongs, and images of Northern and mRNA in situ data.

Analysis of gene function through construction of transgenic mice is just beginning. Our approach is to create transgenic mice carrying YAC clones spanning regions of genetic abnormality and/or cloned genes from these regions in order to assess the function of genes encoded in the YAC. Our long-term plan is to cross the YAC transgenic mice with other transgenic mice known to develop tumors in order to determine the influence of the 20q genes on the rate of tumor progression. Our first transgenic mice will carry a YAC clone spanning the region at 20q13.2 that is amplified in breast cancer.

Publications

C. Collins, S. Hwang, T. Cloutier, T. Godfrey, D. Kowbel, W-L. Kuo, D. Polikoff, J. Rommens, P. Yaswin, M. Tanner, O-P. Kallioniemi, and J. Gray, "Positional Cloning of a Novel 20q13.2 C2H2 Transcription Factor Amplified and Overexpressed in Breast Tumors," in preparation.

S. Hwang, D. Kowbel, T. Godfrey, J. Cochran, K. Myambo, T. Cloutier, W-L. Kuo, D. Polikoff, J. Froula, J. Rommens, M. Tanner, O-P. Kallioniemi , J-F. Cheng, J. Gray, and C. Collins, "Physical Mapping of a 20q13.2 Breast Cancer Amplicon and Discovery of Its Novel Genes," in preparation.

M. Schoenberg-Fejzo, W-L. Kuo, C. Collins, D. Pinkel, and J. Gray, "Definition of a Region of Consistent Abnormality in Breast Cancer and Identification of Candidate Oncogenes in the Region," in preparation.

L. Shayesteh, W-L. Kuo, C. Collins, D. Pinkel, and J. Gray, "Defining a Region of Increase in Copy Number on Chromosome 3q26 in Ovarian Cancer," in preparation.

M. Wang, T. Duell, J. Gray, and H-U. Weier, "High Sensitivity, High Resolution Physical Mapping by Fluorescence in situ Hybridization onto Individual Straightened DNA Molecules," *Bioimaging* **4**, 1–11 (1996).

M. Tanner, M. Trikkonen, A. Kallioniemi, J. Isola, T. Kuukasjarvi, C. Collins, D. Kowbel, X-Y. Guan, J. Trent, J. Gray, P. Meltzer, and O-P. Kallioniemi, "Independent Amplification and Frequent Co-Amplification of Three Non-Syntenic Regions on the Long Arm of Chromosome 20 in Human Breast Cancer," *Cancer Research* **56**, 3441–3445 (1996).

Computational Biology

Principal Investigators: Teresa Head-Gordon and George Oster

Project No.: 96038

Funding: $60,900 (FY96)

Project Description

The Computational Biology group is tackling biological computation at molecular, cellular, and developmental levels. Our goals this fiscal year are the prediction of molecular protein structure from an amino acid sequence, and the simulation of cellular mechanics. Both projects have strong interactions with a mature experimental area, share a need for high-performance computing to realize the desired scientific goals, and are areas of computational biology that address post-genomic research.

The first project is to predict protein structure from an amino acid sequence. A recognized difficulty in protein structure prediction is that a chemically realistic approximation to the conformational behavior of proteins results in an exponentially large number of protein conformations that must be searched in order to find the global (i.e., native structure) minimum. Our computational framework for protein structure prediction is the Antlion conformational search strategy. This strategy smoothes a theoretical protein energy surface to retain only the region near the desired (global) minimum. The smoothing operation involves the design of mathematical functions that are manifestations of neural network predictions of secondary structure. We have developed neural network algorithms that provide our source of protein secondary structure predictions. The mathematical functions are designed to ensure that a one-to-one mapping between the desired minimum on the complex energy surface and that of the simplified surface is maintained. Otherwise, the method may ultimately converge to a higher energy minimum. In collaboration with computer science researchers at the University of Colorado and Argonne National Laboratory, we are developing a joint global optimization approach, based on sampling, perturbation, and smoothing, that has been quite successful working directly on the potential energy surfaces of small homopolymers. The collaboration entails the development of new techniques in the global optimization algorithm that effectively incorporate secondary predictions and supersecondary features and focus on tertiary structure determination for 50 to 100 amino acid proteins.

The second project is the simulation of stochastic trajectories of model motor proteins. This simulation will generate force/velocity curves and when input into Fokker-Planck equations will provide model distributions that are consistent with the experimental statistics. There has been a revival of interest in the class of motor proteins that convert chemical energy into mechanical forces to perform useful work in the cell. Again, advances in experimental instrumentation now make it possible to measure protein ensemble statistics, or even individual motor protein displacement or velocity, as a function of imposed

force at the molecular scale. It is now possible to make realistic models of molecular mechanochemical processes that can be related directly to experimentally observable, and controllable, parameters. These advances in experimental technology have initiated a renaissance in theoretical efforts to readdress the central question concerning operation of protein machines: How do they work? More precisely, how is chemical energy transduced into directed mechanical forces that drive so many cellular events?

Accomplishments

For the first project, all of the algorithmic components have been assembled and are currently being integrated together.

- Thomas Phillips, an undergraduate, has written infrastructure code that serves as the interface between the user and the optimization algorithm.
- Nathan Hunt, a postdoctoral researcher who arrived in September, has helped with the testing of our new neural network predictions of secondary structure, helped formulate the solvent term for our objective function, and coded a simulated annealing algorithm; these components are being incorporated into Phillips's code.
- Ludmilla Soroka, a staff scientist, is currently working on the port of the stochastic/perturbation algorithm from U. of Colorado to the T3D at Livermore, in order to be ready for the port to the T3E at NERSC when it becomes available sometime in January.

Our goal is to actually predict the structure of a 20 amino acid beta-sheet protein and 30 amino acid alpha/beta protein by January.

For the second project, we have developed a numerical method for analyzing statistical behaviour of the bacterial flagellar motor. Using this method, we establish that the motor's force generating mechanism is neither a constant displacement "stepper" nor a constant torque generator. The existing data is best explained by a "stepping force" generator. We delineate the kinds of information that can be gleaned from first passage time statistics and suggest additional experiments that can provide information on the mechanism of force generation.

Publications

T. Head-Gordon, R.C. Yu, and N. Hunt, "Improved Neural Networks for Protein Secondary Structure Prediction Without Use of Sequence or Structural Homologies," submitted to *J. Mol. Biol.* (1996).

G. Oster, "A Detailed Description of the New Numerical Algorithms," in progress. To be submitted to *Phys. Rev.*

G. Oster, "An Application of the Methods to Analyze a New Model for the Bacterial Flagellar Motor," in progress. To be submitted to *Biophysical Journal*.

Mechanism of Chromation Assembly During DNA Replication

Principal Investigator: Paul Kaufman

Project No.: 96039

Funding: $33,300 (FY96)

Project Description

This project focuses on the protein complex termed Chromatin Assembly Factor-I (CAF-I). CAF-I is an evolutionarily conserved factor that assembles nucleosomes in a manner linked to DNA replication in vitro. This project studies the relationship between CAF-I activity and radiation sensitivity in the yeast *Saccharomyces cerevisiae*, which can be studied genetically as well as biochemically.

Many advances in cancer research depend on understanding how eukaryotic chromosomes are assembled and protected from damage. Work published this year shows that human CAF-I will assemble nucleosomes on DNA templates that undergo nucleotide excision repair (Gaillard et al., 1996). Therefore, the initial phase of this project has tested the role of CAF-I in DNA damage sensitivity in vivo. These results have suggested that CAF-I is more important for reformation of chromatin after nucleotide excision repair than after double-strand break repair. Genetic and biochemical reagents for testing this model are currently being prepared.

Accomplishments

We first demonstrated that cell extracts from the budding yeast *Saccharomyces cerevisiae* contained a biochemical activity that would perform DNA replication-linked nucleosome assembly, as had been previously observed in humans, *Drosophila*, and *Xenopus*. Detection of this activity allowed for the biochemical purification of the yeast factor.

We have identified the genes encoding each of the three yeast CAF-I subunits by amino acid sequence analysis of purified protein. Two of these genes are termed *CAC1* and *CAC2* (for Chromatin Assembly Complex). The third gene was previously termed *MSI1*. Identification of these genes demonstrated that each of these genes is homologous to its human counterpart, and allowed for construction of yeast strains lacking individual or multiple CAF-I subunits.

We have established that CAF-I plays a role in protecting the genome from certain types of DNA damage. Specifically, we quantitatively assessed the degree of sensitivity to different DNA damaging agents using cells lacking each of the CAF-I subunits. Ultraviolet light (forming thymine dimers and other photoproducts) and x-ray irradiation (causing double-strand breaks) were tested. Interestingly, mutations in all CAF-I subunits result in increased sensitivity to ultraviolet radiation, but not x-rays. These data suggest that nucleosome assembly by CAF-I is activated by some but not all forms of DNA damage. Biochemical and genetic characterization of CAF-I is underway to determine the nature of the interplay between CAF-I and other factors in the assembly and maintenance of eukaryotic chromosomes.

Publications

P.D. Kaufman, "Nucleosome Assembly: The CAF and the HAT," *Curr. Opin. Cell Biology* **8**, 369–373 (1996).

P.-H. L. Gaillard, E.M.-D. Martini, P.D. Kaufman, B. Stillman, E. Moustacchi, and G. Almouzni, "Chromatin Assembly Coupled to DNA Repair: A New Role for Chromatin Assembly Factor-I," *Cell* **86**, 887–896 (1996).

A. Verreault, P.D. Kaufman, R. Kobayashi, and B. Stillman, "Nucleosome Assembly by a Complex of Chromatin Assembly Factor-I and Acetylated Histones H3/H4," *Cell* **87**, 95–104 (1996).

P.D. Kaufman, R. Kobayashi, and B. Stillman, "Ultraviolet Radiation-Sensitivity and Reduction of Telomeric Silencing in *Saccharomyces cerevisiae* Cells Lacking Chromatin Assembly Factor-I," *Genes Dev.*, in press.

Screening a Combinatorial Peptide Library for Ability to Promote Reversion of Tumor Cells into Nonmalignant Cells

Principal Investigator: Jon Nagy

Project No.: 96040

Funding: $22,900 (FY96)

Project Description

The extracellular matrix (ECM) is a complex network of macromolecules consisting of a variety of polysaccharides and proteins secreted by, and surrounding, cells. The ECM is an important modulator of cell growth, differentiation, and apoptosis (cell death). As such, it has profound influences on cell organization, motility, and gene expression. In human mammary epithelial cells (MECs), competent ECM-cell interactions have been shown to be critical for the suppression of cell proliferation and the induction of morphogenesis. Significant evidence now exists that suggests a tumor suppressor role for the ECM, mediated by cell surface receptors and their associated signal transduction pathways. Thus, aberrations in various checkpoints along these pathways could lead to abnormal cell behavior reminiscent of cancer.

The search for the specific ECM components that are capable of directing this type of regulatory behavior is now underway.

The goal of this proposal is to create and screen a large population of small peptide segments ("peptide library") for their ability to affect cell growth. In this way, new molecules will be discovered that will serve as lead structures in cancer therapy applications.

Accomplishments

The initial resin bead building block for the peptide library has been created. From this support, peptides

are attached in a combinatorial fashion to provide a means for assembling a large set of different analogs. Methodology for screening this library are in the process of being developed.

Theoretical Model for DNA Structure and Function

Principal Investigator: Daniel Rokhsar

Project No.: 96015

Funding: $50,000 (FY96)

Project Description

Theoretical Biology

A-tract DNA serves a variety of genomic functions. Sequences of phased (dA.dT)_n arrays can exist in straight or bent states; the transition between these two forms is presumably important for controlling the tertiary structure of DNA. In collaboration with S. Chan and R.H. Austin of Princeton University, we are developing a statistical mechanical model for this structural transition that will quantitatively explain their spectroscopic and calorimetric data, since a simple two-state model is demonstrably incorrect.

The immature retina of mammals exhibits spontaneous waves of electrical activity. These waves have been implicated in the proper development of retino-thalamic connections between the ganglion cell layer of the retina and the lateral geniculate nucleus. In particular, the detailed spatio-temporal correlations among the ganglion cells are thought to contribute to the formation of the retinotopic map in the thalamus. Our goal is to create a detailed model of the neural circuit in the retina that generates these waves. This work is being carried out in collaboration with Marla Feller and Carla Shatz of the UC Berkeley Molecular and Cell Biology department, who are imaging these waves using calcium-dependent dyes.

Our goals are to create theoretical models for these two biological phenomena (straight or bent state sequences of phased (dA.dT)_n arrays). In both cases, the statistical methods of theoretical physics will be applied to these two problems, which share the common feature of many coupled degrees of freedom. Both projects will be carried out in close collaboration with the respective experimental groups.

Accomplishments

We have resolved an apparent contradiction in the behavior of phased A-tract arrays. The transition between the straight and bent states of such DNA is found to be poorly described by a two-state model, unlike many other structural transitions in biological molecules. We have shown that cooperativity between elements of the phased array is required for the quantitative understanding of physical properties such as specific heat and UV absorption spectra. One consequence of this cooperativity is that under physiological conditions, such phased arrays are poised to act as a sensitive "switch" between the bent and straight states.

We have developed a detailed mathematical model of the neural circuit of the developing mammalian retina. We found that a "single-layer" circuit cannot explain the spatiotemporal properties of the developing retina. A more complicated and anatomically accurate model, involving both the retinal ganglion and amacrine cells, is required for even a qualitative understanding of the early retina. Our model-building has proceeded in close collaboration with the Feller and Shatz experimental group, which is testing specific predictions of our model. This work was presented at the 1996 annual meeting of the Society for Neuroscience.

Publications

D. Rokhsar, R.H. Austin, and S. Chan, "Structural Phase Transitions in A-tract DNA," to be submitted for publication in early 1997.

M.B. Feller, D. Butts, H. Aaron, D. Rokhsar, and C.J. Shatz, "Dynamical Processes Shape Spatiotemporal Properties of Retinal Waves," to be submitted for publication in early 1997.

Role of Recombinational Repair in Mammals: Analysis in Yeast of the Human DNA Repair Gene XRCC3

Principal Investigator: David Schild

Project No.: 96016

Funding: $50,000 (FY96)

Project Description

One strong line of evidence for recombinational repair in mammalian cells comes from the cloning and sequence analysis of the human *XRCC2* and *XRCC3* genes by Dr. Lawrence H. Thompson's group at LLNL. Human *XRCC2* and *XRCC3* genes have recently been cloned by complementation of the mutant CHO cell lines irs1 and irs1SF, respectively, which exhibit some sensitivity (~twofold) to x-rays and UV, but great sensitivity (~fortyfold) to DNA cross-linking agents such as mitomycin C and some psoralens. Both *XRCC2* and *XRCC3* cDNAs have recently been sequenced, and the predicted amino acid sequence shares significant homology with human and yeast *RAD51* proteins and other members of this family. The *RAD51* protein has been shown to have DNA strand-transfer activities, an enzymatic activity required for genetic recombination; it seems likely that *XRCC2* and *XRCC3* also encode strand-transfer proteins. If these proteins are involved in recombinational repair, it suggests that this pathway is critical for the repair of DNA cross-links, although it may be a relatively minor one for UV- and x-ray-induced damage.

To better characterize *XRCC3* and the *RAD51* gene family, the following experiments will be performed:

- Since strand-transfer proteins often form filaments and interact with other recombination and repair proteins, the yeast two-hybrid system will be used to test if *XRCC3* interacts with itself, with *XRCC2*, and/or with human *RAD51* and *RAD52* proteins. We will also test if any of these human proteins can interact with homologous yeast proteins.
- The yeast two-hybrid system will also be used to isolate new human genes encoding *XRCC3*-interacting proteins.
- We will also use other techniques to attempt to isolate additional members of the *RAD51* gene family from human cDNA libraries.

Accomplishments

Using cloned genes supplied by the laboratories of Dr. Thompson and Dr. David Chen (LANL), the two-hybrid system has been used to test for protein interactions between *XRCC3* and human *RAD51* and *RAD52* proteins. *XRCC3* interacts with the human *RAD51* protein but not with itself or the human *RAD52* protein. The region of *XRCC3* involved in this interaction is being determined and it appears that much of *XRCC3* protein is necessary for this interaction with *RAD51*. We have also made a plasmid construction with the human *XRCC2* gene to study its potential protein-protein interactions. We have determine that *XRCC2* does not appear to interact with *XRCC3*, h*RAD51*, h*RAD52*, or itself. We are extending these studies by screening for new human genes encoding proteins that interact with either *XRCC2* or *XRCC3*.

The yeast two-hybrid system has also been used to study the interaction between the yeast and human proteins we are studying. We found that human and yeast *RAD51* proteins do interact, and that the yeast *RAD51* protein interacts with the human *XRCC3* protein. It had already been determined by other groups that the yeast *RAD51* protein interacts with itself, as does the human *RAD51* protein, and as discussed above, we have shown that the human *RAD51* protein interacts with the human *XRCC3* protein. Our new information strongly suggests that this binding activity has been conserved between yeast and humans.

In addition, we are analyzing a potentially new human member of the *RAD51* gene family. This gene was picked up by a computer screen of the EST data base, using the yeast *RAD51* and human *XRCC3* ORFs (Open Reading Frames). We are currently using PCR (Polymerase Chain Reaction) to clone the entire gene. We have very preliminary evidence that the cDNA may be ~1.2 to 1.5 kb long, sufficient to encode a protein similar in size to *RAD51* or *XRCC3*.

Our experiments with *XRCC2* and *XRCC3* are significant in that they help provide further information about a probable recombinational-repair pathway in mammalian cells, and also give us a better understanding of recombinational repair in general.

Publications

The two-hybrid results should be published in the near future.

Crystallization and Structure Determination of Integrin $\alpha_{IIb}\beta_3$, a Platelet Membrane Protein Receptor

Principal Investigator: Peter Walian

Project No: 96017

Funding: $89,900 (FY96)

Project Description

The focus of our project has been to develop a means of producing crystals suitable for high-resolution electron crystallography of the platelet membrane protein receptor GPIIb-IIIa (integrin $\alpha_{IIb}\beta_3$). Integrin $\alpha_{IIb}\beta_3$ mediates the platelet aggregation phase of blood clot formation and plays a critical role in maintaining the delicate balance between the formation of beneficial and potentially deadly blood clots. This protein is also a member of the integrin superfamily of cell adhesion molecules which are essential for a diverse range of biological processes including inflammation, cell development and differentiation, and apoptosis.

To produce two-dimensional crystals of this receptor, we have pursued methods for reconstituting membrane proteins with lipids. In a typical scenario, detergent-solubilized protein and lipids are combined and then dialyzed to slowly remove the detergent. Under appropriate conditions, the lipids and protein come together to form a complex in which the protein is organized into periodic arrays within lipid bilayers. Parameters critical to this process include detergent and lipid type, pH, ionic strength and temperature.

This project is part of an ongoing collaboration with Dr. Joel Bennett of the University of Pennsylvania School of Medicine. The long-range research objective is to determine the atomic structure of $\alpha_{IIb}\beta_3$, thereby providing a basis for understanding the functional mechanisms of this protein in both its normal and disease-associated states.

Accomplishments

We have been able to reconstitute $\alpha_{IIb}\beta_3$ with lipid to form bilayer patches that contain a high density of the receptor. In regions of some of these patches, we have found small arrays of the receptor that occasionally yield weak low resolution diffraction. While these results have been encouraging, they have not yet provided us with the quality of specimen needed to begin electron crystallography-based structural studies. We are continuing to evaluate crystallization conditions.

During the current phase of the project, we placed particular emphasis on improving our microdialysis techniques and equipment. Through this work, microdialysis devices capable of supporting specimen volumes as small as 20 µl were developed, permitting us to assay a much broader range of crystallization conditions for a given specimen preparation. These devices also allow us to visually monitor the progress of the experiment while minimally disturbing the specimen. Additional system improvements included modifications allowing for finer control over temperature and the rate of dialysis, improvements that have helped to increase the average size of the reconstituted patches. We have also conducted studies to better characterize the detergent solubilized proteins. Through these studies, we have identified potential problem areas regarding parameters affecting the conformational stability of the protein during the course of dialysis, detergent purity, and variations in solubilized protein-associated lipids. Based on these findings, modifications to the crystallization and protein purification protocols are currently being evaluated.

Sufficient results were obtained during the course of these studies enabling us to submit an NIH grant application for conducting the additional work necessary to determine the high resolution structure of integrin $\alpha_{IIb}\beta_3$. Techniques developed in the course of this work should be directly applicable to the study of many other membrane proteins that are now available only in extremely limited quantities and for which electron crystallography appears to provide the best way to determine structure.

Isolation of Genetic Suppressor Elements in Human Mammary Epithelial Cells

Principal Investigator: Paul Yaswen

Project No.: 95011

Funding: $40,000 (FY96)
$67,000 (FY95)

Project Description

Inactivation of genes which normally prevent immortal transformation is thought to be a critical factor in progression of breast cancer. In order to directly isolate and identify genes whose normal functions are suppressed during immortal transformation of human mammary epithelial cells, we have employed a phenotypic selection method that allows fast recovery and identification of functional gene fragments. The strategy relies on the ability of small gene fragments to encode dominant-acting genetic suppressor elements (GSEs), which encode inhibitory antisense RNA molecules, or small peptides, which interfere with the function of wild-type genes from which they are derived. The advantage of this method is that it allows phenotypic selection of such genes through dominant inactivation of their products.

We have used the GSE approach in an attempt to directly isolate and identify genes whose inactivated functions are partly or wholly responsible for immortalization of human mammary epithelial cells. Poly(A)$^+$ RNA purified from mid-confluent cultures of adherent normal finite lifespan human mammary epithelial cells has been used to construct a cDNA library in a retroviral expression vector. Defective retroviruses containing the full range of cDNAs have been generated by transient co-transfection of the library along with a plasmid that encodes packaging functions into a highly transfectable cell line. Using a novel retroviral packaging construct and retroviral expression vector, we have consistently obtained infection rates of greater than 60% during a single round of infection in target human mammary epithelial cells.

Successful application of the GSE strategy for identification of genes whose functions are suppressed during immortal transformation of human mammary epithelial cells depends upon the use of target cell populations where there is a good likelihood that only a single change is necessary to get a discernable phenotype. While our cDNA library has been constructed using poly(A)$^+$ RNA from normal human mammary epithelial cell cultures—which contain senescing cells and, presumably, intact transcripts for maintenance of all normal functions—we have used as recipient cultures extended life cells, which have overcome at least one component of the senescence-mediated block to further growth. The extended life cultures, generated by treatment with the chemical carcinogen benzo(a)pyrene, grow for an additional 5 to 10 passages beyond the passage when untreated control cells undergo senescence. Unlike senescent cells, which maintain viability despite growth arrest, extended life cells eventually all die. In two extremely rare exceptions, extended life cultures have previously given rise to immortal cell clones, and are therefore likely to have acquired one or more mutations required for susceptibility to immortalization.

Accomplishments

To date, using the GSE methodology, we have obtained three human mammary epithelial cell lines of indefinite lifespan. However, after cloning and sequencing the cDNA inserts transduced into these lines, we determined that these cDNAs were unlikely to encode true GSEs. We used the inverse PCR technique to obtain genomic DNA flanking the viral insertion site in one of the lines, and determined that a retrovirus had inserted into the gene that encodes the p53 tumor suppressor. In two of the three cases, further confirmation that immortalization occurred as a result of insertional mutagenesis into the p53 gene was obtained by immunoblot analysis showing the absence of p53 expression in the immortalized lines. While we had previously considered the possibility that inactivation of a tumor suppressor could occur by insertional mutagenesis, we considered this possibility remote because both alleles of the target gene would have to be inactivated. The mechanism by which this occurred in the lines obtained remains to be investigated.

Although the experiments described have not yet led to the identification of novel GSEs, they have allowed us to make a new and potentially exciting discovery. After measuring the levels of telomerase activity and the ability to grow in the presence of TGFβ, two traits that correlate well with full immortalization, our observations of the new lines generated by retroviral infection, as well as lines previously obtained after treatment with carcinogens alone (184A1, 184B5),

indicate that there is likely to be an additional, epigenetic stage in the transition of human mammary epithelial cells to full immortality. Our evidence for this third stage, termed "conversion," can be summarized as follows:

- Early post-crisis human mammary epithelial cells are not uniformly resistant to growth inhibition by TGFβ and do not uniformly express detectable levels of telomerase.
- Clonally derived populations of early post-crisis human mammary epithelial cells often contain both TGFβ sensitive and resistant cells—every clone that does not cease growth completely within approximately 10 to 15 population doublings will eventually give rise to cells which are TGFβ-resistant and which display telomerase activity, and in each colony, the acquisition of resistance to TGFβ growth inhibition is gradual.
- In mass cultures of cells which are initially TGFβ-sensitive and do not express detectable levels of telomerase, TGFβ resistance and telomerase activity are first observed coordinately after mean terminal genomic DNA restriction fragment (TRF) length has shortened to less than 2 kb.

These observations have led us to hypothesize that the rare mutational or retrovirally mediated event which occurs during crisis does not affect telomerase activity directly, but allows cells with very short telomeres to continue to divide. Critically shortened telomeres may themselves subsequently trigger telomerase activity without any further mutations. The high frequency with which individual subclones make the transition to telomerase positivity and TGFβ resistance is inconsistent with a separate mutational origin, and is therefore likely to be epigenetic. We are continuing to investigate this phenomenon and its relevance to breast cancer progression.

Materials Sciences Division

New Chemistry for Epitaxial Growth of p-Type Gallium Nitride and Its Alloys

Principal Investigators: John Arnold, Eugene Haller, and Edith Bourret

Project No.: 96018

Funding: $132,900 (FY96)

Project Description

The wide-band-gap semiconductor gallium nitride (GaN) and its alloys are leading contenders in short wavelength applications (blue and UV) such as light-emitting diodes and lasers. Availability of blue diodes is essential to develop flat panel displays (the two other colors needed, red and green, are widely available). In addition, its outstanding chemical and thermal stability, combined with a potential for high-power operation, makes it an attractive material for high-temperature applications in corrosive environments. Such devices can be used as sensors in engines and for control of various industrial processes.

This program is focused on the synthesis of a wide range of potential new precursors to GaN and, in particular, to *p*-type material. A number of crucial issues must be addressed in the design of new precursors. In addition to satisfying the condition that any new chemistry produce molecules which decompose to the desired materials at reasonable temperatures, it is imperative that the compounds are:

- Volatile at ambient pressure (ideally they will be gases or low-boiling liquids)
- Simple and cheap to prepare using conventional synthetic techniques
- Easily purified to extremely high levels
- Safe to handle.

To produce semiconductor-grade thin films with excellent crystallinity, precursor molecules have to decompose—preferably by reaction with the growing semiconductor rather than in the gas phase. To leave the epitaxial reactor evenly, the decomposition products must be highly volatile. Because of the well-established tendency of hydrogen to passivate acceptor and (to a lesser degree) donor dopants, the issue of hydrogen incorporation will have to be thoroughly addressed. We aim to create a hydrogen-free precursor chemistry to eliminate these problems.

Accomplishments

New Nitrogen Sources

Several new nitrogen compounds are now being evaluated as potential sources. These include nitrogen trifluoride, phenylhydrazine, methylamine, and t-butylamine. Since it is vital that we understand the basic chemical reactivity of any new source materials, we have begun a synthetic program not only to prepare new source materials but also to conduct a detailed study of their physical and chemical properties. In the case of nitrogen trifluoride, for example, we are investigating its behavior toward low-valent metal centers to determine:

- Under what experimental conditions we can encourage the formation of metal nitrides.
- Whether the molecule is basic enough to form adducts with Lewis acids (e.g., trimethylgallium).

We are now also beginning work on the synthesis of new fluoroalkyl-substituted nitrogen sources that will be evaluated shortly.

Film Growth and Characterization

Modifications have been carried out on our rf reactor so that liquid precursors, such as alkylamines and hydrazines, can be evaluated. Good quality GaN films (as judged by photoluminescence) have been grown using Ga vapor (from a liquid gallium source) and ammonia on the rf reactor. Work has now begun using nitrogen trifluoride as a nitrogen source, and the initial results are encouraging (characterization of the deposited material is in progress at the time of writing). We are also in the process of testing dimethylamine, t-butylamine, and phenylhydrazine as sources in combination with gallium vapor.

Using our EMCORE reactor, the reaction of t-butylamine with trimethylgallium has been investigated at 200 torr, 650 °C, using hydrogen and nitrogen as carrier gases. Results indicate that the trimethylgallium decomposed but that alkylamines are eliminated from the reaction chamber with either carrier gas. These amines must be identified in order to

understand the details of the chemical reactions and to be able to tailor the process for formation of GaN. We are in the process of fitting a newly acquired residual gas analyzer (MKS RGA model PPt-300EM) onto the reactor for direct mass spectroscopy of the products of reaction. Based on the identity of these products, the operating conditions of the reactor will be modified to prevent formation of the alkylamines. Change of alkyl groups on both the nitrogen precursor and the Ga precursor will also be investigated.

Publications

David W. Peters and John Arnold, "Reactivity of Nitrogen Trifluoride," (tentative title) in preparation.

Synthesis of Oriented Nanoparticulate and Dense Crystalline Ceramic Films Using Biomimetic Membranes

Principal Investigators: Deborah Charych, Lutgard De Jonghe, Amir Berman (UC Davis, Chemical Engineering and Materials Sciences), Marca Doeff, and Pieter Stroeve (UC Davis, Chemical Engineering and Materials Sciences)

Project No.: 96019

Funding: $70,900 (FY96)

Project Description

Inorganic thin films find application in a wide range of technologies as sensors, electro-optic coatings, and magnetic information storage. In many instances, it would be desirable to produce such films either in dense crystalline form or as oriented nanoparticulates such that grain boundary properties—often critical in optical, sensor, or magnetic performance—can be precisely controlled. A variety of high vacuum beam technologies exists for the production of such films, requiring significant post-deposition heating to achieve the desired crystal orientation and structure. Such treatments necessarily limit the possibility of integrating these films with substrate devices that cannot tolerate post-deposition heat treatments (e.g., silicon semiconductor). Ideally, functional inorganic thin films would be deposited in the appropriate patterns near room temperature, with a degree of perfection and microstructural control that would eliminate the necessity of further processing. Biomimetic film synthesis using lipid-polymer membranes offers one such possibility.

In nature, the mineralization of highly oriented inorganic crystals occurs routinely at organic interfaces (e.g., proteins and oligosaccharides). In many cases, large arrays of distinct crystallites are co-aligned relative to the organic matrix. Biosynthesis of these materials evolves in aqueous media and at mild conditions of temperature and pressure. Materials synthesis emulating the essential elements of biomineralization may lead to unique inorganic structures with highly desirable properties. To our knowledge, controlling the absolute alignment of crystallites has not previously been achieved using current methods of organic template-directed crystal growth. Recently, however, we have demonstrated that *total alignment* of a mineral is achieved using self-assembling lipid-polymer membranes. We propose extending this methodology to the synthesis of potentially useful crystalline ceramics such as iron and manganese oxides.

Accomplishments

Iron Oxide

Near-nanometer-sized magnetic iron oxide particles are potentially useful in applications as diverse as information storage, color imaging, bioprocessing, and magnetic refrigeration. Currently, the typical manufacturing procedures for iron oxide particles are carried out in bulk solution and involve kinetic control of the progression of material deposition through the fluid dynamic regime. Alternatively, we have studied the possibility of using organic-template-directed deposition of nanometer-sized iron oxide particles on thin biomimetic lipid-polymer membranes. The polymer film is designed to specifically enhance the deposition and induce alignment between the spatially ordered film and the iron oxide deposit.

It was found that the original lipid polymer membrane, composed of 10,12 pentacosadiynoic acid (PDA), could be modified by forming a co-polymer in the desired composition. In particular, various sulfate-terminated monomer mixtures of 5 to 45 mole percent increase film stability and rigidity and were therefore predicted to provide a better substrate for iron oxide deposition. The organized acidic PDA film binds iron ions at the interface, forming a "quasi" first crystal layer. The ions localized at the film-solution interface are locally at supersaturation, giving rise to mineral deposition at the interface.

Both chemical and electrochemical deposition of the iron oxide mineral were investigated. Iron oxide deposited from solution on 33 to 43 mole percent sulfated-PDA films produces uniquely shaped deposits that do not exhibit any clear alignment with respect to the film. These elongated, spindle-shaped particles are approximately 100 nm long and 10 nm wide, and are polycrystalline as determined by electron diffraction. Interestingly, another observed crystalline phase is an overgrowth layer of the mineral. This layer covers extended regions of the surface (micrometer range) and diffracts electrons as a single crystal, oriented with its hexagonal axis normal to the film plane. The iron oxide deposited using the electrochemical method on 100% PDA films results in well-ordered rectangular crystals in registry with the film. The long axis of the rectangles is perpendicular to the direction of the polymer backbone as deduced by atomic force microscopy.

The results show that it is indeed possible to grow oriented iron oxide crystals. However, the organic layer must be optimized to allow long-range growth of the co-aligned crystals. Measurements of the magnetization of the films with MOKE (magnetooptic Kerr effect) did not yield significant results, suggesting the possible formation of goethite over magnetite or low surface coverage and intrinsically low coercivity. Further investigations on the film deposition and the magnetization are in progress. In addition, the influence of the PDA chemical functionality will be explored by surface modification of the organic template.

Manganese Oxide

The second part of the project focused on the formation of oriented crystallites of MnO_2 at PDA thin films. There are many practical applications for these materials, such as cathode materials for primary and secondary batteries, oxidation catalysts, ion-exchangers, and separation agents. Manganese oxides containing tunnels in one direction (usually along the c-axis) are particularly useful for the latter two applications due to their high selectivity (see Fig. 1). Thin epitaxial films of these tunnel structures have potential applications as rapid-response, highly selective sensors for ions or small molecules. For example, todorokite, a naturally occurring manganese oxide with 6.9 Å tunnels, readily takes up carbon tetrachloride and complexes with actinide ions. In contrast, α-MnO_2, with tunnels approximately 4/9 the size of todorokite, excludes these species on the basis

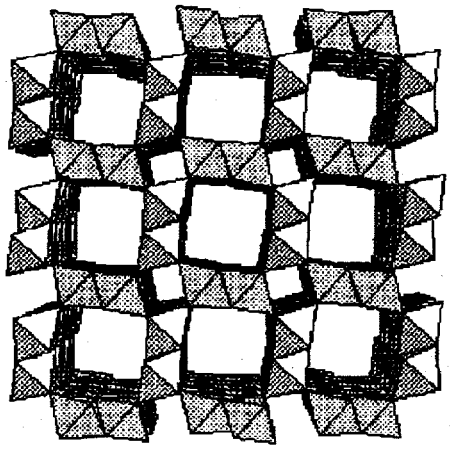

Figure 1. The structure of α-MnO_2 looking down the c-axis.

of size, but will selectively take up Pb^{2+} during ion-exchange processes. Therefore, oriented deposition of the tunnels perpendicular to the film was desired.

The challenges were numerous: manganese (III/IV) oxides display polymorphism; the phase obtained is strongly dependent upon synthetic conditions (solid state reactions, hydrothermal methods, or solution reactions), the temperature, the presence or absence of foreign ions, and many other factors. Products are often poorly crystalline and multiphase, making characterization difficult. Because it is more readily synthesized at low temperatures and often in a single step by solution methods, α-MnO_2 was chosen as the first system for deposition.

A large-scale screening was carried out to determine the best method for the manganese oxide deposition. Unfortunately, due to the high temperature required, those methods that produced the best α-MnO_2 crystals in solution were found to be incompatible with the PDA films. Also, the low solubility of one of the solution phase components (potassium peroxydisulfate) required some temperature elevation (to 45°C). Eventually, a procedure was found in which the PDA film structure was nominally maintained. Glass substrates coated with PDA are exposed to crystallizing solution containing $MnSO_4$. Following addition of $K_2S_2O_8$, the pink solution darkens and a fine brown-black precipitate forms, indicative of α-MnO_2.

The depositions carried out were successful in that the PDA films were coated with a semi-transparent brown film, indicating the presence of α-MnO_2 as

determined by X-ray diffraction with long counting times (130 peak). However, most likely due to the low temperatures employed, the α-MnO_2 produced by this method is poorly crystalline. Although weak, the signal suggests that the α-MnO_2 is preferentially oriented on the sample; however, the tunnels are not perpendicular to the substrate. Other methods, such as atomic force and scanning electron microscopy, should prove useful in further identifying the deposit. Future work will be directed towards the characterization and refinement of the deposition process to produce evenly deposited films in the desired orientation (c-axis normal to the PDA layer). Also, organic deposits that form size-selective cavities will be investigated.

Publications

A. Berman, S. Risbud, D. Charych, and P. Stroeve, "Template Directed Deposition of Iron-Oxide on Thin Polydiacetylene Film," in preparation for *Langmuir*.

Universal Properties at the Critical Point of Quantum Hall Plateau Transitions

Principal Investigator: Dung-Hai Lee

Project No.: 94018

Funding: $50,200 (FY96)
$86,400 (FY95)
$18,300 (FY94)

Project Description

In strong magnetic fields, a two-dimensional electron gas exhibits the quantum Hall effect. The hallmark of this effect is that as a function of the magnetic field, σ_{xy} exhibits quantized plateaus while σ_{xx} vanishes. The quantum Hall effect has completely reshaped our understanding of electronic transport in two space-dimensions. While conventional wisdom predicts that *all* disordered two-dimensional systems are insulators, the quantum Hall effect indicates otherwise. Indeed, when the magnetic field is fine-tuned to values corresponding to the mid-points between Hall plateaus, both $\lim_{T\to 0}\sigma_{xx}$ and $\lim_{T\to 0}\sigma_{xy}$ are nonzero, i.e., the system is metal. The purpose of our research is to understand exactly how the magnetic field resurrects the extended states, and what the properties of these metallic critical points are.

Accomplishments

In the literature, the critical point of plateau transitions has been analyzed under the assumption that electrons do not interact. In 1996, we were able to answer the question of what the effects are of electron-electron interaction on plateau transition critical properties. In this case, we studied the effects of electron-electron interaction on the critical properties of the plateau transitions in the *integer* quantum Hall effect. We found the renormalization group dimension associated with short-range interactions to be -0.66 ± 0.04. Thus the non-interacting fixed point (characterized $z = 2$ and $\nu \approx 2.3$) is stable. For the Coulomb interaction, we found, by dimension counting, that the correlation effect is a marginal perturbation at a Hartree-Fock fixed point ($z = 1$, $\nu \approx 2.3$). Further calculations are needed to determine whether it will maintain its stability upon loop corrections.

The values of electron conductances at plateau transition are universal. We were able to compute not only the conductances but also their mesoscopic fluctuations at transition. Under periodic boundary conditions in the transverse direction, we calculated the averaged zero-temperature two-terminal conductance ($\langle G\rangle$) and its statistical fluctuations ($\langle(\delta G)^{2n}\rangle$ for $n \le 4$) at the critical point of integer quantum Hall plateau transitions. We found *universal* values for

$$\langle G\rangle = (0.58 \pm 0.03)\frac{e^2}{h},$$

and

$$\langle(\delta G)^{2n}\rangle = \left(\frac{e^2}{h}\right)^{2n} A_{2n},$$

where $A_{2,4,6,8} = 0.081 \pm 0.005$, 0.013 ± 0.003, 0.0026 ± 0.005, and $(8 \pm 2) \times 10^{-4}$, respectively. We also determined leading finite-sized scaling corrections to these observables. Comparisons with experiments were also made.

Publications

D-H. Lee and Z. Wang, "The Effects of Electron-Electron Interactions on the Integer Quantum Hall Transitions," *Phys. Rev. Lett.* **76**, 4014 (1996).

Z. Wang, B. Jovanovich, and D-H. Lee, "Critical Conductance and Its Fluctuations at Integer Hall Plateau Transitions," accepted by *Phys. Rev. Lett* (1996).

Determining Macroscopic Materials Properties from Microscopic Calculations

Principal Investigators: Marvin Cohen, Steven Louie, John Morris, Jr., and Daryl Chrzan

Project No.: 96041

Funding: $44,500 (FY96)

Project Description

The goal of this research is to exploit advances in computer hardware and computational techniques, in the fundamental theory of bonding in solids, and in the theory of plastic deformation to construct new predictive models of the properties of real materials.

The project is a collaborative program in which the macroscopic properties of materials ab initio are computed by combining modern methods in theoretical solid state physics and materials science and exploiting the advanced computational facilities under development at Berkeley Lab. The ab initio component involves electronic structure calculations similar to those we performed in the past, but rephrased to exploit new computational methods that take advantage of parallel processing. Using only the atomic numbers and masses of constituent atoms, it is now possible to compute electronic, vibrational, structural, and thermodynamic properties of (and dynamic processes in) materials. These fundamental calculations are used to develop scaling formulae to determine the macroscopic properties of complex materials and to define in-out parameters for property simulations. Systems under investigation include superhard materials, semiconductor clusters, and dislocation dynamics.

Accomplishments

Ability to model the dynamics of a many-dislocation system is essential to development of accurate macroscopic models of plastic flow. Hence, part of this project focuses on developing large-scale simulations of dislocation dynamics. We examined the state of the art in dislocation dynamics simulations. While very impressive, current simulations are limited, first, by computer time, and second, by the approximations in the equations of motion. To produce a means of calculating expected behavior while eliminating the approximations inherent in assumed equations of motion, we therefore began to develop simulations based not on integration of equations of motion, but rather on kinetic Monte Carlo techniques. Development of the code appropriate for the simulation of a single dislocation is well underway.

Clusters or nanocrystals are nanometer-scale aggregates of atoms with size-dependent properties. They exhibit novel phenomena associated with quantum size and Coulomb charging effects and have many practical applications in their optical, electronic, and magnetic properties. In this project, we focus on understanding the electronic and structural properties of semiconductor clusters. In collaboration with J.R. Chelikowsky and Y. Saad of the University of Minnesota, we are carrying out ab initio calculations using a newly developed real-space method that is ideally suited for massively parallel machines. Silicon and other semiconductor clusters containing up to several hundred atoms are being investigated.

Both ab initio computations and empirical studies are performed in search of hard materials rivaling diamonds. We have surveyed the available metallurgical data on exceptionally hard carbides and nitrides, assembled the relevant phase diagrams, and compiled elastic properties. Results suggest that the bulk modulus is, in fact, the most probative single material property to indicate hardness. The hardness of many ultrahard materials increases significantly on alloying, due to a combination of bonding and microstructural effects. Current work includes a critical survey of the available mechanical theories of hardness to clarify the role of the elastic properties (it is not at all clear why the bulk modulus should be the best phenomenological indicator of hardness), and to separate bonding and microstructural effects on the hardness of alloys. Ab initio calculations compute the bulk moduli and elastic constants of the carbides and

nitrides, with the goal of providing a microscopic understanding of the empirical trends. In particular, in collaboration with J. Ihm, a visiting professor from South Korea, we are investigating the titanium-carbide-nitride and tungsten-carbide-nitride alloys. Preliminary results indicated supermodulus effects.

Biological X-ray Microscopy

Principal Investigators: Werner Meyer-Ilse, John Brown, and David Attwood

Project No.: 95023

Funding: $100,900 (FY96)
$ 40,500 (FY95)

Project Description

The goal of this project is to establish x-ray microscopy as a valuable tool in biology. X-ray microscopy provides high resolution images from thick objects, like entire cells, at atmospheric pressure. Samples can be in a liquid environment, similar to their preparation for visible light microscopy.

Accomplishments

Our projects are the first to solve biological problems using x-ray microscopy. We have used XM-1, the soft x-ray transmission microscope operated by the Center for X-ray Optics at the Advanced Light Source, in several biological projects. Among other findings, we have gained new insights in the development of malaria, examined the chromatin organization of sperm, recorded an initial series of parasite development, and imaged metal contents in alga.

- In collaboration with C. Magowan, Life Sciences Division, we studied the intraerythrocytic stages of the malaria parasite *Plasmodium falciparum* (Fig. 2). The repetitive 48-hour life cycle of the intraerythrocytic infection is responsible for the morbidity and mortality of malaria. Efforts to control this deadly disease must be based on an understanding of the parasite's development in the red blood cells. We studied hundreds of images of malaria-infected human red blood cells throughout the life cycle in normal and pathologic red blood cells (Fig. 2 a, b, c). These images established the base for studies of the parasite's development in unfavorable environments. Cysteine protease inhibitors, which have been shown to reduce the survival rate of the parasites (Fig. 2 d, e, f), show striking differences compared to normal parasite development.

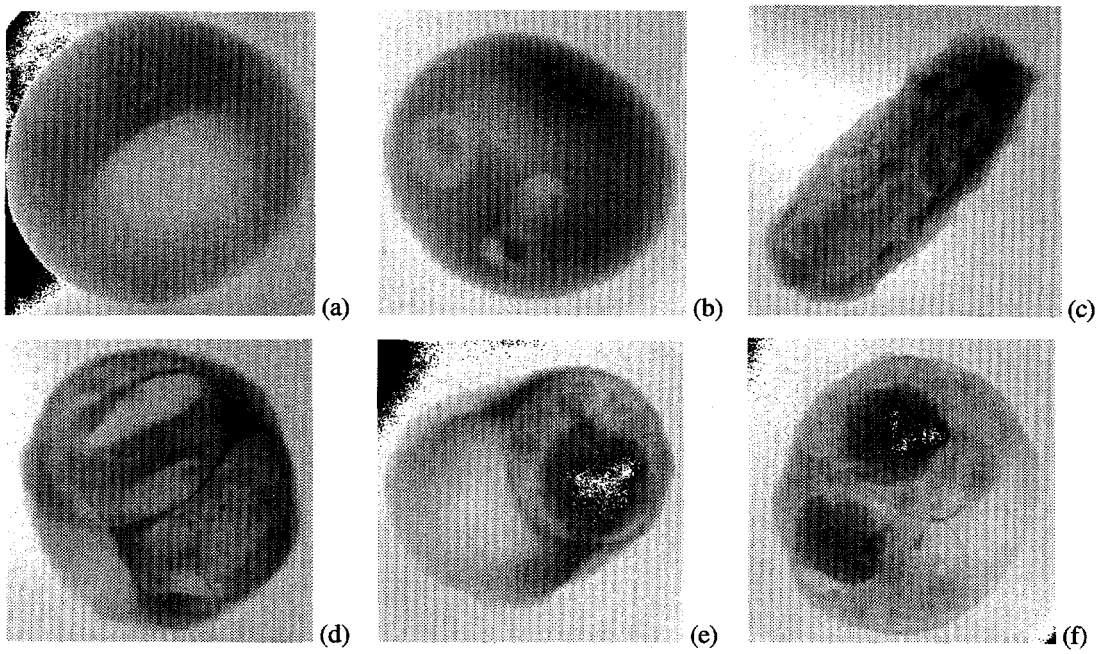

Figure 2. Human red blood cells infected by the malaria parasite Plasmodium falciparum: *(a) uninfected red blood cell, (b) young parasite, (c) parasite in a protein 4.1 deficient red blood cell, (d, e) distinct appearance of parasites in red blood cell treated with protease inhibitor ZFR, (f) parasite in leupeptin-treated cell.*

- In collaboration with R. Balhorn, Lawrence Livermore National Laboratory, we have used XM-1 to examine the uniformity of chromatin organization within the heads of sperm from several mammals [Fig. 3(a)]. Sperm chromatin is particularly well-suited for imaging with x-rays. Since the DNA is packaged in a highly compacted state, x-ray images of the sperm heads show structural details that cannot be observed using other techniques. These images are providing new insight into the importance of the timely synthesis of protamine 1, one of the two nuclear proteins that package DNA in spermatids and sperm.

- In collaboration with C. Petersen, UCSF and San Francisco General Hospital, we imaged *Cryptosporidium*, a parasite commonly found in lakes and rivers, particularly in those contaminated with animal waste and sewage. Occasionally it finds its way into drinking water supplies. The parasite is about 4- to 6-μ large and resistant to chlorination. Recent outbreaks in Las Vegas (1994) and Milwaukee (1993) caused about 140 deaths and approximately 400,000 cases of severe diarrhea and vomiting. We recorded a first series of x-ray microscopy images of *Cryptosporidium*. These images were made from formalin-fixed wet samples. Figure 3(b) shows a sporozoite emerging from the oocyst.

- In collaboration with T. Ford and A. Stead, Royal Holloway University of London, we have investigated the unicellular flagellated green alga *Chlamydomonas* in an unfixed vegetative stage. Images from initially living *Chlamydomonas* were obtained with exposure times of approximately one second [Fig. 3(c)]. These images confirm the existence of x-ray dense spheres reported elsewhere in contact x-ray microscopy and visible light differential interference contrast (DIC) studies. To our knowledge, these spheres have never been reported in electron microscopy studies. By using the absorption changes near ionization thresholds, we were able to detect oxygen, iron, manganese, and cobalt in dried but otherwise unaltered alga. This surprising discovery has implications for understanding the as yet uncharted function of the spheres.

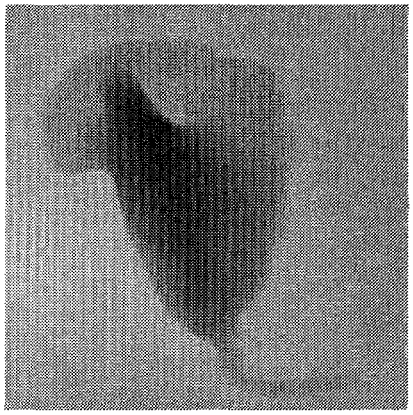
(a)


(b)

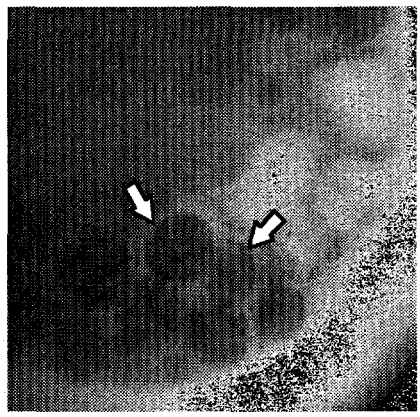
(c)

Figure 3. (a) Spermatid of a mouse sperm cell.
(b) Chryptosporidium *parasite emerging its cyst.*
(c) Chlamydomonas *with the x-ray dense spheres clearly visible.*

Publications

C. Magowan, J.T. Brown, J. Liang, J. Heck, R.L. Koppel, M. Narla, and W. Meyer-Ilse, "Intracellular Structures of Normal and Aberrant *Plasmodium falciparum* Malaria Parasites Imaged by Soft X-ray Microscopy," in preparation.

W. Meyer-Ilse, C.C. Magowan, and M. Moronne, "High Resolution X-ray Microscopy, a New Tool to Investigate Intact Parasites," *American Society of Tropical Medicine and Hygiene*, [Abs]. (1995).

C. Magowan, J.T. Brown, J. Liang, R.L. Koppel, M. Narla, and W. Meyer-Ilse, "Structure of Intracellular Malaria Parasites Imaged by X-ray Microscopy," presented at the 6th International Conference on Cell Biology, Dec. 8, 1996.

D. Attwood, N. Smith, B. Tonner, A. Warwick, F. Cerrina, J. Denlinger, E. Rothenberg, S. Singh, S. Kevan, H. Ade, W. Meyer-Ilse, and J. Underwood, "X-ray Microscopy and its Applications at the Advanced Light Source," to appear in *International Conference on Industrial Applications of Synchrotron Radiation*, edited by Jun-ichi Chikawa (Hyogo Prefecture, Japan, 1996).

Note: The following articles will appear in *X-ray Microscopy and Spectromicroscopy*, J. Thieme, G. Schmahl, E. Umbach, D. Rudolph, eds. (Springer Heidelberg, 1997).

W. Meyer-Ilse, H. Medecki, J.T. Brown, J. Heck, E. Anderson, C. Magowan, A. Stead, T. Ford, R. Balhorn, C. Petersen, and D.T. Attwood, "X-ray Microscopy in Berkeley."

J.T. Brown, C. Magowan, R. Balhorn, J. Heck, T.Ford, A. Stead, and W. Meyer-Ilse, "Biological Applications of XM-1."

R. Balhorn et al., "Application of X-ray Microscopy to the Analysis of Sperm Chromatin."

J. Heck, W. Meyer-Ilse, J.T. Brown, E. Anderson, H. Medecki, and D. Attwood, "Resolution of XM-1."

A.D. Stead, P.A.F. Anastasi, J.T. Brown, T. Majima, W. Meyer-Ilse, D. Neely, A.M. Page, S. Rondot, H. Shimizu, T. Tomie, and E. Wolfrum, T.W. Ford, "If Carbon Discrimination Is More Important to Biologists Than Resolution, Will Soft X-ray Microscopy Become a Useful Biological Technique?"

A.D. Stead, J.T. Brown, J. Judge, W. Meyer-Ilse, D. Neely, A.M. Page, E. Wolfrum, and T.W. Ford, "Use of Soft X-rays to Image Hydrated and Dehydrated Bacterial Spores Using Either Contact Microscopy or Direct Imaging."

T.W. Ford, A.M. Page, W. Meyer-Ilse, and A.D. Stead, "A Comparative Study of the Ultrastructure of Living Cells of the Green Alga *Chlamydomonas* Using Both Soft X-ray Contact and Direct Imaging Systems and an Evaluation of Possible Radiation Damage."

Investigation of Nanometer Magnetism by Using Surface Magnetooptic Kerr Effect (SMOKE)

Principal Investigator: Zi Qiu

Project No.: 96020

Funding: $50,100 (FY96)
$59,800 (FY95)
$25,700 (FY94)

Project Description

The strong correlation between magnetism and crystal structure in transition magnetic metals provides an opportunity to control magnetic properties by controlling crystal structure. The goal of this proposal is to synthesize and investigate new magnetic nanostructures with designed properties. In particular, we investigated how the ferromagnetic and antiferromagnetic phases of metastable face-centered cubic (fcc) Fe films are formed, and the effect of lattice symmetry breaking on magnetic anisotropy. All samples are prepared by molecular beam epitaxy (MBE) and characterized by low energy electron diffraction (LEED), high energy electron diffraction (HEED), and Auger electron spectroscopy (AES). The magnetic properties of the films are investigated in situ by surface magnetooptic Kerr effect (SMOKE), which can detect monolayer magnetism.

Accomplishments

Face-Centered Cubic Fe on Co(100)

We have succeeded in synthesizing the metastable fcc structure of Fe films on a Co(100) substrate. The natural structure of Fe is body-centered cubic. The fcc phase of Fe exists only at high temperatures (>910 °C). Using the MBE technique, we can fabricate up to ~11 atomic layers of fcc phase Fe at room temperature.

With the aid of magnetic interaction with the ferromagnetic Co substrate, the magnetic ordering temperature of fcc Fe has been pushed well above room temperature.

Detailed investigations showed that there are rich magnetic phases in fcc Fe films that are strongly correlated with the structural properties of crystal. By controlling the growth condition, we realized ferromagnetic, antiferromagnetic, and interfacial-live magnetic phases, and altered the ferromagnetic phase in the 5- to 11-monolayer range into the antiferromagnetic phase by annealing the low temperature growth film at 150 °C. We also realized oscillatory magnetic coupling across an fcc Fe spacer layer for the first time.

Our results demonstrate that we can not only synthesize new phases of magnetic materials, but also can control and design their magnetic properties. This is a significant step towards the "atomic engineering" necessary to develop a new realm of materials.

Symmetry-Breaking Induced Magnetic Anisotropy

Magnetic anisotropy is one of the most important quantities in low dimensional magnetism. Since magnetic anisotropy originates from spin-orbit interaction, it must respect the symmetry of the lattice. To understand how magnetic anisotropy behaves, it is very important to investigate how breaking lattice symmetry induces magnetic anisotropy.

We use well-defined atomic steps (~10 Å) on a Ag(001) surface to break the fourfold rotation symmetry of the surface. The steps are created by vicinal cutting of the crystal with a small angle. Fe films were grown on the stepped Ag(001) substrate and investigated in situ by SMOKE. A step-induced uniaxial magnetic anisotropy was observed with the easy magnetization axis parallel to the step edges. Using the idea of curved surface, we were able to explore the relation between step-induced anisotropy and step density. Surprisingly, induced anisotropy depends quadratically on step density. Subsequent analysis indicated that the quadratic relation is solely determined by the symmetry of the lattice at the step edge. A consequence of symmetry-breaking at the step edges is that the perpendicular magnetization in the Fe/Ag(001) system should be stabilized at a higher film thickness. This prediction was also confirmed by our experiment.

This work explored the underlying symmetry of magnetic anisotropy. It will help to design new structures with preferred magnetization direction.

Publications

R.K. Kawakami, Ernesto J. Escorcia-Aparicio, and Z.Q. Qiu, "Investigation of fcc Fe Thin Films Using Wedged Samples," *J. of Vac. Sci. and Tech. B* **14**, 3164 (1996).

R.K. Kawakami, Ernesto J. Escorcia-Aparicio, and Z.Q. Qiu, "Antiferromagnetic Coupling in Co/fcc Fe/Co Sandwiches," *J. Appl. Phys.* **79**, 4532 (1996).

Ernesto J. Escorcia-Aparicio, R.K. Kawakami, and Z.Q. Qiu, "Structural and Magnetic Properties of fcc Fe Films Grown on Co(100)," *J. Appl. Phys.* **79**, 4964 (1996).

Ernesto J. Escorcia-Aparicio, R.K. Kawakami, and Z.Q. Qiu, "An Investigation of the fcc Fe Films Grown on fcc Co(100)," *Phys. Rev. B* **54**, 4155 (1996).

R.K. Kawakami, Ernesto J. Escorcia-Aparicio, and Z.Q. Qiu, "Symmetry-Induced Magnetic Anisotropy in Fe/Ag(100) Systems," *Phys. Rev. Lett.* **77**, 2570 (1996).

Functionally Graded Ceramic-Metal Architectures for High Temperature Applications

Principal Investigators: Antoni Tomsia and Rowland Cannon

Project No.: 96021

Funding: $70,800 (FY96)

Project Description

We undertook a novel approach to fabricating ceramic/metal functionally graded composites (FGMs). The idea was to develop a colloidal science for high temperature systems, one that will make it possible to understand and control the wetting and colloidal behavior of particles dispersed in high temperature liquids and to relate this behavior to the relevant interfacial chemistry. Our final objective is to use the acquired knowledge to develop new fabrication routes for processing metal/ceramic systems by which material gradients, composition

microstructure, interfacial chemistry, and residual stresses and properties can be controlled.

Accomplishments

This project examined systems of interest for high temperature applications, such as refractory silicate glasses in combination with Al_2O_3, Si_3N_4, or refractory metals and intermetallics (W, Mo, Ni, Co, NiAl, CoAl). Basic wetting and penetration studies for liquid metals and oxides were undertaken. The microstructure of the interfacial zone has been determined by atomic force and scanning electron microscopy (AFM and SEM). Compositional studies have been carried out, both by energy- and wavelength-based X-ray spectroscopy (EDX and WDX). In parallel, the colloidal behavior of ceramic and metallic particles in high temperature liquids has been identified.

Our basic wetting studies have determined the effect of triple point deformation (ridging) on spreading kinetics and measured contact angles. The interpretation of contact angle experiments utilized to measure interfacial energies is usually based on Young's equation. This implies that the substrate can be treated as absolutely rigid and insoluble, and that only equilibration of the interfacial forces in a direction parallel to the substrate surface is necessary (one-dimensional approximation). However, our results clearly show that the one-dimensional approximation is not accurate for high temperature systems. In such systems, the amount of surface diffusion or solution precipitation is so large that the substrate is not rigid. Capillary forces induce a deformation at the triple junction in order to achieve complete two-dimensional equilibrium. We have studied ridging on several metal/ceramic and glass/metal systems. Analytical expressions have been found for ridge growth and spreading velocities, depending on the ridging mechanisms. Unlike most low temperature wetting experiments, we found that in high temperature systems, spreading kinetics is controlled by the movement of the ridge. We have identified the limited conditions in which wetting results can be interpreted in terms of one-dimensional equilibrium, allowing us to accurately use contact angle results to measure interfacial energies.

Our experiments have shown a close relationship between the infiltration and colloidal behavior of high temperature melts. As a first step to creating a colloidal description of high temperature systems, we have classified their behavior attending to their tendency to aggregate (flocculate). This can alternately be stated as the tendency of the liquid to infiltrate grain boundaries or dense compacts. We have found three systems:

- Systems with zero dihedral angle. Liquid infiltrates the grain boundaries of a dense preform. In parallel, a suspension of the solid particles in the melt will remain completely dispersed (deflocculated). For example, silicate glasses totally penetrate alumina preforms—the final state consists of ceramic particles dispersed on the glass. Penetration kinetics is dependent on glass or grain boundary composition (e.g., adding small amounts of TiO_2 to the glass enhances infiltration)
- Systems with non-zero dihedral angle. Liquid does not penetrate grain boundaries; solid particles dispersed in the liquid will attract each other and flocculate, leaving a clean (or "dry") interface. By control of oxygen partial pressure or addition of active elements, contact angles can be manipulated so that molten metals infiltrate porous ceramic preforms. However, these metals do not penetrate grain boundaries and the preform keeps its structural stability. In parallel, metal particles dispersed in molten silicate glass flocculate and sinter.
- Similar non-zero dihedral angle systems, but with an equilibrium layer between solid particles ("wet" boundary). Silicon nitride particles dispersed in silicate glasses flocculate, leaving an equilibrium layer. Equilibrium thickness has been observed in Si_3N_4 sintered with different additives.

It is expected that, as a result of the present project, new processing techniques for the fabrication of ceramic/metal FGMs (e.g., controlled sedimentation on high temperature melts, controlled infiltration, or dense preforms) could be developed in the future.

Publications

E. Saiz, A.P. Tomsia, and R.M. Cannon, "Ridge Formation Effects on Spreading of Liquids on Solids," in preparation. To be submitted to *Acta Materialia*.

L. Esposito, E. Saiz, A.P. Tomsia, and R.M. Cannon, "High Temperature Colloidal Processing for Glass/Metal FGMs," in preparation. To be submitted to *Ceramic Microstructures 96*.

L. Esposito, E. Saiz, A.P. Tomsia, R.M. Cannon, and A. Bellosi, "FGMs Through High Temperature Colloidal Processing: An Example in the System Silicon Nitride/Silicon Yttrium Silicate Glass," in preparation. To be submitted to *Acta Materialia*.

MSD Theory and NERSC Computation for ALS Experiments

Principal Investigator: Michael Van Hove

Project No: 96042

Funding: $86,000 (FY96)

Project Description

The project offers needed theoretical interpretation of experimental data measured at the Advanced Light Source (ALS), where current experimental results await the application or development of computational codes and models. A number of important issues in the information and materials sciences await more developed analytic tools. We are focusing on data that will only yield scientific information after being interpreted calculationally. The required large amounts of computer time and power are provided through NERSC (National Energy Research Supercomputer Center), now at Berkeley Lab.

In order to interpret the vast amount of available and soon-to-be-produced experimental data, powerful theoretical methods must be developed and used. For example, to deal with the complex electronic multiple scattering that underlies methods like photoelectron diffraction and holography, methods for improving programming efficiency, in addition to parallelization, are being implemented. Extensions of existing methods and new approaches will be introduced in response to the ALS users' needs and requests.

Accomplishments

This project was initiated in late summer, so effort in FY96 concentrated on establishing the necessary base for FY97 work. The first task was to hire a scientist. After a world-wide search, the best candidate, Dr. Yufeng Chen, was found at Berkeley Lab: he stood out in particular because he was already actively involved in programming precisely the theoretical methods of photolectron diffraction of maximum interest. While awaiting permanent residence status from INS, Dr. Chen continued his programming efforts, keeping the project on schedule. Procurement of the necessary workstations was also accomplished. First application to the interpretation of experimental data should yield initial results early in FY 1997.

National Energy Research Scientific Computing Division

Electron and Photon Collisions with Molecules, Clusters, and Surfaces

Principal Investigators: C. William McCurdy and Thomas Rescigno

Project Number: 96043

Funding: $88,100 (FY96)

Project Description

Electron and photon collisions, in a variety of species and environments, play a key role in plasma etching and deposition processes, as well as in a number of waste remediation processes currently under development at DOE laboratories. Relatively little is known about such collisions, despite the important role they play in surface characterization, plasma-wall interaction, electron-induced desorption, and reorganization of adsorbed particles. Although the past few years have witnessed tremendous progress in the development of sophisticated ab initio methods for treating collisions of slow electrons with isolated small molecules, the practical need to study electron collisions with the complex molecules and fragments encountered in real-world plasma-processing environments, as well as with molecules in complex environments (e.g., at interfaces, on surfaces, or in clusters) taxes present methods far beyond their current capabilities.

The purpose of this research is to develop theoretical and computational tools for treating electron and photon interactions with targets that are presently beyond the grasp of ab initio methods. We want to develop new methods for dealing with heavier molecules, complex molecular clusters, and, ultimately, molecules bound to surfaces and interfaces. Moreover, we also want to extend our capabilities to intermediate energies from the ionization threshold to a few hundred electron volts—a region that presents a formidable challenge for ab initio theory.

The approach will build on our unique capabilities, based on the complex Kohn variational method, for calculating cross sections for gas phase electron scattering (elastic, vibrational excitation, electronic excitation, dissociation, and attachment) and photoionization processes involving small polyatomic molecules. The formalism will be extended to include pseudopotential methods, complex optical potential interactions, and scattered flux operator techniques.

Accomplishments

A common property of many of the species found in reactive chemical plasmas is the presence of one or more heavy atoms in the target molecule. The inner-shell target electrons associated with these heavy atoms add enormously to the computational time needed to produce cross sections. To address this problem, we have investigated the use of standard ℓ-dependent effective core potentials and carried out the modifications necessary to use them in algebraic variational scattering codes that do not rely on specific analytic schemes for computing matrix elements. Using these techniques, we reported the results of an extensive study of low-energy electron scattering by HBr, an important etching gas—including elastic and dissociative excitation cross sections. We also completed a study of electron scattering by CH_3Cl—a process important for waste remediation strategies and for understanding how solvents change during storage with radioactive materials. This study is being prepared for publication.

We have also made progress in several areas of new theory. The common thread connecting these developments is the need for practical schemes for calculating cross sections in energy regions characterized by a dense level of excited states, including ionization continua. For photoionization applications, we have shown that by employing several continuum basis functions in a single calculation, we could develop a method that obtains the cross section over a continuous range of energies without explicitly resolving the variational equations at each desired energy. This is especially useful in cases where the cross section is dominated by autoionizing resonances. Figure 1 shows a calculation of the photoionization cross

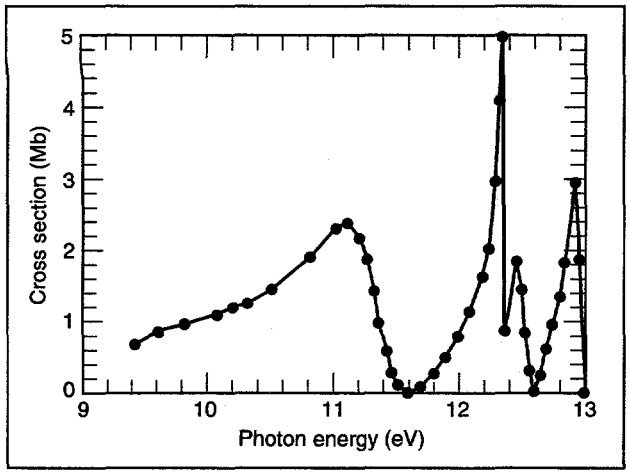

Figure 1. Photoionization cross section of Be calculated at discrete energies, using conventional Kohn wave functions (•), and from a single calculation of the resolvent, using several energy dependent basis functions (solid line).

section of atomic Be in the autoionizing region between the $1s^2 2s$ and $1s^2 2p$ states of Be^+.

We have also made progress in developing practical methods, based on analyticity, for studying electron scattering at intermediate energies (above the threshold for ionization). We have been investigating the use of finite element methods in connection with complex scaling and, as a test, applied this method to a standard model problem—electron-hydrogen atom scattering in the spherical model. Our results for excitation and ionization are probably the most accurate values ever obtained for this model and are being prepared for publication. During the course of this work, we discovered a new way of expressing excitation and ionization cross sections using projection operators; the expressions do not require detailed specification of boundary conditions for the three-body Coulomb problem. We also answered some open questions associated with both complex scaling and complex basis function methods and developed a generalization of complex scaling that allows it to be used in collision problems involving long-range interactions. We will continue to investigate ways to apply these techniques to problems of practical interest.

Publications

T.N. Rescigno and C.W. McCurdy, "Effective Potential Methods in Variational Treatments of Electron-Molecule Collisions I. Theoretical Formulation," *J. Chem. Phys.* **104**, 120 (1996).

T.N. Rescigno, "Effective Potential Methods in Variational Treatments of Electron-Molecule Collisions II. Application to HBr," *J. Chem. Phys.* **104**, 125 (1996).

T.N. Rescigno, A.E. Orel, and C.W. McCurdy, "Algebraic Variational Approach to Atomic and Molecular Photoionization Cross Sections: Removing the Energy Dependence from the Basis," accepted by *Phys. Rev. A*.

T.N. Rescigno, "Dissociative Excitation in Electron-Molecule Collisions," accepted by *Comments At. Mol. Phys.*

C.W. McCurdy and T.N. Rescigno, "Electron-Molecule Scattering," to be published in *Encyclopedia of Computational Chemistry*, edited by P. von Ragué Schleyer (Wiley, New York, 1997).

T.N. Rescigno, M. Baertschy, D.A. Byrum, and C.W. McCurdy, "Can Complex Scaling Be Made to Work for Long Range Potentials?" in preparation.

T.N. Rescigno, A.E. Orel, and C.W. McCurdy, "Low-Energy Electron Scattering by CH_3Cl," in preparation.

C.W. McCurdy, T.N. Rescigno, and D.A. Byrum, "An Approach to Electron Impact Ionization That Avoids the Three-Body Coulomb Asymptotic Form," in preparation.

Nuclear Science Division

A Third-Generation ECR Ion Source

Principal Investigator: Claude Lyneis

Project No.: 96022

Funding: $157,600 (FY96)

Project Description

The development of a third-generation ECR (Electron Cyclotron Resonance) source at Berkeley Lab will upgrade the 88-inch cyclotron by providing higher energy heavy-ion beams as well as continue to advance ECR source technology. One of the goals of the third-generation ECR would be the production of ions with charge states and intensities high enough to increase the usable mass range up to uranium. Recent results with two-frequency heating, high mirror ratios, and enhanced supplies of cold electrons indicate that significant advances in ECR technology are possible. To incorporate these ideas into a new, third-generation ECR source presents significant technical challenges, but improving ion source performance continues to be a cost effective method of improving heavy-ion accelerator performance.

The goal of the project is to develop a design addressing the cryogenic, superconducting, and ECR physics issues for a new high-performance ESR ion source. The key technical development for the new source centers on the design, fabrication, and performance of the superconducting coils needed to produce high magnetic fields. Main issues include determining the optimum coil geometry to produce the required magnetic field topology, examining the constraints placed on the design by the properties of the superconducting wire, developing solutions to the large mechanical forces generated between the solenoid and sextupole coils, and integrating the cryogenic constraints into the design.

Accomplishments

Three-dimensional TOSCA code calculations were used in developing the superconducting magnet structure and evaluating designs to support the coils against the inter-coil forces. The magnetic interaction between sextupole and solenoid coils results in very large forces, particularly at the sextupole ends, because they require substantial structural support and careful assembly to minimize coil deformation and quenching. In addition, an innovative design was developed that incorporates iron pole pieces in the sextupole to increase the radial field and reduce the axial field in the center region. The initial plan had been to build a subset of the magnet system to explore fabrication and assembly issues. However, the acquisition of sufficient superconducting wire from surplus SSC wire at no cost made it feasible to build a complete prototype magnet system within the scope of this project.

During FY96, a preliminary design was made of a Superconducting Magnet System for the third-generation ECR source, and a full-sized, prototype nine-coil magnet assembly was built. Design specifications are listed in Table 1. Coil parameters, including number of turns, operating current, inductance and Lorentz forces are given in C. Taylor (see *Publications*, below).

All of the superconducting magnets were wound at Wang NMR, Inc., using 48 km of surplus superconducting wire from the SSC project. The sextupole has 0.8-mm-diameter NbTi wire insulated with 0.05-mm Kapton tape. Each coil was wound and vacuum-impregnated using tooling that resulted in a precise I.D., O.D, and an azimuthal arc of 60 degrees. The 80-cm-long poles, which are a permanent part of each coil, have 35 cm of iron in the center and non-magnetic stainless steel ends. The ends of pole pieces

Table 1. Prototype Nine-Coil Magnet Assembly Design Specifications.

I.D. of plasma chamber	16 cm
Mirror field on axis	4 T, 3 T
Mirror-mirror spacing	50 cm
Central field (variable)	0 to 1.0 T
Minimum field at I.D. of plasma chamber	2 T

Figure 1. Sextupole coils after vacuum impregnation prior to assembly.

were shaped to facilitate layer winding of the 1748 turns. Figure 1 shows the six separate sextupole coils after winding and potting, but before assembly on a cylindrical form that fits into the bore of the mirror coil assembly. Figure 2 shows the completed mirror coil assembly with three mirror coils wound on a common coil form and vacuum-impregnated. The complete coil assembly will be tested in a vertical cryostat in January and February, 1997.

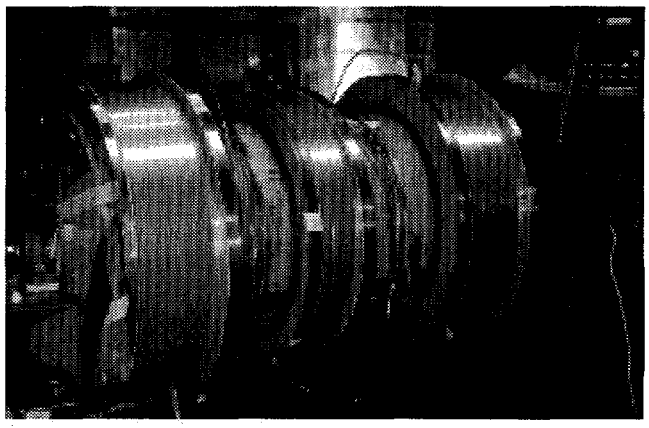

Figure 2. Completed mirror coil assembly.

Publications

C. Taylor, "Specifications—Build and Test Prototype ECR Magnet Systems," *SC-MAG 547* (9 April, 1996, revised 16 July, 1996).

C.M. Lyneis, Z.Q. Xie and D.J. Clark, "LBNL 88-Inch Cyclotron Improvements," *Proceedings of the 14th International Conference on Cyclotrons and Their Applications*, Cape Town, S. Africa, October 8-13, 1995, p. 173.

Physics Division

Pixel Detectors for Charge Particle Detection

Principal Investigator: Murdock Gilchriese

Project No.: 96024

Funding: $119,600 (FY96)

Project Description

Pixel detectors are the next step in instrumentation for charged-particle detection in high-rate particle physics experiments. Silicon strip detectors are widely used in high energy physics experiments. The basic detection element in strip detectors is a 50-to-200-microns-wide-by-a-few-to-18-cm-long strip, with integrated circuit electronics for amplification and signal processing wire-bonded to the end of the strip. In high rate environments, a much greater degree of segmentation is required to avoid overlap and confusion. This segmentation is achieved in pixel detectors by subdividing the detector substrate (e.g., silicon) into pixels, cells typically 50 x 300 microns in size. Readout electronics must be joined directly to the pixels. This can be achieved by using bump bonds and flip chip assembly to mate the readout integrated circuit (IC) to the segmented detector substrate.

The enabling technologies to allow successful operation of pixel detectors are integrated circuits, for amplification and signal processing, and bump bonding and flip-chip technology, for allowing the detector substrate to be mated reliably with the integrated circuits. Berkeley Lab (LBNL) has been involved for some years in the development of integrated circuits for readout of pixel detectors. However, very little work has been done on the bump bonding and flip-chip technology that will be required to bond detectors to integrated circuits and make modules, the building blocks of larger systems. Furthermore, the process of depositing bumps on silicon detector substrates may affect the radiation hardness of the detectors. This proposal was to evaluate bump bonding and flip-chip technologies and to fabricate testable prototypes.

Accomplishments

The intent of this program was to investigate the U.S. capabilities for fine-pitch solder bump deposition via plating techniques and flip-chip assembly, and to utilize such capabilities, if found, to determine the effect, if any, of the bumping process on basic silicon detector properties.

Test structures to evaluate bump bonding were fabricated in the Microsystems Laboratory. Two classes of test structures were fabricated: simple arrays were used to measure bump yield by continuity measurements and active detector test diodes and other structures, and larger area arrays were designed and fabricated on additional wafers for measuring bump yield.

After a search for low-cost vendors, two solder bump vendors were contacted: Aptos, in California, and MCNC, in North Carolina. After extensive contact and negotations, Aptos decided that it was not capable of providing the required fine-pitch bumps on a timely basis. Therefore, a contract was drawn up with MCNC to deposit 30-micron-diameter solder bumps on wafers containing the small continuity test structures and wafers with active detector elements. MCNC had previously demonstrated the ability to deposit 40-micron bumps. MCNC was also to assemble some structures via the flip-chip process.

Wafers and masks were designed and provided by LBNL. However, MCNC had great difficulty in properly depositing bumps. Some wafers were broken; the bump process was tried numerous times under different conditions. This resulted in a greatly delayed schedule, and, in the end, MCNC could not meet the bump requirements. A few continuity test assemblies and bumped active devices were delivered in late 1996, more than six months behind schedule. Preliminary continuity tests show that the bump yield is not zero. More measurements are underway. Should the yield be sufficient, the active test structures will be irradiated, as planned, and measured, although many months later than expected.

Photosensor for Use in a High Magnetic Field

Principal Investigators: Hans Wenzel and Richard Kadel

Project No.: 96025

Funding: $120,800 (FY96)

Project Description

The purpose of this project was to investigate the use of low pressure gas parallel plate detectors to detect photons in the vacuum ultraviolet. VUV photons are converted on a photocathode (e.g., CsI), and the resulting photoelectron is amplified in a low pressure (10 to 100 torr) gas in an electric field of order ~5000 V/cm. Our specific long-term goal was to develop a photosensor for use in a threshold Cerenkov counter to permit particle identification in the Collider Detector at Fermilab (CDF), a large 4 π detector designed to measure $p-\bar{p}$ collisions at 1800 GeV. The particular physics to be addressed by the Cerenkov counter was particle identification for the momentum range 1 to 6 GeV in B meson decays. In this particle identification application, the geometry of the CDF detector requires detection of single photons in a 15 kG magnetic field.

Accomplishments

We first designed a large vacuum vessel in which to conduct our tests. This vacuum vessel was designed to work together with our existing VUV monochromator, which has a separate vacuum enclosure and pumping system. The requirements for the vacuum vessel were to obtain a modest vacuum (better than 10^{-5} torr), to allow for the introduction of light in the 125-to-200-nm range, and to permit computer-controlled component movement inside the vacuum in at least two orthogonal directions (vertical plus horizontal). Design of the vacuum vessel and related plumbing was completed and given to the main shops for fabrication. The completed vacuum vessel was assembled and vacuum proof-tested. Commercial vacuum x-y and linear translators were delivered in the summer, and software (LABVIEW) was then written and tested to allow positioning of translators under program control.

Using our apparatus, we conducted tests of several CsI photocathodes in a variety of amplifying gases: CH_4, C_2H_6 and CF_4. Tests of the amplifying gas were conducted from 100 to 10 torr , and relative gains of up to 10^6 were made. The CsI photocathodes showed sensitivity in these ranges: 125 to 200 nm (CF_4), 140 to 200 nm (CH_4) and 155 to 200 nm (C_2H_6). After about 6 months, our first CsI photocathode showed about a factor of three drop in gain from its original value. This performance drop is not adequate for a long term detector, but we anticipate that better storage and fabrication techniques could potentially lead to lifetimes of a few years. For these time scales, the critical issue is component outgassing and the purity of the amplifying gas.

Therefore, coincident with these hardware projects, we did some analysis on the transportation and storage of CsI photocathodes, which are quickly damaged by humidity (i.e., exposure to air) and contact with some metals. After consultation with A. Lyon in the vacuum plating shop, we had all of our photocathodes deposited on electropolished stainless steel. We experienced none of the aging problems associated with copper substrates, typical when CsI is used on printed circuit boards (copper is known to react with CsI). After some empirical testing ranging from individual vacuum containers to "open racks" in a large evacuated volume, we found the lifetime of the photocathodes to be longest in the latter configuration. Baking the CsI photocathodes appeared to have little affect on their longevity or efficiency.

Preliminary results were also obtained on a 1-μm-thick KCl photocathode which had been irradiated by VUV light for several days to form point defects in the crystal lattice. Using CH_4 as the amplifying gas, we found this photocathode was photosensitive in the 140-to-165-nm range, where the lower limit comes from the CH_4 gas and the upper limit is from the photosensitivity of the KCl. We were only able to obtain relative gains up to a factor of ~5000, compared to 10^6 in the case of CsI/CH_4 systems. The response of the photocathode was extremely unstable, both in time and as a function of the wavelength of the light detected.

In August, the hardware and software were in a state such that we expected to conduct detailed tests of the absolute quantum efficiency and transverse uniformity of our photocathodes. Unfortunately, our $5,000 calibrated VUV photomultiplier tube failed and had

to be returned to the factory for repair under warranty. It has not yet been repaired, despite repeated inquiries.

Given the failure of our calibrated photomultiplier, in the fall of 1996 we conducted a candid assessment of our experimental choices. This reassessment was strongly motivated by the April 1996 decision of the CDF experiment to eliminate a particle identification system for the foreseeable future (at least the next 15 years), as well as the departure of one of the authors (H. Wenzel), scheduled for January 1997. We concluded that it would take several years to develop useful devices, and, given the aforementioned decision of the CDF experiment, there was no foreseeable use for these devices in the next decade. Consequently, the project was terminated.

System Design and Initial Electronic Engineering for a km-Scale Neutrino Astrophysical Observatory

Principal Investigators: David Nygren, Douglas Lowder, Martin Moorhead, Gilbert Shapiro, George Smoot, and Robert Stokstad

Project No.: 96026

Funding: $138,000 (FY96)

Project Description

Detection of ultra-high energy neutrinos of astrophysical origin is an unexplored frontier of great scientific interest to particle physics as well as astrophysics. Because neutrinos interact weakly, large detector volumes—ultimately on the kilometer scale—are required to detect a statistically significant signal. The best methodology, using the Cerenkov technique, involves strings of photomultiplier tubes located in deep, clear ocean water or in deep ice at the South Pole. The design and realization of such a large detector presents numerous technical and practical challenges. An innovative engineering approach to this design and realization has already been developed at Berkeley Lab (LBNL). Complementing this engineering effort, new computing methods that will efficiently and accurately simulate the optical properties of the water environment are needed to clearly understand the scientific reach of possible detector arrays.

Accomplishments

Our simulation effort focused on designing an accurate and efficient code to represent the generation, propagation, and detection of the Cerenkov light. This includes scattering and absorption during propagation as well as geometric effects at the detector. Our basic simulation code structure has been adopted by the AMANDA collaboration. Some very instructive new results have been obtained, although the full reconstruction of events has not yet been attempted.

The basic architecture of a kilometer-scale detector has been defined: a highly decentralized digital system, with semi-autonomous optical modules embedded in a logically configurable, easily expandable network.

At the detector level, a new family of waveform-recording, full-custom ASICs (Application Specific Integrated Circuits) has been conceived, designed, and put into operation. The new ASICs are called Analog Waveform Transient Recorders (ATWRs). The ATWR devices capture several waveforms simultaneously, permitting capture of information with extremely high dynamic range and nanosecond time resolution, without the use of highspeed clocks. In collaboration with JPL (Pasadena), a digital optical module (DOM) has been developed, based on the LBNL system concept and the ATWR ASIC. Two DOMs have been constructed and tested in the laboratory, and are scheduled to be deployed at 2 km depth in the South Pole ice in early 1997. An advanced version of the ATWR, with internal analog-to-digital conversion, has been submitted for fabrication.

The DOM concept requires an internal clock to timestamp events at the nanosecond level of accuracy. Tests performed at LBNL have demonstrated that modestly priced ($25) quartz oscillators can provide astonishing short-term accuracy. The measured results for an ensemble of these devices indicate frequency drift of less than 1×10^{-10} per minute. These tests provide proof that the DOM can provide the necessary timestamping accuracy, with a negligible level of system activity to measure clock drift. The oscillators operate at a very convenient 15.36 MHz.

An engineering study showed that a relatively simple, very low power microprocessor is sufficient to distinguish between single photoelectron signals and more complex waveforms, permitting substantial data compaction within the DOM.

Bright optical beacons based on GaN LEDs (light emitting diodes)—a new item of commerce—were

developed and deployed in deep ice at the South Pole; pulsed dc modes could be remotely selected, both with variable brightness. Such beacons should be equally useful in the deep ocean environment. Further development of the circuitry is needed, so that the GaN LEDs can be an internal DOM component.

At the system level, a specific concept has been developed at LBNL, called the Shared Boundary Ring Structure (SBRS). The SBRS offers a very natural path of incremental growth, topological flexibility to avoid most single point failure mechanisms, and possibly an optimum match to the physics goals. Most of the engineering work remains to be done for a real array design.

Exploring Scientific-Computational Collaboration: NERSC and the Supernova Cosmology Project

Principal Investigators: Saul Perlmutter, Gerson Goldhaber, Donald Groom, and Alex Kim

Project No.: 96044

Funding: $44,400 (FY96)

Project Description

Over the next few years, we will use astrophysics techniques developed in the Supernova Cosmology Group to measure the fundamental parameters of cosmology. Because future data sets are beyond our current capabilities, this project requires unusual computational environments and capabilities. Innovations will be needed for near-real-time computation, fast access to large data sets, tools for scientific visualization, networking and "collaboratory" environments—all of which are research interests of NERSC. As a first step in the collaboration, we will use supercomputer calculations to interpret our supernova spectra.

The key to successful cosmological measurements is to eliminate statistical and systematic errors. To reduce statistical errors, it is necessary to move to significantly larger data sets so that larger samples of supernovae can be studied at greater distances. We are now scaling up our supernova search, using larger wide-field cameras and multi-telescope coordination to produce data sets that are 5 to 20 times larger than standard, and thus beyond our current computational resources. We also aim to reduce systematic errors associated with minor variations in intrinsic brightness among Type Ia supernovae by calibrating on features of the supernova spectrum. This spectral work requires supercomputer simulations of supernovae atmospheres to produce "synthetic spectra." By preparing simulated spectra, we will be able to understand distant supernova spectra and thus calibrate the supernova's brightness.

Accomplishments

The project was funded at the end of FY96. We have hired Dr. Peter Nugent as the postdoctoral fellow for this project and purchased and installed his workstation. Working with the Supernova Cosmology research group and NERSC, preparation has started on a supernova spectral synthesis code that can be run on the NERSC machines. Studies to understand which features are most likely to be accessible at high redshift have also begun on the supernova spectral data already collected by the Supernova Cosmology Project.

Level Set Methods for Medical Image Analysis

Principal Investigators: Ravi Malladi and James Sethian

Project No.: 96023

Funding: $48,900 (FY96)

Project Description

The goal of the project is to reconstruct anatomical shapes given a time-varying sequence of dense volumetric scans of a particular region in the human body, say the thorax. Shape recovery schemes have many applications in medical image analysis; we are principally interested in visualization, organ volume extraction, measurement, and tracking.

The main challenge in three-dimensional shape recovery is to devise a modeling framework that is topologically adaptable, especially so when one attempts to recover an unknown tumor volume or the shape of heart chambers together with connecting valves. Also, from an algorithmic point of view, it is important to propose a fast shape recovery solution in

order to achieve realistic off-line processing times. We address both these issues in our work.

Our approach to shape recovery is an evolutionary one. In other words, we let the physician specify an initial shape or a set of shapes in the image domain, preferably inside the shape he/she intends to recover. These initial shapes, typically spheres or just a set of mouse clicks, are then made to propagate in the image domain by solving a partial differential equation. Steady state of our solution describes the desired shape.

Accomplishments

We have made progress on two fronts during the past year.

First, we now understand the role of anisotropic diffusion in preprocessing of images. This step is an alternative to the low-pass filtering commonly used for image smoothing. The anisotropic diffusion schemes that we used are edge-preserving: they filter out noise without destroying the crucial edge information necessary for shape recovery.

Second, we have developed a very fast solution scheme called the Marching method to solve our governing equation. This scheme is motivated by some of our previous work on narrow-band methods to solve curve and surface evolution problems. The main idea is to recast the equation of motion in an arrival-time framework and explicitly solve for the solution by sweeping the domain from smaller to larger time values. We restrict the sweeping zone to a narrow band around the current position and use a heap data structure to store points on the surface. The result is an $O(N \log N)$ algorithm in time where N is the total number of points in the domain.

(a) (b)

Figure 1. Examples of three-dimensional shape recovery. (a) Liver. (b) Spleen.

As an example, in Fig. 1 we show the shapes of liver and spleen that have been extracted from an MRI image of the abdominal section.

Publications

R. Malladi and J.A. Sethian, "An O(N log N) Algorithm for Shape Modeling," *Proceedings of National Academy of Science, USA* **93**, 9389–9392 (1996).

R. Malladi and J.A. Sethian, "Level Set and Fast Marching Methods in Imaging Processing and Computer Vision," *Proceedings of IEEE International Conference on Image Processing*, Lausanne, Switzerland, September 16–19, 1996.

R. Malladi and J.A. Sethian, "Shape Modeling in Medical Images with Marching Methods," LBNL-39541, University of California, Berkeley, October 1996; submitted to *IEEE Transactions on Medical Imaging*.

R. Malladi, R. Kimmel, D. Adalsteinsson, G. Sapiro, V. Caselles, and J.A. Sethian, "A Geometric Approach to Segmentation and Analysis of 3D Medical Images," *Proceedings on IEEE/SIAM Workshop on Mathematical Methods in Biomedical Image Analysis*, 244–252, San Francisco, California, June 1996.

Structural Biology Division

Synthesis, Crystallization and Characterization of 5S Ribosomal RNA

Principal Investigators: Stephen Holbrook and Rosalind Kim

Project No.: 96045

Funding: $130,800 (FY96)

Project Description

The purpose of this project is to determine by X-ray crystallographic methods the three-dimensional structure of 5S ribosomal RNA (5S rRNA), specifically the sequence from the hyperthermophilic Archaea *Pyrodictium occultum*. Specific goals include:

- In vitro synthesis of milligram amounts of a homogeneous species of 5S ribosomal RNA of *Pyrodictium occultum*.
- Crystallization of this 5S ribosomal RNA.
- Co-crystallization of 5S rRNA with ribosomal protein isolated from *Thermus thermophilus* (TL5).

Accomplishments

To date, despite extensive efforts by others, the best crystals of 5S rRNA diffract only to low resolution (~7 Å). These were obtained from thermophilic organisms. Our approach has been to use 5S rRNA from a hyperthermophile, *Pyrodictium occultum*, which grows at 90°C. It is expected that this RNA will be very stable and rigid, thus more amenable to crystallization. The predicted secondary structure of this RNA is shown in Fig. 1. In order to avoid impurities and biological heterogeneity and to allow engineering of the sequence, the RNA is synthesized *in vitro*.

The following systems have been developed:

- Double-stranded DNA containing the T7 RNA polymerase promoter, 5S rRNA (*Pyrodictium occultum*), sequence and a self-cleaving ribozyme sequence was synthesized. This DNA was amplified by the polymerase chain reaction and 5S rRNA was synthesized by runoff transcription with T7 RNA polymerase. The uncleaved molecule was 185 nucleotides (nt) but upon self-cleavage, a 138 nt 5S rRNA molecule was generated along with a 44 nt ribozyme as shown in

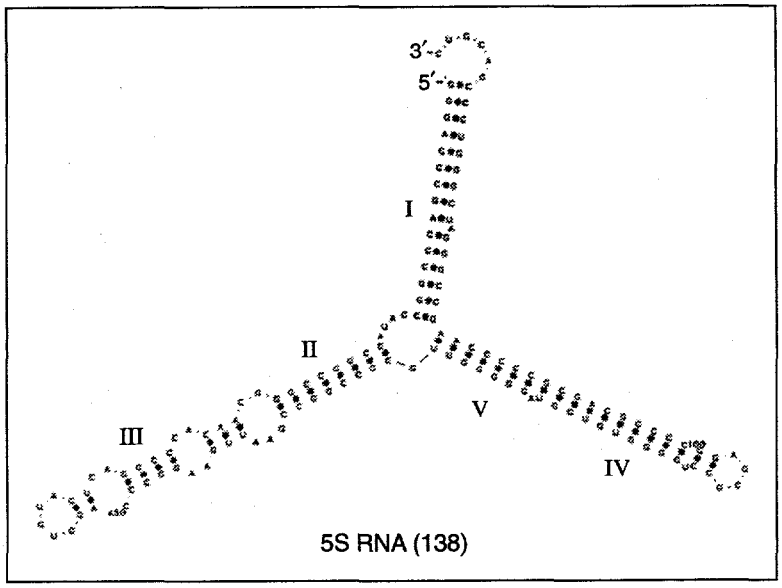

Figure 1. Expected secondary structure of the 138-nucleotide 5S rRNA from Pyrodictium occultum.

Fig. 2(a). This latter molecule was purified by gel elution from a 10% TBE polyacrylamide urea gel. To check for purity, the 5S rRNA was analyzed by chromatography on a Tosohaas DEAE-5PW column as shown in Fig. 2(b).

- Using this procedure, we have isolated milligram amounts of purified 5S rRNA for crystallization. Crystallization experiments have been initiated using sparse matrix screening and hanging drop vapor diffusion techniques. There have been indications of microcrystals, but these need to be further improved.
- We have established a joint project with Dr. Maria Garber of the Institute of Protein Research, Puschchino, Russia, to try to crystallize a complex of *Pyrodictium occultum* 5S rRNA and TL5, a ribosomal binding protein from *Thermus thermophilus*, known to bind to 5S rRNA. We have been successful in showing by gel shift assay that these two molecules do interact with each other. Co-crystallization experiments will begin soon.

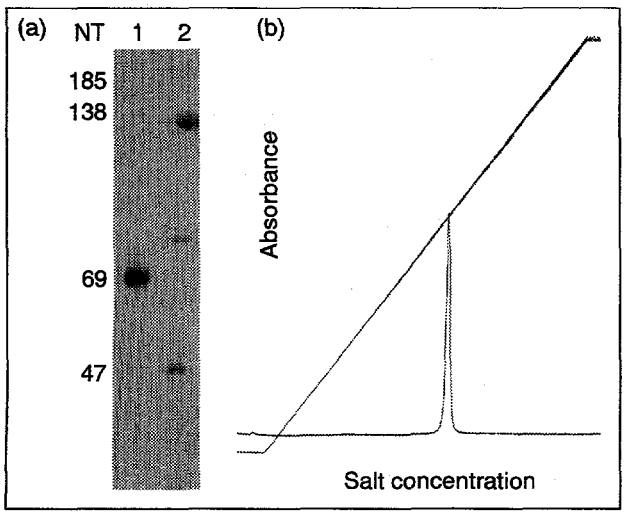

Figure 2. (a) 10% Tris-borate EDTA polyacrylamide urea gel. Lane 1: RNA marker: 69 nt. Lane 2: In vitro *transcription of 5S rRNA: 185 nt (uncleaved RNA), 138 nt (cleaved product), 47 nt (cleaved product). (b) Scan of the 138 nt 5S rRNA loaded on a Tosohaas TSK-DEAE-5PW column and run on a Waters 650 Fast Protein Liquid Chromatography system. Sample was loaded in 0.4 M sodium acetate, 0.1 M Tris, 0.2 mM EDTA, pH 6.9 and eluted in a linear gradient to 1.5 M sodium acetate, 0.1 M Tris, 0.2 mM EDTA, pH 7.3.*

Determination of Macromolecular Structure by ab initio *Phasing of Crystallographic Diffraction Data*

Principal Investigator: Stephen Holbrook

Project No.: 96046

Funding: $57,200 (FY96)

Project Description

The goal of this project is to develop a simple, automatic method for solving macromolecular crystal structures which utilizes the power of high-speed parallel computers and avoids preparation and crystallization of heavy atom derivatives or the need for an approximate structural model.

Our approach is to start with a limited number of experimental diffraction intensities, then to calculate a large number of electron density maps by Fourier transformation using randomly assigned phase sets, and, finally, to develop a method for selecting a map or set of maps closest to the "correct" map. A molecular envelope is then defined based on this map and the solvent content. Evidence in macromolecular crystallography has shown that once a reasonable molecular envelope can be identified, it is possible to obtain a final solution by density modification and refinement techniques. Currently, we are exploring procedures of map averaging and clustering as a means of selecting the proper phase set.

If successful, this approach will greatly accelerate the determination of macromolecular crystal structures and make possible the solution of structures which have resisted traditional methods of phase determination.

Accomplishments

Feasibility

We have determined the minimum number of reflections in centric and non-centric cases required to produce a good approximation of the "correct" electron density map and molecular envelope. This number of reflections is small enough to allow a complete search of all possible phase combinations if

phases are sampled every ninety degrees in the non-centric case.

Map Averaging

Real space averaging of electron density maps calculated with correct phases and maps calculated with incorrect phases was shown to yield average maps highly correlated with the correct map. Thus, the correct electron density map is robust even when averaged with incorrectly phased maps.

Density Modification

We have begun to explore the use of density modification (DM) applied to 10 Å maps with molecular envelopes obtained from correct, partially correct, and incorrect maps. We hope to identify the correct map from the others according to the behavior of the DM process.

Map Clustering

We have developed an algorithm to cluster maps with similar features. The procedure will do the following:

- Randomly sample a set of quadrant phases of selected reflections.
- Fourier transform these reflections and obtain the maps in real space.
- Calculate the correlation coefficients of this map to all existing map clusters.
- Add this map to the cluster with highest correlation above a selected correlation threshold.
- If the correlation coefficient of this map to all existing clusters is lower than the threshold, the map itself starts a new cluster.

We have shown that a correlation cut off of 20% generates about 20 stable clusters; 40% yields 60 clusters and 50% creates 200 clusters regardless of the number of maps generated (> 1000). Further, averaging the strongest clusters improves agreement with the correct map over the average correlation of the individual clusters. Finally, we have observed an interesting and potentially very important aspect of the number of maps in the clusters. Usually, there is one cluster containing many more maps than all the others. This cluster often is the one with highest correlation to the correct map. This clustering procedure has been developed, debugged, and tested on an SGI Indigo II workstation with a 195 Mhz R10000 CPU. It is easily expandable to any number of reflection sets, correlation threshold, number of phase sets sampled, type of phases assigned, and number of clusters. It takes about 40 hours on this workstation to generate and cluster 10,000 maps with about 200,000 correlation calculations between the two 44×28×36 maps. In order to increase the number of phase sets we can sample and maps we can cluster, we plan to port the procedure to the new NERSC T3E parallel computer.

The outcome of this clustering procedure is not limited to our main project. We foresee the potential application of this technique to conventional crystallographic methods such as multiple isomorphous replacement and molecular replacement. We plan to develop these applications as well along with our major project.

Publication

S.R. Holbrook, L.W. Hung, and S.H. Kim, "Map Clustering and Its Applications to Macromolecular Crystallography," in preparation.

Cross-Divisional

New Chemistry for Pollution Prevention: Selective Catalyst

Principal Investigators: Robert Bergman, Mark Alper, Jonathan Ellman, Peter Schultz, Alexis Bell, Enrique Iglesia, Heinz Frei, and Jay Keasling

Project No.: 96027

Funding: $378,800 (FY96)

Project Description

A major issue in the development of environmentally benign synthetic processes is lack of selectivity, which results in disposal problems of unwanted byproducts, energy-intensive separations, and inefficient use of starting materials. Development of selective catalysts that promote only the desired reaction is therefore of great importance. Catalyst use also allows introduction of different reaction conditions which can be less energy-demanding and may decrease dependence on toxic or wasteful solvents and reactants. The focus of this research is the exploration of four approaches to selective catalysis:

- In one study, a combinatorial approach to catalyst optimization is explored with the expectation that it will improve dramatically the time-consuming and costly trial-and-error process currently practiced.
- In the second study, the problem of selective conversion of low alkanes to bulk chemicals and fuels is addressed. The inertness of alkanes constitutes a real challenge, but the importance of these feedstocks makes efficient and selective catalysts for these conversions particularly urgent.
- In the third study, visible-light-assisted chemistry of reactants occluded in molecular sieves is explored for selective monochlorination of small hydrocarbons, and for the direct conversion of alkenes and aromatics to epoxides and alcohols using oxygen as terminal oxidant. Substantial environmental benefits over existing processes are expected from new routes to these important commercial products.
- In the fourth study, microbial pathways are explored for the synthesis of biodegradable polymers. The use of engineered microorganisms promises high selectivity as well as the use of renewable feedstocks for plastics manufacture.

Accomplishments

A Combinatorial Approach to Catalysis

The discovery of new catalysts and optimization of existing ones can have a large impact on chemical manufacturing processes in terms of energy efficiency and environmental friendliness. Unfortunately, a detailed understanding of catalyst structure and its influence on transition state energy is largely lacking in catalyst discovery and development. Moreover, the nature of the interactions between catalyst and support that influence catalyst performance is not well understood. These difficulties have led to a very empirical, trial-and-error approach to catalyst discovery and optimization. We hope to impact this process by application of combinatorial approaches—the ability to cost-effectively design, execute and analyze tens of thousands of experiments in parallel versus one at the time. Initial focus is on two systems:

- Late metal metallocene catalysts for olefin polymerization.
- Transition metal-phosphine ligand complexes for the asymmetric hydrosilation of alkenes.

Our efforts have focused thus far on the development of a general synthetic approach to the "Brookhart" family of olefin polymerization catalysts. These are currently the subject of considerable effort, in large part due to their ability to copolymerize olefins containing heteroatom substitutes and produce long chain polyolefins. A highly efficient solution route has been developed that allows us to generate *bis* imines with control over the substituents on the carbon and nitrogen atoms of the *bis* imine skeleton. The combinatorial synthesis of Brookhart catalysts can be accomplished in seven straightforward steps (Fig. 1).

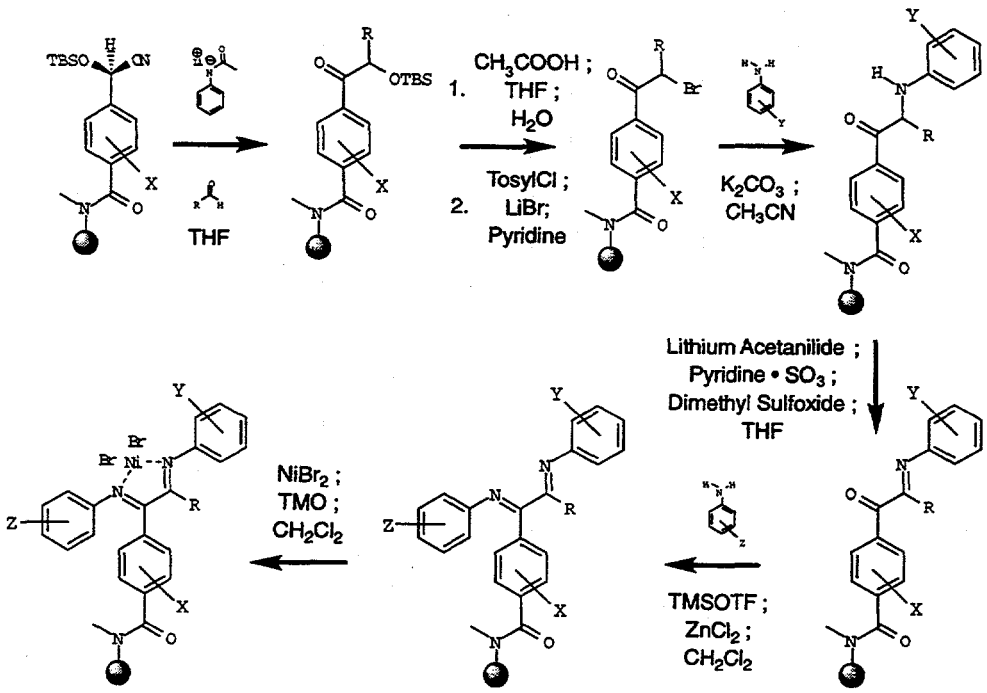

Figure 1. Synthesis of Brookhart catalysis.

For the successful implementation of a combinatorial approach to transition metal-based catalysts with phosphine ligands, a general strategy had first to be developed for the combinatorial synthesis of diverse phosphine ligands. We have selected chelating phosphine ligands for our initial efforts because they form more stable complexes, and because different structures of the tethering elements can provide a range of bite angles and/or chiral environments with which we can modulate the reactivity and selectivity of the catalyst. Of the many possible choices for chelating ligands, we selected 2-phosphinobenzoic acid derived ligands because of their already established use in a number of reactions; access to a variety of bite angles and chiral environments from a large number of commercially available diols, diamines, and amino alcohols; and ease and high yield of synthesis. The synthesis sequence for generating a library of chelating phosphine ligands is shown in Fig. 2.

Catalytic Oxidation of Alkanes at Low Temperature

In the light of the importance of low alkanes as new feedstocks for industrial chemicals and as fuels, development of catalysts for their selective conversion to bulk and fine chemicals and fuel additives is a crucial aspect of pollution prevention. Methane activation is especially attractive as it constitutes the main component of natural gas. Partial oxidation and combustion of methane are opposing extremes, yet the processes share common aspects whose simultaneous study promises to benefit both. One aspect of our work focuses on the latter process, namely the complete catalytic combustion of methane.

Preliminary research revealed that the methane oxidation activity of PdO is sensitive to the structure of dispersed microcrystallites. It is therefore imperative to establish the influence of particle morphology and the means by which desired sizes and morphologies can be obtained. We have approached this by stabilizing PdO with refractory metal oxide supports such as ZrO_2. Indeed, strong effects of the structure and the extent of Pd oxidation on the rate of methane oxidation on Pd/ZrO_2 catalysts were uncovered. In-situ Raman spectroscopy of PdO species during methane oxidation is employed. These studies have identified the details of the mechanism of Pd to PdO transformation during catalysis and suggest the requirement for both surface oxygen and free Pd sites for the rate limiting C-H bond activation step.

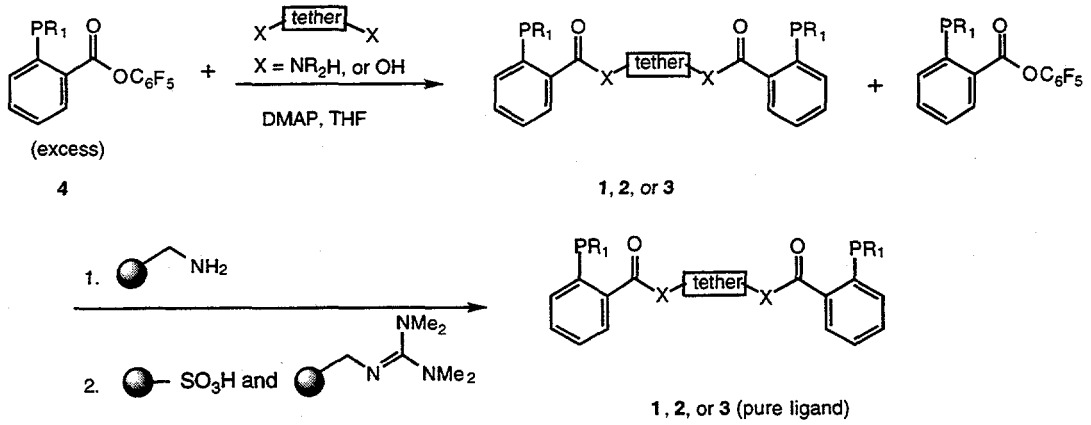

Figure 2. Parallel synthesis of pure ligands 1, 2, or 3.

Work has been initiated on the selective oxidation of $C_2 - C_4$ alkanes. This effort involves the synthesis of well-characterized metal-oxo units incorporated into either amorphous or zeolitic matrices. The catalyst samples are characterized by a variety of spectroscopic techniques to establish the structure of the metal-oxo units after synthesis and catalyst pretreatment.

Light-Assisted Functionalization of Small Hydrocarbons

We have recently discovered a method for highly selective oxidation of low alkanes, alkenes, and alkyl-substituted aromatics by O_2 to commercially important carbonyl products. The method consists of exposure of the reactant gas mixture, loaded into alkali or alkaline-earth zeolites, to visible light at ambient temperature. The three-dimensional nanocage network of the zeolite (type Y) allows the formation of high concentrations of collisional hydrocarbon-O_2 pairs. We are exploring photochemistry of collisional pairs in nanocage matrices for two types of commercially important processes:

- The selective monochlorination of small hydrocarbons by Cl_2.
- Direct oxidation of benzene to phenol by NO_2, a process that uses O_2 as terminal oxidant.

Nitrogen dioxide dismutates spontaneously to NO_2^+ and NO_2^- in alkali zeolites because of the high electrostatic fields: Cl_2 may be too reactive towards olefins in these zeolites and react indiscriminately in the dark. Non-ionic molecular sieves such as $AlPO_4$ or high-silica sieves may be more suitable for these systems. These sieves are much less polar than cation-exchanged zeolites, and may offer the additional benefit of facile removal of polar reaction products from the matrix. Therefore, we started the project by synthesizing $AlPO_4$-5, $AlPO_4$-11, VPI-5, and high-silica faujasite materials. We have found that dark thermal reaction of small olefins in these sieves occurs at substantially lower temperature than in conventional phase, presumably because of the high concentration of reactant collisional pairs in the molecular-size cages. Photochemical studies of Cl_2 with alkene, alkane, and toluene under red and near-infrared light are in progress.

The concept of visible-light-driven benzene-to-phenol conversion by NO_2 is attractive because the coproduct NO can rapidly be reoxidized by O_2 to NO_2 in the dark. We have demonstrated this reoxidation in $AlPO_4$ and high-silica sieves at temperatures as low as 150 K. Therefore, NO acts as catalyst and O_2 is the oxidant consumed.

Metabolic Engineering for Intracellular Synthesis of Biopolymers

Genetic manipulation of storage biopolymer-producing microorganisms offers opportunities for the production of biodegradable polymers such as polyhydroxyalkanoates. While living organisms do not produce such desirable polymers, it is possible to assemble the appropriate enzymatic pathways in them by giving them new genes. To optimize production, it is desirable to use normal cell products as precursors and balance the flow of the multitude of pathways in the organism. The primary objective of this project is to develop a methodology to redirect bacterial metabolism to produce desired products from inexpensive raw materials. This will be achieved through the movement of genes from one

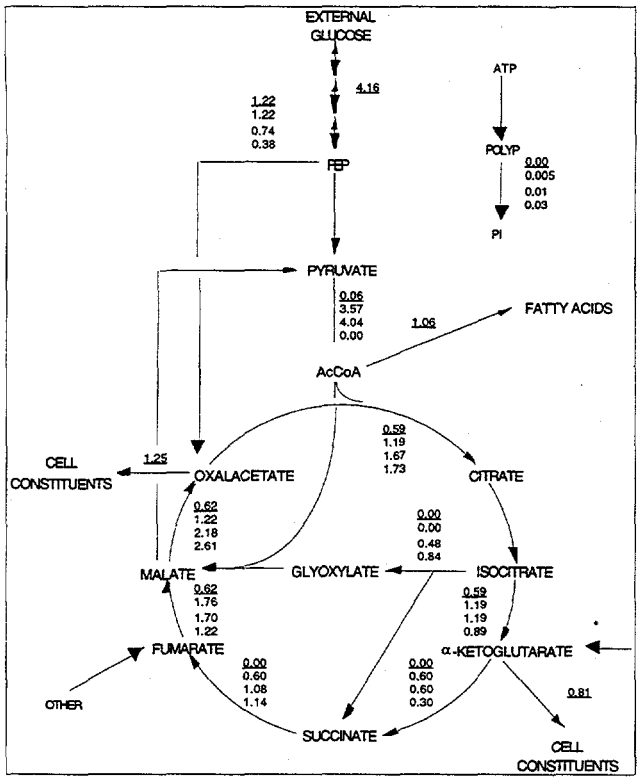

Figure 3. Solutions from the flux-based metabolic model for wild-type cells and cells overproducing PPK and PPX.

organism to another and by using mathematical models to describe and then manipulate the flow of reactions in the organism. As a first step towards our goal, we manipulated the accumulation of the long-chain biopolymer polyphosphate in *Escherichia coli*.

The genes involved with polyphosphate metabolism in *E. coli* were cloned behind different inducible promoters on separate plasmids. The gene coding for polyphosphate kinase (PPK), the enzyme responsible for polyphosphate synthesis, was placed behind the P_{tac} promoter. Polyphosphatase (PPX), a polyphosphate depolymerase, was similarly expressed using the arabinose-inducible P_{BAD} promoter. The ability of cells containing these constructs to produce active enzymes only when induced was confirmed by polyphosphate extraction, enzyme assays, and RNA analysis. Experiments were performed in which the *ppk* gene was induced early in the growth, overproducing PPK and allowing large amounts of polyphosphate to accumulate. The *ppx* gene was subsequently induced, and polyphosphate was degraded to inorganic phosphate. Therefore, these constructs allow independent manipulation of synthesis and degradation pathways. A mathematical model of steady state fluxes through metabolic pathways was used to evaluate the effect of polyphosphate metabolism on cell growth (Fig. 3).

Publications

J.D. Keasling, S.J. Van Dien, and J. Pramanik, "Engineering Polyphosphate Metabolism in *Escherichia coli*," *Biotechnol. Bioeng.*, submitted 1996.

S.J. Van Dien, S. Keyhani, C. Yang, and J.D. Keasling, "Independent Synthesis and Degradation of Polyphosphate in *Escherichia coli* Using Inducible Promoters to Control Enzyme Levels," *Appl. Env. Microbiol.*, submitted 1996.

Biology of Boron Neutron Capture Therapy (BNCT)

Principal Investigators: Eleanor Blakely, Thomas Budinger, William Chu, and Theodore Phillips

Project No.: 96002

Funding: $128,900 (FY96)

Project Description

To assist in fulfilling the necessary requirements for an Investigational New Drug (IND) application, this project proposes acquiring scientific data on pharmacokinetics and on the toxicity of boron compounds in cells, small animals, and large mammals. IND Phase I clinical trials of specific boron compounds will be done in preparation for boron neutron capture therapy (BNCT). This is a bi-modal therapy where tumors are selectively loaded with a boron-rich compound prior to irradiation with neutrons. Boron neutron capture results in fission that produces two particles (^{4}He and ^{7}Li) with short tissue pathlengths of less than 9 μm. These high linear energy transfer (LET) particles damage adjacent cellular structures, and knowledge of the intracellular compartment where the boron localizes is important for understanding the potential effectiveness and underlying mechanism of tumor cell damage from BNCT. Berkeley Lab (LBNL) and the UCSF laboratory are performing technical and clinical BNCT tasks. A proposed accelerator-based BNCT capability

for Phase I and II clinical studies, to be located at LBNL, has received enthusiastic support from the West Coast medical community (including UCSF, Stanford University, University of Washington, and Loma Linda University).

Stephen Kahl, of the UCSF Pharmaceutical Chemistry Department, developed a boronated protoporphyrin (BOPP) that has shown very promising tumor-concentrating capability in small animal models. FDA approval of such a boronated drug is necessary before clinical trials can be started. The immediate goal of this project was to measure the biodistribution, biological half-life, and binding sites—as well as the transport kinetics—of the boronated compounds in the 9L-rat gliosarcoma model. These can be studied *in vitro*, as well as with intracranial or flank transplantation. Two human tumor cell lines, the SF-767 glioma and the SSC-25 squamous cell carcinoma, were proposed for study *in vitro* and in the flank of nude mice. Biodistribution of the compounds in four dogs was also proposed. In addition to the tissue specificity and biological half-life in these different systems, the effects of drug concentration and time of exposure were to be determined. In the 9L model, we also proposed studying the effects of reduced pH, oxic status, and cell cycling on cytotoxicity. Results from these investigations would assist the IND application for Phase I clinical trials of the boron compounds.

An additional goal of this project is to develop the protocols by which the uptake, clearance, and metabolic fate of proposed BNCT compounds can be monitored *in vivo* in both animal models and human patients. We propose radiolabeling the compounds with positron-emitting isotopes (^{18}F, ^{64}Cu, ^{11}C) and using our Positron Emission Tomography (PET) facility to follow the biodistribution of these compounds via radioimaging. The information obtained from these and related studies will:

- Allow for the comparative evaluation of the potential BNCT compounds so that the best candidate for clinical studies can be selected based on determinations of clearance rates, metabolic turnover, and tumor/blood and tumor/normal tissue ratios.
- Provide the information needed to calculate the final boron concentration in the tumor so that therapeutic dose delivery can be calculated.
- Allow for the optimization of treatment and injection strategies.
- Provide the information to tailor these strategies to the individual patient.

Key personnel for this project included: Eleanor Blakely, Daniel Callahan, Trudy Forte, Javed Afzal, Thomas Budinger, Scott Taylor, James O'Neil, and William Chu of LBNL and Dennis Deen, John Fike, Stephen Kahl, and Theodore Phillips of UCSF.

Accomplishments

Milestones achieved during the funding period largely accomplished the proposed goals and even expanded the scope of the investigation. *In vitro* and *in vivo* cytotoxicities and pharmacokinetics were measured in replicate experiments with human glioma cells derived from brain tumor biopsy material. Selective tumor uptake of BOPP has been reported in CBA mice bearing an implanted intracerebral glioma with tumor ratios at high as 400:1 relative to normal brain (Hill et al., *Proc. Natl. Acad. Sci. USA* **89**: 1785-1789, 1992). In collaboration with W. Bauer at INEL, we have analyzed boron content to determine BOPP uptake in exponentially growing tumor cells over a range of concentrations (including 0.01, 0.05 and 0.1 mM) for periods of exposure ranging from 2 to 72 hrs. We find BOPP uptake within 2 hrs and saturation within 24 hrs. Cytotoxicity studies indicate approximately 50% cell killing with exposure to 0.07 mM BOPP for 24 hours. Results of initial studies on cells *in vitro* show that the cytotoxicity of BOPP is affected by microenvironmental conditions. Further studies are now underway.

In studies using the fluorescence microscope, the fluorescence of BOPP allows one to determine the intracellular localization of the compound. Hill et al. (1992) reported discrete localization into perinuclear mitochondria. We also observe discrete BOPP subcellular localization distributed into punctate perinuclear bunches (see Fig. 4), but our co-localization studies with rhodamine-123 and Lysotracker-red indicate that the BOPP (20 μg/ml for 32 hours) appears to accumulate primarily in the lysosomal compartment with adequate proximity to the nucleus for effectiveness in BNCT. We expanded the scope of the investigations by testing the role of lipoproteins on the uptake of BOPP and have evidence that low density lipoprotein (LDL)

receptor-deficient cells have a significant reduction in BOPP uptake. The physiological basis for the differential uptake by tumor versus normal cells is still under investigation. We are currently screening several more human glioma biopsy specimens for LDL-receptor status.

In vivo testing of BOPP has included measuring biodistribution and toxicity in rat glioma models and in human xenograft models. One day after BOPP injection, the 9L rat intracerebral tumor model showed tumor/blood and tumor/normal brain ratios of 0.5 and 19, respectively. The corresponding ratios for the xenograft model, in which SF-767 human brain tumors were grown in the flanks of athymic mice, were 0.5 and 13.

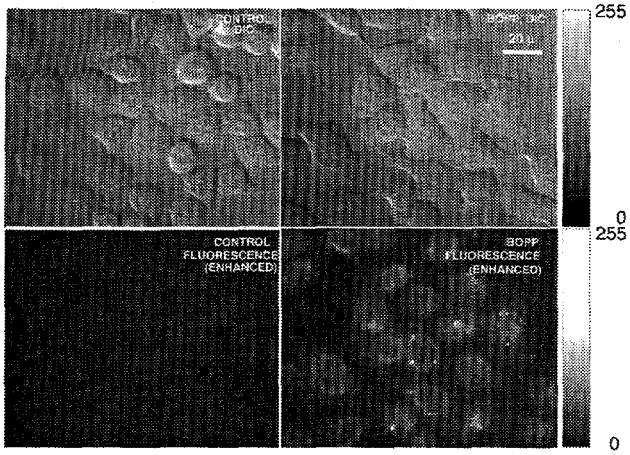

Figure 4. Digital images of living human glioma SF-767 cells obtained with an inverted optical microscope at the Life Sciences Microscope Resource (LSMR).

***Panel 1** (Control, DIC): DIC (differential interference contrast) image of cells that have not been exposed to the fluorescent compound BOPP (boronated protoporphyrin).*
***Panel 2** (Control, Fluorescence) Fluorescence image of the same cells as Panel 1. No fluorescence signal is visible in these control cells.*
***Panel 3** (BOPP, DIC): DIC image of cells exposed to BOPP (20 μg/mL) for 24 hours. Scale bar indicates 20 microns.*
***Panel 4** (BOPP, Fluorescence): Fluorescence image of same cells as Panel 3. Image has been digitally enhanced to the same extent as control cells (Panel 2). Fluorescent signals are due to BOPP accumulation in intracellular lysosomes and magnitude of fluorescent signal is related to amount of BOPP in the cells.*

In addition, the pharmacokinetics, tissue localization, and toxicology of BOPP in normal adult male beagle dogs has also been investigated. Three sets of four dogs have been exposed to BOPP (35 mg/kg) for 25 hrs, 79 hrs, or 10 days. At the end of the exposure period, tissue specimens from numerous organs were taken for either tissue fixation and embedding, for later microscopic examination of ultrastructure, or for analysis of boron content. Clinical toxicities noted in these preliminary experiments include periphereal venous thrombosis near the injection sites, reversible hematopoietic system response, and reversibly elevated liver enzymes. Further toxicity studies are still to be done. Boron associated with BOPP appears to be concentrated in the liver, lymphatic tissues, and the adrenal glands of canine subjects. Boron levels in the cerebrum, cerebellum, cerebral spinal fluid (CSF), and intraocular fluid remained at or below 1 μg/g at all time points. Plasma boron pharmacokinetics appear to follow a multicompartment behavior with a long terminal half-life. Preliminary histopathologic examination of livers of these subjects suggest some minor changes in the morphology of the liver.

We have successfully inserted ^{64}Cu into BOPP at high radiochemical yields. This PET agent was used in biodistribution studies and in imaging studies with animal models. Biodistribution, tumor/tissue ratios, and metabolism of the compound were found to be nearly identical to the studies done with non-radiolabeled BOPP.

Publications

S.M.J. Afzal, E.A. Blakely, D. Callahan, W. Chu, S. Kahl, J. Tibbits, A. Bollen, L. Hu, J. Fike, W. Bauer, T.C. Phillips, and D.F. Deen, "BOPP: A New BNCT Compound," presented in a workshop at the 44th Annual Meeting of the Radiation Research Society, 14-17 April 1996, Chicago, Illinois.

E.A. Blakely, S.M.J. Afzal, D. Callahan, W. Chu, S. Kahl, J. Tibbits, A. Bollen, L. Hu, J. Fike, W. Bauer, T.C. Phillips, and D.F. Deen, "BOPP: Cytotoxicity, Pharmacokinetics and Intracellular Localization in a Human Glioma Cell Line and Biodistribution in a Canine Model," presented at an International Particle Therapy Meeting (PTCOG XXIV), 24-26 April 1996, Detroit, Michigan.

D. Deen, J. Afzal, E. Blakely, A. Bollen, D. Callahan, W. Chu, L. Hu, S. Kahl and T.L. Phillips, "BOPP: Cytotoxicity, Pharmacokinetics and Intracellular Localization in a Human Glioma Cell Line," presented at the 7th International Symposium on

Neutron Capture Therapy for Cancer, 4-7 September 1996, Zurich, Switzerland.

D. Callahan, T. Forte, J. Afzal, D. Deen, S. Kahl, K. Bjornstad, W. Bauer, T. Phillips, and E. Blakely, "Boronated Protoporphyrin (BOPP) Localizes in Lysosomes of the Human Glioma Cell Line SF-767 With Uptake Modulated by Lipoprotein Levels," in preparation.

J. Afzal, E. Blakely, L. Hu, J. Fike, S. Kahl, K. Bjornstad, T. Phillips, and D. Deen, "BOPP: Cytotoxicity and Pharmacokinetics in a Human Glioma Cell Model," in preparation.

T. Ozawa, J. Afzal, J. Wang, A. Bollen, J. Wyrick, J. Fike, E. Blakely, G. Ross, T. Phillips, and D. Deen, "BOPP: Cytotoxicity and Biodistribution in Rodent Tumor Models," in preparation.

J. Tibbitts, J. Fike, A. Bollen, W. Bauer, T. Seilhan, T. Phillips and S. Kahl, "Pharmacokinetics and Toxicology of BOPP in the Normal Canine," in preparation.

SELECT: An Integrated Framework for Assessing Transport, Exposure, Health Risk, and Clean-up Cost for Subsurface Contamination

Principal Investigators: Thomas McKone, Sally Benson, Nancy Brown, Joan Daisey, Lois Gold, and Jane Macfarlane

Project No.: 94031

Funding: $322,700 (FY96)
$434,400 (FY95)
$375,300 (FY94)

Project Description

Regulatory agencies turn to health and environmental scientists for systematic and scientifically defensible approaches to evaluating potential impacts and/or ranking potential hazards from occupational, residential, and ambient exposures to chemical agents. To assist this process, scientists at Berkeley Lab have formed an interdisciplinary team to assess potential health and environmental risks posed by toxic agents at hazardous waste sites. This team has produced a prototype computer framework, SELECT, that links and integrates the activities of site characterization, contaminant transport (with and without remediation technology), human exposure, hazard and risk assessment, and cost estimation.

The first step in the methodology is to assess the current and future state of the contaminant plume and the effects over time of each remediation alternative being considered. This is followed by estimating the exposures to a given contaminant for a specified population. Using rodent carcinogenic potency values and human exposure estimates, including (often profound) estimates of uncertainty, cancer risks are estimated. Where possible, pharmacokinetic analyses and mechanisms of carcinogenesis are incorporated in cancer risk assessments. Possible cancer hazard is compared to similarly estimated hazards from typical exposure to rodent carcinogens, e.g., to natural chemicals in the diet, or background exposures to airborne chemicals. Costs associated with a specific remediation action are integrated with risk estimates to identify cost-effective strategies. Secondary risks produced by remediation are also evaluated. Visualization tools are used to present information in an understandable form that site managers can use to formulate remediation strategies.

When fully developed, SELECT will accelerate the transfer to industry and regulators of state-of-the-art models and up-to-date information from the national laboratories and will provide the concerned public with a tool that makes the decision process easier to understand.

Accomplishments

The goal of the SELECT project is to design and develop a flexible, PC-based, object-oriented software system that will integrate, analyze, and present environmental information to managers, engineers, scientists, regulators, and the public. The software assists the user in selecting cost-effective environmental remediation strategies. Progress toward this goal in FY96 is summarized below.

Continued Prototype Development

We have developed a SELECT prototype that runs on a PC and is used to illustrate a simplified version of the site characterization; a graphic visualization of the development of the concentration field over time; and displays of exposure, risk, and cost effectiveness. The prototype demonstrates the vision of the SELECT software and implements portions of the SELECT methodology. The prototype currently includes the following elements:

- Contaminant transport simulations using T2VOC.
- Air dispersion transport model based on ISCLT, [New].
- Integration of transport results into the exposure spreadsheets of the CalTOX software used by the state of California.
- An easy-to-use interface.
- Real-time estimation of exposure and risk, including risk comparisons.
- Integrated cost spreadsheets.

Uncertainty/Sensitivity Analyses

During the last fiscal year, we demonstrated that SELECT could be used to carry out an integrated uncertainty analysis, linking a Monte Carlo analysis in the T2VOC simulation with a Monte Carlo analysis carried out with the CalTOX model. The result of this analysis is a two-dimensional uncertainty surface that allows one to explore how the uncertainties in the two simulation systems combine when the models are integrated. This process is illustrated in Fig. 5. Concentration distributions and their uncertainties were calculated with the subsurface transport simulator T2VOC (using the associated ITOUGH2 code for error analysis) for a three-dimensional system in which TCE migrates in both the vadose and saturated zones over extended distances and time scales. In this study, the subsurface concentration distributions and variance were passed to the exposure model CalTOX. Monte Carlo methods were used in both the subsurface transport and exposure models for the propagation of error due to parameter uncertainty. Several analyses were completed to evaluate the contributions of uncertainty from both modeling efforts as well as individual parameters on the distribution of risk.

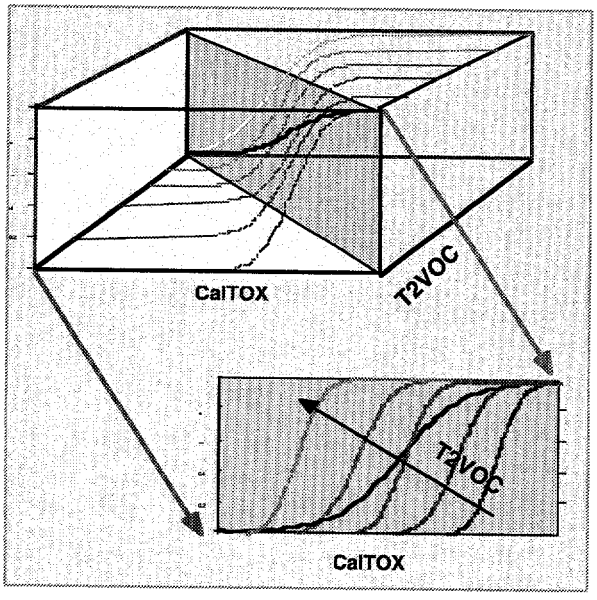

Figure 5. An example of the type of two-dimensional uncertainty surface that allows us to explore how the uncertainties in CalTOX and T2VOC combine in an exposure assessment.

Homepage Release

During 1996, the SELECT Homepage on the World-Wide Web was completed and released at **`http://omega.lbl.gov/select/`**. The homepage provides a demo of the SELECT prototype and allows easy access for all potential SELECT users.

Exposure Assessment

Multimedia, multiple pathway exposure models are used in CalTOX to estimate average daily doses within a human population in the vicinity of hazardous substance release sites. The exposure models encompass twenty-three exposure pathways. The exposure assessment process consists of relating contaminant concentrations in the multimedia model compartments to contaminant concentrations in the media with which a human population has contact (personal air, tap water, foods, household dust, soils, etc.). During FY96, a number of modifications were made to the CalTOX model in order to address some of the limitations that were identified in the early version of the model. These modifications to CalTOX include:

- Redefining the equations so that there can be both batch and continuous inputs to the root-zone soil.
- Altering the way the plants compartment interacts with soil and air.
- Allowing CalTOX to handle chemical concentrations in soil that exceed the aqueous-phase solubility limit.
- Adding the ability to simulate off-site transfers of contaminants through the ground water and air pathways.

Air Model

We have developed for SELECT a site-specific atmospheric dispersion model to predict contaminant

concentrations in the air at receptor locations near the contaminant source or treatment site. We are using the EPA ISCLT2 program to develop this model, which requires long-term, site-specific meteorological data. We have located such data for a five-year period for the McClellan/Sacramento area. The McClellan-specific model has been interfaced to the SELECT prototype.

Risk: Ranking Potential Health Hazards

The Carcinogenic Potency Database (CPDB) is an integral part of the SELECT system. Based on rodent carcinogens in the CPDB, a comparison is presented in SELECT of possible carcinogenic hazards from exposures to site contaminants and a variety of exposures to natural chemicals. A database of information that is relevant to developing cancer risk assessments has been created and put in an accessible form within SELECT. Included in this database system are:

- Carcinogenic potency estimates for approximately 600 rodent carcinogens based on (a) TD50 from CPDB, (b) q1* from the U.S. EPA, and (c) q1* from California EPA.
- Mutagenicity evaluations for about 400 rodent carcinogens.
- U.S. OSHA permitted exposure levels (PEL) and California OSHA PELs.
- Ranking of possible carcinogenic hazards based on (a) HERP on 80-rodent carcinogens, and (b) PERP on 75-rodent carcinogens.
- Maximum Concentration Limits (MCL) in drinking water set by the U.S. EPA and the California EPA.

We continued our efforts to obtain PBPK-based risk estimates for TCE that are based on animal no-observed-adverse-effect levels (NOAELs) and a peak-blood-concentration dose metric, and have illustrated estimation of NOAEL-based MCLs for human exposures to TCE using novel methods. Our results indicate that the current U.S. MCL for TCE in drinking water may be about 40 times lower than the no-effect level. The new methods support quantitation of cancer potencies required in SELECT for volatile organic water contaminants such as TCE.

Total Risk Integrated Methodology

We have began to work with the U.S. EPA Office of Air Quality Planning and Standards to support their Total Risk Integrated Methodology (TRIM). We provided input for a report that the EPA prepared on a framework for multimedia exposure assessment for air emissions to comply with requirements of the 1990 Clean Air Act.

Publications

K.T. Bogen and L.S. Gold, "Trichloroethylene Cancer Risk: Simplified Calculation of PBPK-Based MCLs for Cytotoxic Endpoints," accepted for publication in *Regulatory Toxicology and Pharmacology*.

T.E. McKone, "The Reliability of a Three-Compartment Fugacity Model for Estimating the Long-Term Inventory and Flux of Contaminants in Soils," accepted for publication in *Reliability Engineering and Systems Safety*.

T.E. McKone and R.L. Maddalena, "Soil Contamination and Human Exposure: A Comprehensive Assessment Framework," accepted for publication in *The Journal of the American College of Toxicology*.

T.E. McKone, D. Hall, and W.E. Kastenberg, "Modifications of CalTOX to Assess the Potential Health Impacts of Hazardous Waste Landfills," a draft report prepared for the California Environmental Protection Agency, 1996.

C.M. Oldenburg, A.L. James, "Linear and Monte Carlo Error Analysis," accepted for publication in *Water Resources Research.*

Use of rRNA Gene Sequencing and Signature Lipid Biomarker Analysis to Assess and Monitor Microorganisms in Damaged Environments

Principal Investigators: Stanley Goldman and Tamas Torok

Project No.: 96047

Funding: $251,000 (FY96)

Project Description

Microbial communities in nature are complex, highly integrated, dynamically changing, and diverse assemblies. Characterization of these communities is a major prerequisite for any in situ or ex situ bioremediation effort. Standard practice in microbial

ecology has traditionally relied on isolating and growing microorganisms. However, available media and isolation techniques have typically helped grow and identify less than 1% of naturally occurring microorganisms. Thus, this project was designed to use molecular-level methods to characterize microbial communities in damaged environments. Our goal was to build a microbial phylogenetic core capability so that we could establish and adapt necessary sample preparation techniques, and generate rRNA gene sequences and fatty acid methylester (FAME) profiles of microorganisms.

Accomplishments

Sample Preparation Techniques

Some basic sample preparation methods for both DNA and phospholipid extraction are familiar. However, their adaptation has been challenging, especially for whole microbial communities from natural, contaminated environments. Soil humic substances that co-precipitate with DNA can render subsequent polymerase chain reactions (PCRs) impossible. On the other hand, most steps used to eliminating soil humic substances will cause major yield losses in DNA extraction. By using several DNA extraction protocols, we are finally in the position of being able to extract representative total microbial genomic DNA from most natural environments. As for phospholipid extraction, the technique of working with whole cells is routinely used in our laboratory.

Several sites with very different ecophysiological parameters—representing a wide variety of scenarios, humic substance concentrations, and contaminants—were chosen for the project. The matrixes included groundwater, sand, soil, sediment and rock.

16S rRNA Gene Sequences

The extracted DNA is used to amplify 16S or 16S-like rRNA gene sequences in a PCR. To identify members of naturally occurring microbial communities, PCR products are cloned and ultimately sequenced, edited, and aligned with database entries. Lately, we have been working on economically and environmentally important samples from the Central Valley. Twenty microorganisms were isolated from heavy metal, selenium-contaminated sites. Twelve have been sequenced and eight were in good agreement with existing database entries. Further sequence analysis is needed to determine whether the remaining strains have unique sequences representing potentially novel microorganisms.

Fatty Acid Methylester Profiles of Microorganisms

The same samples used for DNA extraction have been used to prepare specimens for FAME analysis. The GC-based microbial identification system (MIS), available in our laboratory, is designed to identify pure microbial cultures. Among other advantages, MIS can compare FAME chromatograms even if the system could not use the run for identification. This latter feature will allow for characterization of complex microbial communities. Using a wide variety of media and isolation techniques, we grew large numbers of microorganisms and generated FAME profiles for analysis. In a relatively short period (MIS was purchased late July, 1996), more than 100 FAME profiles have been generated. Judging by the high similarity index, most identification results were satisfactory. In other cases, though the microbes were characterized by a large number of named peaks and extremely small deviation from the standards, a very low similarity index showed that either the FAME profile was not typical for the species or the database entry needed new considerations.

In support of these efforts, we had the necessary infrastructure for housing the microbial phylogenetic core facility built and purchased two key pieces of equipment (a PerSeptive Biosystems Model 8909 Expedite DNA synthesizer and a Perkin Elmer Model ABI Prism 377 DNA sequencer).

Acronyms & Abbreviations

AES	Auger electron spectroscopy
AFM	atomic force microscopy
ALS	Advanced Light Source
ANAS	Alameda Naval Air Station
ASIC	application-specific integrated circuit
ATWR	analog transient waveform recorder
BLISS	Building Life-Cycle Information Systems
BNCT	boron neutron capture therapy
BNL	Brookhaven National Laboratory
BOPP	boronated protoporphyrin
bp	base pairs
CAC	chromatin assembly complex
CAF	chromatin assembly factor
CCD	charge-coupled device
CCN	cloud condensation nucleous
CDF	The Collider Detector at Fermilab
CERN	European Organization for Nuclear Research
CMT	computed microtomography
CPU	central processing unit
CSF	cerebral spinal fluid
D-D	deuterium on deuterium
D-T	deuterium on tritium
DBC	double-buffered counter
DCE	dichloroethene
DIC	differential interference contrast
DM	density modification
DNA	deoxyribonucleic acid
DNAPL	dense non-aqueous phase liquids
DOE	United States Department of Energy
DOM	digital optical mode
DSP	Digital Signal Processor
ECM	extracellular matrix
ECR	electron cyclotron resonance

EDX	energy-length-based x-ray spectroscopy
EPA	The Environmental Protection Agency
ESNet	The Energy Sciences Network
ESR	electron paramagnetic resonance
ESRF	The European Synchrotron Radiation Facility
FAME	fatty acid methylester
FGM	functionally graded composites
FNAL	Fermilab National Accelerator Laboratory
FWHM	full width at half maximum
GaN	gallium nitride
GM	General Motors
GSE	genetic suppressor element
HEED	high energy electron diffraction
HVAC	high-voltage alternating current
IAI	International Alliance for Interoperability
IC	integrated circuit
I.D.	inside diameter
IND	Investigative New Drug
INEL	Idaho National Engineering Laboratory
IR	interaction regions
ISSC	inner-sphere surface complex
JPL	Jet Propulsion Laboratory
K-B	Kirkpatrick-Baez
KEK	Japanese National Laboratory for High Energy Physics
LBNL	Ernest Orlando Lawrence Berkeley National Laboratory ("Berkeley Lab")
LDL	low density lipoprotein
LED	light-emitting diode
LEED	low-energy electron diffraction
LET	linear energy transfer
LHC	The Large Hadron Collider
LLNL	Lawrence Livermore National Laboratory
LSMR	Life Sciences Microscope Resource
MBE	molecular beam epitaxy
MC/MD	Monte Carlo/molecular dynamics

MCL	maximum concentration limits
MCP	microchannel plate
MEC	mammary epithelial cell
MINSY	Mare Island Naval Shipyard
MIS	microbial identification system
mM	milli-molar
mmO	methane monooxygenase
MOKE	magnetooptic Kerr effect
MRI	magnetic resonance imaging
NAPL	nonaqueous phase liquid
NDE	nondestructive evaluation
NERSC	National Energy Research Scientific Computing Center
NIST	National Institute of Standards and Technology
NOAEL	no-observed-adverse-effect level
NOW	network of workstations
NSLS	The National Synchrotron Light Source
nt	nucleotide
O.D.	outside diameter
ORF	open reading frame
OSHA	Occupational Safety and Health Administration
OTT	Office of Transportation Technologies, DOE
PAH	polycyclic aromatic hydrocarbon
PBPK	physiologically based pharmacokinetic
PC	personal computer
PCB	chlorinated hydrocarbons (polychlorinated biphenyl)
PCE	tetrachloroethene
PCR	polymerase chain reaction
PDA	pentacosadiynoic acid
PET	Positron Emission Topography
PPK	polyphosphate kinase
PPX	polyphosphatase
PVM	parallel virtual machine (code)
rf	radio frequency
RHIC-STAR	Relativistic Heavy-Ion Collider—Solenoidal Tracker at RHIC
rRNA	ribosomal RNA
SBRS	shared boundary ring structure

SC	superconducting
SDC	Silicon Detector Collaboration
SELECT	a computer framework
SEM	scanning electron microscopy
SETAC	(National) Society of Environmental Toxicology & Chemistry
SMOKE	surface magnetooptic Kerr effect
SSC	The Superconducting Super Collider
STAR	Solenoidal Tracker at RHIC
SWIC	sediment-water-interface corers
TCE	trichloroethene
TEM	transmission electron microscopy
TPPE	two-photon photoemission
TRF	terminal genomic DNA restriction fragment
TRIM	Total Risk Integrated Methodology
U.K.	The United Kingdom
URL	universal resource locator
U.S.	The United States
UV	ultraviolet
VC	vinyl chloride
VULCAN	commercial software
VUV	vacuum ultraviolet
WDX	wavelength-based x-ray spectroscopy
XANES	x-ray absorption near-edge spectroscopy microprobe
YAC	Yeast Artificial Chromosomes